Abstract

GHARDE, AVONI AMARNATH. Carpet Recycled Polyester (PET): Characterization, Fiber Formation, and Applications. (Under the direction of Dr. Behnam Pourdeyhimi and Dr. Abhay Joijode).

In the past decade, a significant amount of attention has been given to recycled PET made from plastic bottles and containers that are thrown away by consumers, where in reality, we can recycle PET from both post-industrial scrap and post-consumer materials. Post-consumer carpets serve as a valuable source of raw materials that can be reused. This research investigates the challenges that are found within the material and fiber extrusion process stream.

To analyze this, initial characterization was conducted, which included thermal, rheology, chemical analysis, and a few preliminary extrusion trials. Thermal analysis included TGA and DSC; rheological properties were studied by measuring melt flow properties, gel time, and solution viscometry, and molecular weight analysis was studied by the gel permeation chromatography method. SEM-EDS elemental analysis and FTIR tests were conducted as well. We anticipated challenges in fiber formation, such as filter clogging and fiber breaks due to inferior material properties.

We found limited success on the extrusion lines. During fiber formation trials, melt-blown media were produced, and parameters for melt-spinning on homocomponent and bicomponent lines were also optimized. The first investigation gave us an understanding of the polymer composition and quick learnings about the same. It drove us to dig deeper into interpreting and recognizing the components within the carpet recycled PET system, that were causing fiber formation failure.

To establish a limit for the impurity content of $CaCO_3$ (ash) and Polypropylene (PP), ‘dirty’ designer PET pellets were created and analyzed for extrusion trials. Virgin commercial PET was

compounded with varying amounts of PP and ash to mimic the materials received. With these controlled experiments, we could relay information based on this study to our suppliers. By ensuring a thorough cleaning and efficient recycling process, we received new grades of material with a significantly lower amount of impurities. We concluded the addition of modifiers, in this case, a compatibilizer, as a possible solution to improve the inherent polymer properties that would aid in successful fiber formation. The compatibilized recycled PETs were blended with virgin PET at 5:95, 10:90, 15:85, 20:80, 25:75, and 30:70 ratios. There was stable meltblown fabric manufactured with an average fiber diameter of $\leq$10μm in blends containing 5-20% of recycled polymer content.

Carpet Recycled Polyester (PET): Characterization, Fiber Formation, and Applications

by
Avoni Amarnath Gharde

A dissertation submitted to the Graduate Faculty of
North Carolina State University
in partial fulfillment of the
requirements for the degree of
Doctor of Philosophy

Textile Technology Management
Fiber Polymer Science

Raleigh, North Carolina

2020

APPROVED BY:

_____	_____
Dr. Behnam Pourdeyhimi	Dr. Abhay Joijode
Committee Co-Chair	Committee Co-Chair
_____	_____
Dr. Trevor Little	Dr. Eunkyoung Shim
_____	
Dr. Saad Khan	

Dedication

I would like to dedicate this dissertation to my mother, Dr. Rita Gharde, who unfortunately passed away during my first semester of graduate studies abroad. I also dedicate this dissertation to my father, Mr. Amar Gharde, and all my family members who have supported me through life.

Biography

Avoni Gharde received her Bachelor of Technology degree in Fibres and Textiles Processing Technology in 2015 from the Institute of Chemical Technology, Mumbai (India). It was here that her interest peaked in textiles and sustainability in the global industry. She joined North Carolina State University, USA, to pursue her Master of Science in Textiles and switched to the Doctoral Program in the second semester. She is pursuing her Ph.D. in Textile Technology Management and a co-major in Fiber Polymer Science, with a specialization in Nonwovens Science and Technology.

Acknowledgments

As Walter Elliot rightly said – *"Perseverance is not a long race; it is many short races one after the other,"* my journey has also been filled with several pit stops supported by a large group of people who have cheered me on.

Throughout the project, I am incredibly grateful to my advisors Dr. Behnam Pourdeyhimi and Dr. Abhay Joijode, who have been so patient, inspiring, and fantastic guides. I would also like to thank Dr. Saad Khan, Dr. Eunkyoung Shim, and Dr. Trevor Little for serving on my committee and providing suggestions and feedback.

I want to extend my thanks to Carpet America Recovery Effort (CARE), especially Dr. Bob Peoples, Glenn Odom, and Frank Endreyni for funding this project and being great mentors. Special thanks go to Eric Lawrence of the Fiber Science Lab for teaching me to operate on a few of the testing equipment, Amy Minton, of the analytical testing lab for her assistance during testing. A thank you to Tri Vu, who helped me in the spinning trials as well, and everyone who is part of The Nonwovens Institute (NWI) for being a fantastic support system.

There are a few invisible hands who have helped me keep my head up high, and I would like to name them as well. Firstly, thanks to Ritesh Porey for his patience, support, and encouragement. Thanks to all my friends – Erin, Srivatsan, Arjun, Sushant, Yash, to name a few; my school friends – Beverley, Radhika, Suhani, Ava, Malvika, Pooja, NWI student group, and family members in India. I also want to thank my peers and professors at North Carolina State University. To Devesh Udasi, without whom I would not have taken this leap of faith and moved forward into the Ph.D. program. Your support has been a key ingredient to my success. Finally, a big thank you to my mother and father again, who have always taught me to be bold, independent, and create a path where others fear to tread.

Table of Contents

LIST OF TABLES

LIST OF FIGURES

1. Chapter 1: Introduction

Although nearly all kinds of carpets can be reused and recycled, about 4 percent of used carpets are reused and recycled in the U.S (LeBlanc, The Business Opportunity in Carpet Recycling, 2017). Recycled carpets can be used to produce carpet fiber, carpet underlayment, automotive parts, erosion control products, plastics, sports surfaces, roofing shingles, stepping stones, carpet cushion, railroad ties, and different engineered materials. One of the various challenging aspects of carpet recycling is that there is no simple, routine method to recycle old carpet. One of the most common approaches to carpet recycling involves identifying and grouping carpets by their component fibers, mostly plastic, and nylon. The carpets are run through either a shearing machine or shredder to separate different layers of the carpets (LeBlanc, The Business Opportunity in Carpet Recycling, 2017). Further processing is needed to form the plastic into various products like automobile parts.

Carpets have been recycled in the U.S. for nearly 25 years. However, the lack of widespread demand has translated into inconsistent opportunities for carpet recycling entrepreneurs (LeBlanc, The Business Opportunity in Carpet Recycling, 2017). The recovered polyester from carpets had limited end-use markets. There were still relatively healthy and viable streams for post-consumer nylon 6 and nylon 6,6. The single most significant market for nylon 6 was Shaw's Evergreen nylon recycling facility in Georgia. It had a capacity of 100 million pounds, while nylon 6,6 had already established engineered resin markets. A comparatively high melting point makes it a suitable material in vehicle parts. Then came the fall of oil prices, which combined with rising domestic natural gas capacity from fracking to drive down virgin PET prices, making an unfavorable recycled material even less attractive (Helm, 2016).

At present, carpet recycling is highly challenging, and its feasibility will depend on local market conditions (LeBlanc, The Business Opportunity in Carpet Recycling, 2017).

1.1. Textile Recycling

Waste is inadvertent in any process, and for the betterment of the environment, it has to be used again. The importance of recycling textiles is increasingly being recognized and established in the industry. Over 80 billion apparel and clothing products are produced annually worldwide. In 2010, about 5% of the US municipal waste system was textile scrap, totaling 13.1 million tons. The recovery rate for textiles was only 15%. As such, textile recycling is a significant challenge to be addressed as the industry strives to move closer to zero landfill society. Once in landfills, the natural fibers can take hundreds of years to decompose; they may release methane and carbon dioxide into the atmosphere. Synthetics, on the other hand, are not designed to disintegrate. In the landfill, they may release toxic substances into groundwater and the surrounding soil (LeBlanc, The basics of textile recycling, 2017). This is a significant concern.

One of the solutions to the reduction of the carbon footprint in the textile/apparel supply chain would be the use of recycling (Muthu, Li, Hu, & Ze, Carbon footprint reduction in the textile process chain: Recycling of textile materials, 2012). Textile waste materials can be broadly categorized into two categories. They are (i) pre-consumer textile wastes (Pr CTW), and (ii) post-consumer textile wastes (Pt CTW) (Vadicherla, Saravanan, & Muthu, Polyester Recycling—Technologies, Characterisation, and Applications, 2015).

Pr CTW is the waste that never makes it to the consumers, and which comes directly from the original manufacturers. Few examples include ginning wastes, opening wastes, carding wastes, comber noils, combed waste yarns, roving wastes, ring spinning waste fibers, ring-spun waste

yarns, open-end spinning waste fibers, open-end spinning yarn wastes, knitting waste yarns, weaving waste yarns, fabric cutting wastes, fabric wet processing wastes, and apparel manufacturing wastes. Pt CTW is the waste recovered from the consumer supply chain, and these are the materials that are ready for disposal or landfill. Famous examples include recycling of the accessories and beverage bottles to make recycled polyester (Vadicherla, Saravanan, & Muthu, Polyester Recycling—Technologies, Characterisation, and Applications, 2015).

1.1.1. Types of Recycling

Recycling technologies can be divided into primary, secondary, tertiary, and quaternary methods (refer to Table 1). Primary recycling involves recycling a product into its original form; secondary recycling involves mechanical processing of post-consumer plastic products into a new product that has a lower level of properties. The tertiary approach involves processes such as pyrolysis and hydrolysis, which convert the plastic wastes monomers or fuels. Quaternary recycling means burning the fibrous solid waste and utilizing the heat generated. Fibers and fabrics are recycled using all four approaches (Scheirs, 1998; Wang, Recycling in Textiles, 2006).

Table 1. Recycling Technologies.

Methods	**The raw material for recycling**
Primary	Industrial Scraps
Secondary	Mechanical processing of post-consumer products
Tertiary	Pyrolysis/hydrolysis of polymeric wastes to get monomers or fuels
Quaternary	Burning the fibrous solid wastes and utilizing the heat generated

In the technological considerations, the first and foremost issue is the fiber composition of the textile material made out of and also the compatibility of fiber blends, if it is a blended textile product. The other compounded factors are issues/difficulties in separating the blended components, the efficiency of separation, quality of separated material, and hence the recycled material's quality, and so on. When these issues are considered in the life cycle assessment angle, the life cycle inventory of the recycling process becomes much more complicated and energy-intensive, which again leads to the carbon footprint. A good amount of literature was reviewed in this area (Vivek, 2009; Michaud, Farrant, Jan, Kjær, & Bakas, 2010; Muthu, Li, Hu, & Ze, Carbon Footprint Reduction in the Textile Process Chain: Recycling of Textile Materials, 2012).

1.2. PET Recycling Process

PET recycling represents one of the most fruitful and widespread examples of polymer recycling. The main driving force responsible for this extreme increase in the recycling of post-consumer products (Raheem & Uyigue, 2010). Polyester clothing can be recycled and reused in the new polyester product, and polyester clothing can be made from recycled PET. It is useful to sort materials before recycling.

The percentage of plastic waste in the municipal solid waste stream in the U.S. increased to 12 % in 2008; it was less than 1 % in 1960. In 2008 alone, the total amount of plastic waste in the U.S. was approximately 30 million tons. This included 13 million tons of plastic packaging and containers, 11 million tons of durable plastic products, and the remaining 6 million tons was categorized as non-durable plastic items. Each year, almost 25 million dollars is spent in California state to dispose of plastic waste in landfills (LeBlanc, Plastic Recycling Facts and Figures, 2017).

Reusing valuable resources more feasibly contributes to sustainable living. There are several continuous lines of research for the reuse of products made from non-renewable resources

(Awaja & Pavel, 2005). PET is used extensively for beverage bottles and textile fibers. While PET bottles are recycled to a large extent, recycling of PET fabrics is much more challenging, mainly because they are mixed with other fibers (Awaja & Pavel, 2005). A significant portion of PET (39 million tons of PET out of 49 million tons used in 2008) was utilized in the textile industry. About 74% of the PET used in the textile industry is used to make staple fibers. These staple fibers are mostly mixed with cotton fibers to produce cotton/PET blend fabrics (Zou, Reddy, & Yang, 2011; Oerlikon, 2009). The blended fabrics must be disposed of after use, and often they are incinerated to regain energy. However, the most part ends up in landfills (Zou, Reddy, & Yang, 2011). The degradation of PET is slow, and there are environmental problems. Also, the valuable non-renewable petroleum-based resource is wasted (Ramamoorthy, Persson, & Skrifvars, 2014).

Here are some economic facts about recycling plastics around the world and in the US, as published by LeBlanc (Plastic Recycling Facts and Figures, 2017):

- Between 2004 and 2014, the global production of plastics grew to 311 million tons from 225 million tons.
- According to PlasticsEurope, 7.7 million tons of plastics were recycled globally in 2013, including greater than 3.5 million tons of post-industrial and post-consumer plastic scrap in the US, according to the Institute of Scrap Recycling Industries (ISRI).
- About 2000 gallons of gasoline can be saved by recycling just one ton of plastics.
- Producing plastic products from recycled plastics reduces energy requirements by 66%.

1.2.1. Primary Recycling

Primary recycling is also known as re-extrusion. It is one of the oldest ways of recycling PET. It refers to the '*in-plant*' recycling of the scrap materials that have features similar to the original products. This process, although it ensures simplicity and low cost, requires

uncontaminated scrap, making it an unpopular choice for recyclers (Al-Salem, 2009; Al-Salem, Lettieri, & Baeyens, 2009).

1.2.2. Secondary Recycling

Secondary recycling creates opportunities for finding new ways to incorporate materials from used products into things we already produce, and into new things, we may not have thought of before. When recycling provides "new" sources of useful materials, fewer finite resources are being used up in production. For example, shredding used tires for rubber offers a source of valuable rubber products without having to harvest more natural rubber or use resources to produce synthetic varieties, thereby saving natural resources. Secondary recycling can also be very efficient because it takes less time and equipment than processes that require the disintegration of materials chemically. The purpose of recycling is conservation, after all, so saving energy makes recycling all the more worth it (EcoGreen Equipment, 2017).

1.2.3. Tertiary Recycling

Tertiary recycling (also known as feedstock recycling) is the process of converting waste into fuels or basic chemicals. A few methods of plastic feedstock recycling have been investigated in recent years (e.g., depolymerization, catalytic cracking/reforming) with the goal of either recovering monomers or, more commonly, oils and waxes. Also known as thermolysis, pyrolysis is a process of thermal and chemical decomposition, generally leading to smaller molecules. As Municipal Solid Waste (MSW) plastics are predominately thermoplastics, they serve as an excellent feedstock for this process. Pyrolysis is conducted in an oxygen-depleted environment. It is operated at a wide range of temperatures to target specific products (typically between 400-700°C for predominant liquid yield; > 700°C for predominant C1- C3 light

hydrocarbon). There is also considerable literature on different reactor designs and the influence of catalysis (Sharobem, 2010).

1.2.4. Quaternary Recycling

At the fourth level in the recycle hierarchy, a method of vaporizing polymers in solid waste (also termed "quaternary recycling") exploits the calorific content. Polymers have a high heat content so that incineration with energy reclamation offers a way of winning back some value from polymer wastes (where the level of contamination or degree of mixing makes any other process economically unattractive) (Hind, 1999).

1.3. Carpet Waste

Although environmental regulations have forced many industries to change their ways of manufacturing, the primary driving force behind carpet recycling is believed to be economical. There has been an increase in the consumption and production of consumer goods – resulting in a growing waste problem that needs to be addressed. The problem is two-fold, environmental as well as economical. The goods still have value but end up in landfills and incinerators. In the face of climate change and depletion of natural resources, the global community cannot keep expanding landfills. We end up polluting the environment with incinerator emissions and use virgin resources that are limited, such as fossil fuels, to continue producing consumer goods. As increasing portions of the global population join the ranks of the middle class and are becoming more significant consumers, global production and waste systems must evolve to recover better, reuse, and recycle discarded products and bring them back into the global economy (Gaia, 2016).

Gaia (2016) also reported that the U.S. represents five percent of the world's population. However, it produces half of the world's solid waste (Scientific American, 2012) and consumes a quarter of its fossil fuel resources. One solution to the consumption and waste challenge is to

rethink the linear production system consisting of resource extraction, production and consumption of goods, and disposal of waste. But what if there was an entire paradigm shift towards efficiency and designing products not to become waste? It is now needed towards a more circular economy where at the end of life, products are not disposed of but recovered and restored into other valuable products, creating a closed-loop system.

In 2014, the carpet industry in the United States (U.S.) produced 11.7 billion square feet of carpet and rugs. Approximately 3.5% of all waste disposed of in U.S. landfills (4 billion pounds) is carpet discard. Despite the existence of the industry-led Carpet America Recovery Effort (CARE) initiative to responsibly manage carpet waste, an astounding 89% is discarded in a landfill, 6% is incinerated, and less than 5% is recycled. Of the 5% that is recycled, 20% is recycled in a closed-loop, i.e., turned back into carpet, as the rest is down-cycled into less valuable products. That translates to the fact that barely 1% of carpet discards are recycled back into carpet each year (Gaia, 2016). While carpet is benign and accounts for a relatively small amount of total landfill waste, it does represent an opportunity to conserve valuable landfill space. For example, from 20,000 pounds of collected carpet 8,000 pounds of fiber (nylon) and 4,000 pounds of polypropylene (backing) can be recovered. Carpet also represents a form of fossil fuel, and therefore, carpets should be recycled. Not only to conserve landfill space, but also to conserve valuable/non-renewable resources.

It is quite challenging to convince the general public to incorporate recycled and refurbished goods to be a part of our everyday lifestyle. A huge concern with the market is the quality of recycled products that need to be a selling point.

1.4. Carpet Recycling

Tufted carpets are traditionally made of face fibers (Nylon, Polypropylene, and Polyester) that are stitched into a backing material. The face fibers may be cut to create a walking surface. This particular “cut pile” carpeting creates a face fiber that is “U” shaped with the bottom of the “U” in the backing material. The carpet's backing material consists of two polypropylene mesh layers that sandwich a Styrene-Butadiene (SB) latex bonding agent. The topmost layer is considered the primary layer and has the face fiber stitched through it. The secondary layer is the bottom-most layer, which encloses the SB latex bonding agent material. The SB latex bonding agent contains a calcium carbonate filler and binds the two layers and the bottom “U” of the face fibers together (US Patent No. US20140251545 A1, 2014).

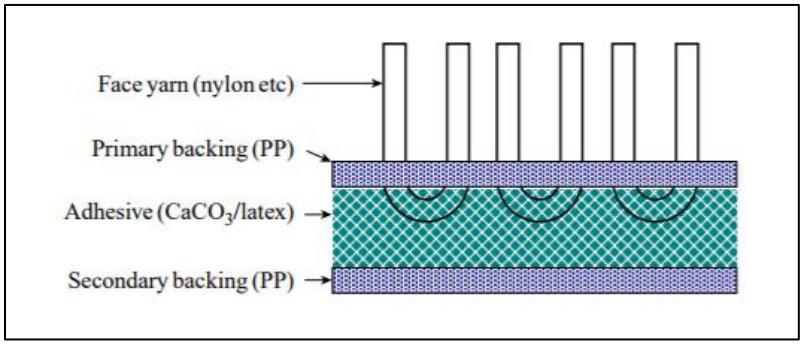

Figure 1. Tufted carpet structure.

The most valued portion of the carpet is called the “face fiber” material, also described as “pile,” which is often polyester or nylon, and usually makes up from about 35 to about 65 weight % of the carpet (US Patent No. US8864057 B2, 2014).

One conventional method for recovering the face fiber material typically involves shearing. It is a method for removing face fiber material analogous to shearing a sheep to remove its fleece. In such cases, the balance is generally discarded. An advantage of this method is that most of the non-face fiber portion (which includes the backing and adhesive) is separated from the face fiber. A disadvantage of the technique is that shearing is quite labor-intensive. Pieces of carpet are

unrolled, cut into appropriately-sized pieces, and manually fed one-by-one into a shearing unit. The carpet that is fed into the shearer must be in the proper orientation – with the face fiber oriented toward the shearing blades, making the sheared fiber susceptible to contamination with the backing material (US Patent No. US8864057 B2, 2014).

Another conventional method of carpet recycling is the complete carpet shredding. The entire carpet is merely shredded into fibers, and a portion of the adhesive (latex or inorganic fillers) are removed as sand or dust. However, this method has a drawback of leaving the backing of polypropylene fibers intermixed with the face fibers. The bottom end of each face fiber (the U-shape) retains a significant portion of the latex and inorganic filler, making this face fiber unsuitable for uses that require a more purified recycled face fiber (US Patent No. US8864057 B2, 2014).

US Patent No. US6752336 B1, (2004), describes a method that uses a carpet feedstock which includes only face fibers having a density higher than 1.0 g/cm^3 (e.g., nylon fibers or polyester fibers) and an olefin fabric backing that includes fibers having a density less than 1.0 g/cm^3 (e.g., polypropylene fibers). The carpet is reduced to size-reduced fibers (i.e., size-reduced face fibers and size-reduced olefin backing fibers). Then, the size-reduced fibers are slurried in an aqueous liquid medium. Finally, the size-reduced fibers are centrifuged to advantageously separate the face fibers from the olefin fabric backing (i.e., the olefin backing fibers).

1.4.1. Carpet Recycling Policies and Legislations

California's Carpet Stewardship Law: California is the first US state to found a private sector designed and managed statewide carpet stewardship program which follows producer responsibility principles. It ensures the discarded carpets are sustainably reused or recycled as carpet has been identified as one of the ten most common waste materials in California landfills.

In 2010, California passed a law, AB 2389, to increase the recycling and diversion of post-consumer carpets in California. The law requires all the carpet manufacturers to include a stewardship assessment fee of $0.50 per square yard carpet sold in the state from July 2011. There is also a penalty for non-compliance with the law (LeBlance, 2017).

Illinois Carpet Stewardship Act: Carpet Stewardship Act in Illinois requires individual producers or stewardship groups to implement and finance a statewide carpet stewardship program that manages the product by lessening the generation of waste by the product. Also, it promotes carpet reuse and recycling. The Illinois Environmental Protection Agency must approve each carpet stewardship plan. Also, the act requires stewardship groups to pay specified administrative fees and submit annual reports to the agency. The bill has been active since January 2015 (LeBlance, 2017).

1.5. Challenges

The current problems of PET carpet recycling can be summarized in two key points:

1.5.1. Economics

First, the economic aspects of PET are a bit different when compared to other popular recyclable materials, nylons, for example. The price of virgin nylon is quite high, which allows this material to be recovered and recycled with a large profit margin. On the other hand, the cost of virgin PET and resulting products are often much lower. Combined with global over-supply and even lower-priced recycled bottle flake, this narrows the possibility of real profitability for recyclers.

1.5.2. Properties

Continuing our comparison, recycled nylon material can be used to create construction materials, automotive parts, and more, while the PET's next life is limited to carpet fiber pads or

felts. There is not a broad breadth of new products that could be created from recycled post-consumer carpet derived PET content (C.A.R.E., 2014). In ensuring no loss in properties, it is crucial to ensure the recycled material is thoroughly cleaned and does not cause issues during re-processing and extrusion. By tackling these issues, I hope to expand this product breadth through my Ph.D. research.

2. Chapter 2: Polyester

2.1. Introduction

World production of polyester fibers and yarns based on polyethylene terephthalate (PET) today exceeds 50 million metric tons. Statistics show the production of polyester fibers worldwide from 1975 to 2017; in 1975, there were 3.37 million metric tons of polyester fibers being produced. By 2017, that number increased to 53.7 million metric tons (Garside, M., 2019). Production of PET textile yarns exceeds the production of staple fiber. It indicates that international practice emphasizes polyester yarns, which is one of the essential types of textile raw material (Geller, 2016).

Polyesters, for our purpose, may be defined as condensation/step-growth polymers that contain ester units as their chain linkage. They are made by a reaction of a dicarboxylic acid with a diol or by self-condensation of ω-hydroxy acid. The earliest known work on polyesters was by W.H. Carothers at DuPont in the late 1920s, where almost all his materials were based on aliphatic molecules (Mark & Whitby, 1940). The polyesters, however, could not be utilized as garments and apparel as they were quickly dissolved in dry-cleaning solvents (East, 2004). This made Carothers turn towards corresponding aliphatic polyamides. They were insoluble in such solvents. Carothers's discovery led to the invention and commercialization of nylon.

During the days of World War II, J.R. Whinfield and J.T. Dickson were working at the Calico Printers Association Laboratories in England, when they synthesized high molecular weight PET from terephthalic acid and purified dimethyl ester by reacting them with ethylene glycol. This new polymer was melt-stable, colorless, and could be melt-spun into fibers. All these properties were desirable. However, the dark times restricted from commercializing the fibers. After the end of the war, the Imperial Chemical Industries (ICI) in Britain developed the PET under the name

Terylene®, while in the USA, DuPont Corporation introduced it as *Dacron*® (London Patent No. 587 079, 1946).

With the commercial success, other manufacturers in Germany and France took the licenses to produce their version of PET fibers. As a result, Whinfield and Dickson's work became a pioneering example. Further on with their experiments, they also were able to synthesize polymers such as poly (tetramethylene terephthalate), poly (trimethylene terephthalate) and other polyesters derived from 1,2-bis (4-carboxyphenoxy) ethane, known merely as 'O-acid.' O-acid is famous as an industrial fiber (East, 2004).

Poly (butylene terephthalate) was also a popular alternative to PET back in the early 1950s. Its properties were more attractive than PET. However, it never achieved the heights of success like PET, due to the high pricing of 1,4-butanediol.

Today, due to rising environmental concerns, one can observe the trend towards awareness of eco-friendly products and practices. Plastics are the most prominent contributors to waste. They pose considerable problems for humanity (Vadicherla, Saravanan, & Muthu, Polyester Recycling—Technologies, Characterisation, and Applications, 2015). The most traditional concept of 3R's comprises of reuse, reduce, and recycle. Recycling is an old concept and has a long history.

Polyesters are examples of condensation polymers. Polyethylene terephthalate (PET) is a typical linear polyester. It is depolymerized, and the terephthalic acid is recovered by the hydrolysis of the ester linkages, using potassium hydroxide in refluxing pentanol.

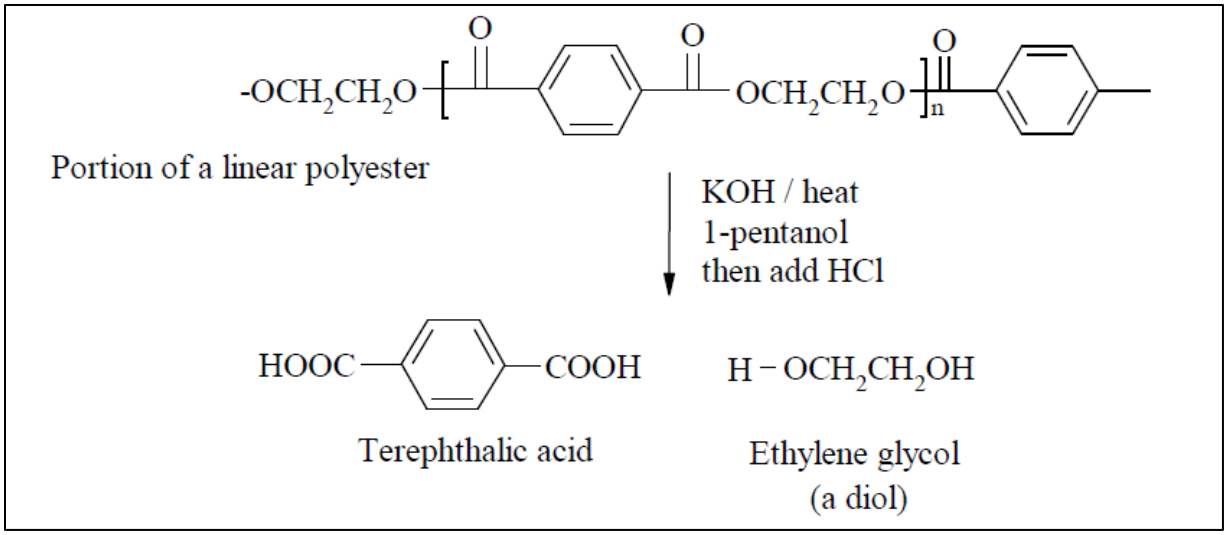

Figure 2. Depolymerization of PET.

In principle, it is entirely possible to use the product to produce other polymers and chemicals. A linear polyester can be prepared as follows:

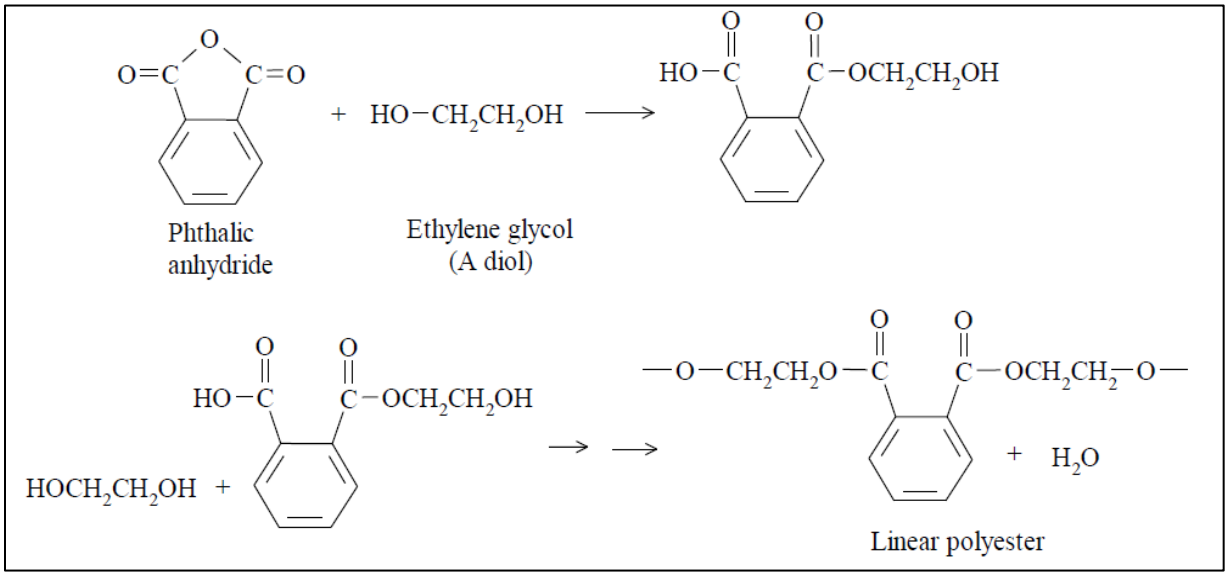

Figure 3. Preparation of PET.

If there are more than two functional groups are present in one of the monomers, the polymer chains cross-link to form a three-dimensional network. Such structures are rigid in comparison to the linear structures. They are also useful in making paints and coatings and are classified as thermosetting plastics (University of Calgary, 2020).

2.2. Raw Materials

2.2.1. Terephthalic Acid

For ease, we will refer to terephthalic acid as TA. TA is a crucial ingredient in many polyesters. Produced from the C-8 aromatic distillate fraction, which is isolated in petroleum refining, the fraction contains ethylbenzene plus three isomeric xylenes (dimethylbenzene). The primary reaction step is the air oxidation of *p-xylene* in an acetic acid solvent, under pressure, with a mixture of transition metal catalysts such as cobalt and manganese acetates, activated by a little bromide anion. An isolation step will give the insoluble crude TA. Crystallization removes impurities that may be present. As crude TA is highly insoluble in water at atmospheric pressure, it is recrystallized from superheated water under high pressure and, at the same time, hydrogenated over a fixed noble metal catalyst. The result after isolation and drying is pure TA of fiber production quality (East, 2004).

2.2.2. Dimethyl Terephthalate

Dimethyl terephthalate (DMT) is a colorless crystalline solid that can be distilled under a very high vacuum and recrystallized (under pressure) from methanol. Before the process of obtaining pure TA was developed, the essential intermediate for PET was DMT. In the early days of manufacturing PET, the *p-xylene* was oxidized with aqueous nitric acid, which gave a product contaminated with many undesirable by-products. These included nitroaromatic compounds and carbazole derivates, all of which were harmful to polymer color and quality. It was simpler to convert the crude TA into its dimethyl ester by esterification under pressure with methanol and an acid catalyst (East, 2004).

2.2.3. Ethylene glycol

The other main PET component is ethylene glycol (EG). EG is manufactured on a commercial scale by a two-stage process from ethylene. The first step is the oxidation of ethylene gas directly with air to ethylene oxide (EO), followed by the ring-opening of EO by reacting it with water (East, 2004).

2.3. DMT Method and Direct Polymerization Method

Typical manufacture methods for PET include the DMT method, which uses dimethyl terephthalate (DMT) and ethylene glycol (EG) as the starting materials and the direct polymerization method (TPA method) to start from terephthalic acid (TPA) and EG. In the beginning, the DMT method was adopted. DMT was popularly used because of its simple refining processes such as distillation and recrystallization compared to TPA, which had no boiling point, poor solubility, and great difficulty in refining (Aoyama & Tanaka, 2016).

However, it can also be said that the DMT method contains an additional process to replace the methanol added to TPA, which is added to facilitate purification, with EG and collect by transesterification during the PET production processes. Because of this, the direct polymerization method became more popular and had become the mainstream today as a technique to manufacture TPA with high purity (called PTA) was developed later.

Manufacture of PET mainly comprises of the transesterification process, which forms the intermediate bis-hydroxyethyl terephthalate (BHT or BHET) from DMT and EG; or the direct esterification reaction (DE reaction) to form BHT from TPA and EG in the first part and the polycondensation reaction to form PET polymer from BHT in the second part. In transesterification reaction, DMT and EG are heated and made into a homogeneous phase in a reaction tank. The reaction is facilitated by the existence of an appropriate catalyst and atmosphere

of normal pressure while removing methanol, which is a reaction by-product. Since DMT has a melting point of approximately 140˚C, reaction uniformity and production efficiency can be improved by melting it in a separate dissolver and supplying it into the EI reaction tank as necessary. However, it can also be injected into the reaction tank as powder or flakes. The factors that affect the EI reaction rate include the reaction temperature, the ratio of charged quantities of DMT and EG (molar ratio), and EI reaction catalysts. Catalysts are especially important as they also have a significant influence on the quality of the polymer that is formed in the end (Aoyama & Tanaka, 2016).

While DE reaction is classified as an esterification reaction between carboxylic acid and alcohol, which are well known, it is somewhat tricky to handle in studies on reaction kinetics as TPA has poor solubility to EG. Thus creative measures are required in industrial processes. As the DE reaction is an autocatalytic reaction in which proton from the acid functions as a catalyst, the reaction continues by mixing and heating TPA and EG together and removing water, which is the reaction by-product. This reaction starts in a mixed system (slurry state) from the beginning until the middle of the process since TPA is poorly soluble in EG, as discussed above. Therefore, how this TPA/EG slurry properties are controlled is one of the most critical points in controlling the DE reaction. Examples of various creative measures in industrial processes to improve the handleability and fluidity of slurry and ES reactivity include optimization of the size and shape of TPA particles as well as mixture ratio with EG and use of BHT instead of EG (Aoyama & Tanaka, 2016).

2.4. Thermal Properties

Depending on its processing and thermal history, PET may exist both as an amorphous (transparent) and as a semi-crystalline (opaque and white) material. In particular, amorphous PET

is of little commercial value since it has poor mechanical properties, low dimensional stability, and high gas permeation ratel; on the other hand, crystalline PET has higher strength, excellent dimensional stability, and chemical resistance. It is widely used in fibers, in beverage containers, and so on. The degree of crystallinity of a polymer is temperature-dependent, and in comparing its effect on material properties, it is vital to carry out experiments at the same temperatures, i.e., at ambient temperatures and not the melting point. There are various analytical methods to determine the crystallinity, and measure thermal properties such as degradation temperatures, glass transition temperatures, and melting temperatures. Differential Scanning Calorimetry (DSC) and Thermogravimetric (TGA) are probably the most widely used techniques. TGA, in conjunction with DSC, can lead to a critical understanding of the true nature of the polymer thermal events. Typically, crystallization, partial melting, annealing, recrystallization, and complete melting can occur during the heating of a sample (Kong & Hay, 2002). Thermal history plays a vital role as the presence or absence of exothermic crystallization peaks in thermoplastic materials is dependent on it. Therefore, DSC results may not be reproducible if the thermal history of the sample is not tightly controlled (Leonard C. Thomas, 2020).

Commercial virgin PET starts to degrade slowly around 380°C before the weight starts to decrease significantly around 400°C. Glass transition temperature can range from 70-78°C. Peak melting begins around 250°C until 260°C, with a degree of crystallinity around 33-35% (Pattabiraman, Sbarski, & Spurling, 2005).

2.5. Molecular Weight

Molecular weight is an essential fundamental property that can influence the mechanical properties as well as forming processability when used as fiber. The average molecular weight for PET used in fiber for clothes is approximately 20,000 (g/mol) with a degree of polymerization

approximately 100 and an intrinsic viscosity [IV] about 0.62–0.65. This value of molecular weight is similar to that of biaxially oriented polyester film used for packaging or general industrial material applications. Compared to this, PET for tire cords and seatbelts that are required to have high strength usually has a molecular weight of 30,000 (degree of polymerization 150 and intrinsic viscosity 0.80) or higher. Furthermore, the PETs used in fiber for clothes typically have the melt viscosity of around 2000 poises (200 Pa-s) at 290˚C, which can be stirred. Thus PET can be manufactured with the specified molecular weight by only melt polymerization. However, PETs of higher molecular weights have an extremely high viscosity, which prevents uniform stirring of melt and continuation of melt polymerization. Therefore, the solid-state polymerization method is used to further increase the molecular weight after melt polymerization (Aoyama & Tanaka, 2016).

2.6. Mechanical Properties

The tensile strength of material becomes essential when the material undergoes stretch or is kept under tension. Tensile testing is one of the most widely used mechanical tests on materials. By measuring the force required to elongate a specimen to breaking point, material properties can be determined that can allow design engineers to predict how materials and products will behave in their intended applications (Westmoreland Mechanical Testing & Research, 2020). Tensile testing provides data on the strength and ductility of materials under uniaxial tensile forces.

To measure the tensile strength of a sample, we simply stretch it in one direction (uniaxial testing). A machine like Instron will have clamps that will hold each end of the sample while stretching it, measuring the amount of force is it exerting (F). We divide this by the cross-sectional area (A). Stress (σ) can be calculated by:

$$\sigma = \frac{F}{A}$$

We continue to increase the amount of force on the sample until it breaks. The stress needed to break the sample is the tensile strength of the material. The units are usually N/m^2. Stress (and strength) can also be measured in megapascals (MPa) or gigapascals (GPa) (How Polymers Work, 2020).

All strength tells us is how much stress is needed to break something; it does not give us much information about what happens to the polymer sample while trying to break it. Elongation comes into play here. It is a type of deformation. Deformation is simply a change in shape in anything that undergoes stress (How Polymers Work, 2020). We talk of percent elongation which is the length of the polymer sample after it is stretched (L), divided by the original length of the sample (L_o), multiplied by 100:

$$\frac{L}{L_o}\ x\ 100 = elongation\ \%$$

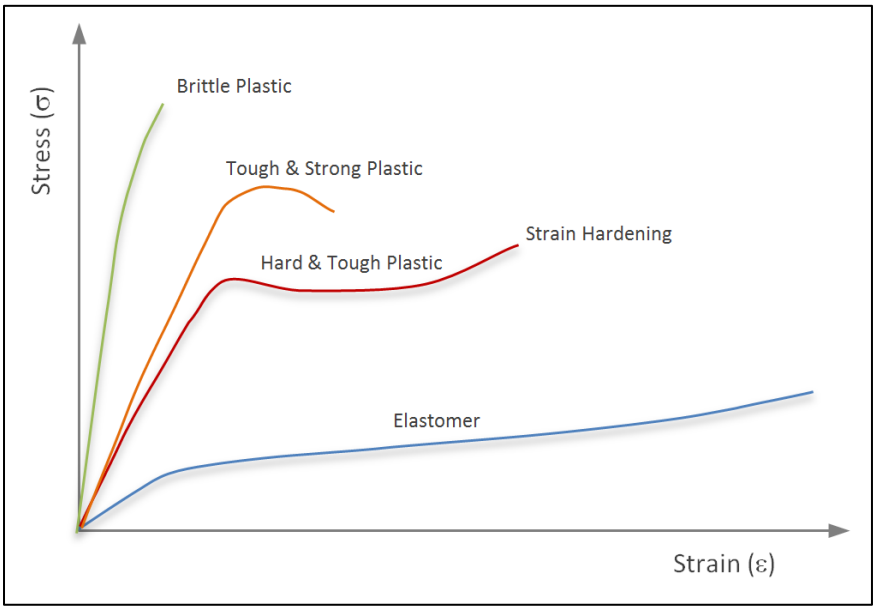

Figure 4. Stress-strain behaviour of polymers.

The mechanical properties of plastic materials depend on both the strain (rate) and temperature. At low strain, the deformation of most solids is elastic; that is, the deformation is

homogenous. After removing the deforming load, the plastic returns to its original size and shape (Polymer Database, 2015). In this regime, the stress (σ) is proportional to the strain (ε):

$$\sigma = E\varepsilon$$

where *E* is the tensile (or Young's) modulus of the plastic and is a measure of the stiffness of the material, this relationship is known as Hooke's law. The maximum stress up to which the stress and strain remain proportional is known as the *proportional limit*. If a plastic material is loaded beyond its elastic limit, it does not return to its original shape and size, or a permanent deformation occurs. With an increase in load, a point is eventually reached at which the material starts to yield. This point is known as the *yield point*. A further increase in strain occurs without an increase in stress. For some polymers, steady stretching with a stress minimum and break at much higher stress is observed. This phenomenon is known as "*strain hardening*" and "*stress-induced crystallization*." It is caused by the orientation and alignment of polymer chains in the direction of the load. This increases the strength and stiffness of the plastic in stretch direction and explains the observed increase in (true) stress. The opposite of strain hardening is *strain softening*. Amorphous polymers, when physically aged, sometimes exhibit true strain softening (Polymer Database, 2015). Flexibles plastics like PET do not resist deformation as well, but they tend not to break. Initial modulus is high, but if enough stress is applied, it will eventually deform (How Polymers Work, 2020).

3. Chapter 3: Polyesters in Nonwovens – Literature Review

The majority of polyester fabrics in use are spunbond, utilizing a continuous filament process which produces a flexible, nonwoven reinforcement fabric. Typically, the polyester fabrics range from 170 to 250 grams/square meter in weight. Lighter weight fabrics are available and in use. The fabrics provide excellent tensile, elongation, and tear strength (Dupuis, Nelson, & Soane, 1991). In the experiments that follow, the polyester filaments will be produced by the process of melt spinning. The next section will discuss this in detail.

3.1. Melt Spinning

Melt spinning is one of the most popular methods for manufacturing polymeric filaments. While there are several methods available for filament production, melt spinning is considered to be the most economical approach due to the absence of solvents and the simplicity of the process. In melt spinning, the polymer pellets or granules are fed into an extruder consisting of a screw for melting using heat, and then the polymer melt is pumped through a spinneret under pressure. The extruded polymer is then quenched with cold air, and the molten mass is solidified into filaments. The spun filaments lack adequate strength for industrial applications. Hence, melt spinning is followed by the mechanical drawing of the extruded filament resulting in the alignment of molecular orientations along the filament axis. This results in improved physical and mechanical characteristics. The mechanical drawing of filaments consists of many fold elongations of the filaments (starting from 2x), which can be achieved directly after spinning or carried out separately with an undrawn extruded polymer as input material. Polymers such as poly(ethylene terephthalate), polyurethanes, polyolefins, and polyamides are melt-spun (Rawal & Mukhopadhyay, 2014).

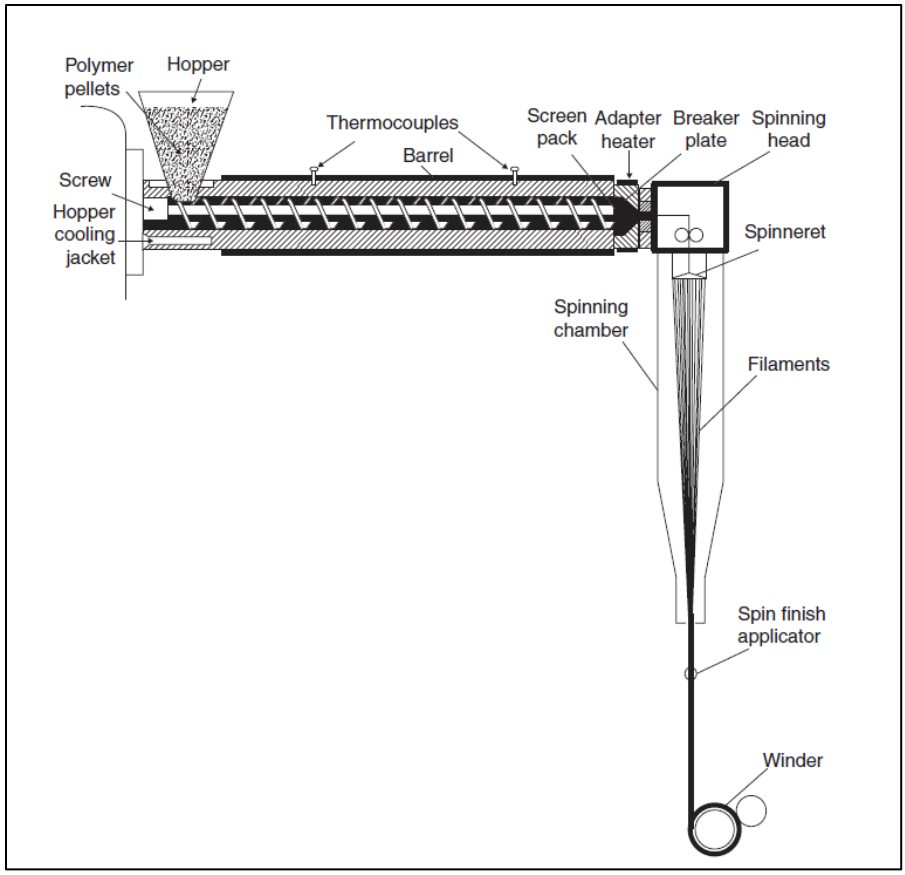

Figure 5. Melt spinning process.

The typical melt spinning process requires a constant mass flow rate of molten polymer, which is maintained by a metering or a spinning pump positioned inside the spinning head. The molten polymer is channeled into some individual capillary holes or slots of defined shapes and sizes present inside the spinneret. Each orifice is responsible for individual filaments. Subsequently, the long continuous filaments extruded through the spinneret orifices are cooled-off, solidified, and collected on a winder (Rawal & Mukhopadhyay, 2014). The take-up speed is kept higher than the average extrusion speed or throughput rate at the spinneret, and the ratio of take-up speed (v_f) to average extrusion speed (v_0) is defined by the draw down ratio (DDR). Hence,

$$\mathrm{DDR} = \frac{v_f}{v_0}$$

Another method that can draw on the properties of two different polymers is the bicomponent fiber extrusion (Mooney, et al., 2018). A bicomponent fiber is defined by the American Society of Testing Materials (ASTM) as a "fiber comprised of two chemically or physically different (or both) polymers" (ASTM Standard, 2003). Bicomponent fibers are typically melt-spun by using two single screw extruders connected to a spinneret block. The spinneret block contains multiple polymer distribution plates, with the end of the block having a die consisting of several holes (the number varies from 20-80) (Hills Inc., 2013; Patent No. EP1241284 A1, 18 Sept. 2002; Hegde, Dahiya, Kamath, Jangala, & Kotra, 2016). Created by DuPont in the mid-1960s, the approach of using a series of plates to guide the flow of the two polymers was not introduced until 1989.

Bicomponent fibers can be made in many configurations, including tipped, side-by-side, micro-denier, and sheath/core (Cooke, Bicomponent Fiber, 1996; Parsons, 2013). The sheath/core configuration is defined as having the core wholly surrounded by the sheath, where the sheath is the smaller multiple cores or channels (Mooney et al., 2018). By employing a lower-melting-temperature polymer in the sheath and a higher-melting-temperature polymer in the core, the fibers can be used in nonwoven webs to thermally bond the webs together without losing the fiber shape or integrity of the binder fiber. This allows more bond points, which improves fabric strength and allows increased line speeds (Textile World, 2010).

3.1.1. Molten state rheology

Rheology is the study of the deformation and flow of matter. This field is dominated by inquiry into flow behaviour complex fluids such as polymers, foods, biological systems, slurries, suspensions, emulsions, pastes, and other compounds. For any processing technology of a

thermoplastic polymeric material (injection molding, calendering, extrusion-blowing, compression molding, spinning, etc.), it is the material flow that defines the suitability of the method considered. Viscosity is the most commonly sought after rheological quantity and is a qualitatively different property for Newtonian and non-Newtonian fluids (Morrison, 2001).

The rheological properties of a polymer depend mainly on chemical structure and molecular weight, as well as temperature. The possible presence of additives and their concentration is also a key parameter relating to the rheological behavior of a polymer (Devaux, 2014). Viscosity η (expressed in Pa.s) for an ideal liquid is independent of the shear rate. During flow, such a fluid follows Newton's law, which expresses the relationship between the shear stress γ and the gradient rate of deformation $\frac{d\gamma}{dt}$.

$$\sigma = \eta \frac{\mathrm{d}\gamma}{\mathrm{d}t}$$

At higher shear rates, three types of deviations are observable when compared to ideal Newtonian flow (Figure 6).

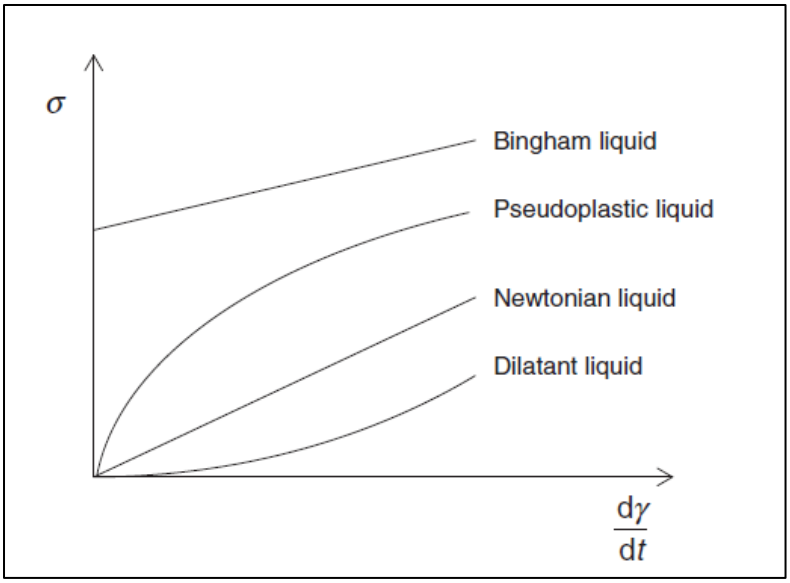

Figure 6. Different kinds of deviations when compared to the Newtonian flow, shown as a function of the shearing rate.

The first kind of deviation relates to the existence of a flow threshold (yield point). Yield is the tendency of a material to flow only when stresses are above threshold stress. This is a non-Newtonian effect—Newtonian fluids will always flow when a stress is applied, no matter how small the stress. For example, honey is a food that has a high viscosity, but it is nonetheless Newtonian (Morrison, 2001). In the case of a Bingham fluid, flow occurs only when the yield stress is exceeded. The second type of deviation is shear thickening, observed where the viscosity increases with shear rate. This is the case for a dilating fluid, behavior which is seldom apparent in polymers. Last, where the viscosity decreases with an increase in shear rate, fluxing is observed, and such fluids are usually referred to as pseudo-plastic fluids. This last phenomenon is a general characteristic of thermoplastic polymers. Flow effects may also be time-dependent. Where viscosity does not depend only on the shear rate, but also on the duration of the applied stress, fluids are thixotropic. Polymers in a molten state thus behave as pseudo-plastic fluids having thixotropic characteristics. Viscoelastic fluids subjected to stress also deform, but when stress is removed, the stress inside the viscoelastic fluid does not instantly vanish. For these types of fluids,

the internal molecular configuration of the fluid can sustain stress for some time. This time, called *relaxation time*, varies widely among materials. Moreover, because a viscoelastic fluid has internal stresses, the fluid will deform on its own even after the external stress has been removed (Morrison, 2001).

In a shear flow with a constant applied shear rate, a shear banding fluid can separate into two and possibly more shear bands, where the local shear rate differs from the applied one. Shear banding occurs when the fluid microstructure cannot stabilize to match the applied shear rate, and instead, the fluid responds by partitioning into shear rates with stable microstructures. The location of the interface between the two shear bands has been shown to scale with the applied shear rate. Even in shear flow, more complex behavior can arise; examples of this include velocity fluctuations in the vorticity direction and fluctuations in the shear rates or wall slip. The stability of the interface between the two shear bands has also shown complex behavior that can manifest in velocity variations along the vorticity direction and in time-dependent flows (Salipante, Little, & Hudson, 2017). At increased mechanical stress, molten plastics are characterized by a decrease in viscosity. This reduction in viscosity can be explained as increasing mechanical stresses gradually destroy the structured organization of the molten polymer.

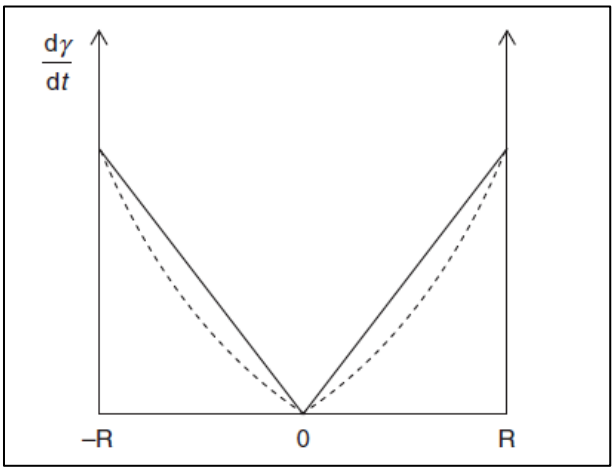

Figure 7. Shearing rate profiles in a spinning capillary.

Polymer viscosity is also affected by several factors, such as temperature, pressure, shear rate, molecular weight, and the presence of additives. Flow occurs in the molten state when the macromolecular chains slip over each other. The ease of this movement depends on the mobility of the polymeric chains, the intermolecular forces, and the sequences ensuring the material cohesion. Most long-chain polymers exhibit fading memory, and it impacts polymer manufacturing processes since trapped stresses (and frozen-in molecular orientation) can weaken or strengthen a part made of polymers (Morrison, 2001).

For a constant shear rate, viscosity decreases with an increase in temperature, and this effect increases with increasing shear rate. In most transformation processes, the flow of polymers in the molten state results from intense shearing; thus, the dependencies of temperature and apparent viscosity have considerable practical importance. Shear-thinning is the result of micro-structural rearrangements occurring in the plane of applied shear. It is observed for dispersions, including emulsions and suspensions, as well as polymer solutions and melts. At low shear rates, materials tend to maintain a random order with a high zero shear viscosity resulting from particle/molecular interactions and the restorative effects of Brownian motion (erratic, random fluctuations/movement of particles suspended in a fluid). At shear rates or stresses high enough to overcome these effects, particles can rearrange or reorganize into string-like layers, polymers can stretch out and align with the flow, aggregated structures can be broken down and droplets deformed from their spherical shape (Malvern Instruments, 2016).

A consequence of these rearrangements is a decrease in molecular/particle interaction and an increase in free space between dispersed components, which both contribute to the significant drop in viscosity. The higher the shear rate, the easier it is to force polymers to flow through dies and process equipment. During single-screw extrusion, shear rates may reach 200 s^{-1} in the screw

channel near the barrel wall, and much higher between the flight tips and the barrel. At the lip of the die, the shear rate can be as high as 1000 s^{-1}. A low shear rate on a die wall implies the slow movement of the polymer melt over the metal surface. At very high shear rates, a flow instability known as melt fracture occurs (Vlachopoulos, 2019).

3.1.2. Polymer behavior during filament spinning

Devaux (2014) mentions several strategies to obtain a melt or a solution with adequate viscosity. For example, it is possible to decrease the molecular weight of the polymer, which appreciably increases the fluidity of the liquid material. However, this reduction in the molecular weight has significant consequences for the final properties of the yarn, and in particular, on its mechanical behavior. The addition of a plasticizer makes it possible to decrease the thermal transitions of the polymer and increase its fluidity. The processing temperature of the polymer is also a relevant parameter in decreasing its viscosity. It must not, however, exceed the thermal degradation limit of the material.

3.1.3. Drawing: changes in morphology and properties

A *drawn fiber* is an industry term used to describe a filament extrusion that has been stretched, pulled, or drawn down post extrusion. This term refers to the characteristic that the fiber has been made thinner as a result of the drawing process; thus, it has been drawn down in size (diameter). In the melt phase, the chains are arranged in a random or disordered state. The extrusion process initiates the orientation of the chains in the extrusion direction. Drawing on the extruded filament further orients the polymer chains in the machine direction resulting in more close packing polymer chains within the fiber structure. The overall effect of the draw-down process is increased polymer chain density and strength. Therefore, drawn fiber typically possesses superior and often preferable mechanical attributes than simple extruded monofilament (Bigham, 2018). At

the die exit, and particularly in the case of melt spinning, the polymer is at a higher temperature than its melting point. Simultaneous with the swelling phenomenon at the die exit, the material is gradually brought back to room temperature. As the temperature decreases, the apparent viscosity of the polymer increases. Under the action of the tensile force, the polymer flow is refined, and the filament diameter decreases until reaching its final value. This deformation occurs between the die and a point where the material reaches its glass transition temperature T_g, i.e., between a liquid and a rubbery state. Below this critical temperature, the polymer reaches a glassy state where it is comparable to a non-deformable material (Devaux, 2014).

Between the molten state and the end of the rubbery state, the polymeric filament undergoes a very strong tension, which compensates (at least partially) the Barus effect. The following relation defines the Barus effect:

$$B = \frac{D}{D_0}$$

where D represents the diameter of the extrudate and D_0 the diameter of the die. This ratio of swelling B lies between 1 and 4 but can reach much higher values in the case of polymer alloys. The flow rate in the capillary is another parameter which conditions swelling at the exit of the die. The Barus number increases with the shear rate γ up to a breaking value, at which point certain flow defects appear. At this breaking value of γ, B passes through a maximum and then sharply decreases. This threshold, often called the 'rupture of melting,' can be characterized by small irregularities on the extrude at the surface (roughness, shark skin), by corrugated or helicoidal deformations, or by periodic deformations or breakage. This critical phenomenon was first observed by Barusin in 1893 but was more correctly analyzed by Merrington in 1943 (Merrington, 1943).

The drawing ratio lies between 2 and 4. This ratio can go up to 6 in the case of a few high-performance fibers. Drawing is accompanied by a self-heating phenomenon, which can cause a temperature rise beyond the glass transition temperature without external heating of the yarn (in particular for polyamide 6,6). The phenomenon of striction also occurs, which is fixed and located on a metallic part of the drawing device. The identification of the striction point should not be confused with the appearance of a constriction point obtained during the cold drawing of a static specimen. In a dynamic industrial drawing, the striction point is imposed by a mechanical device, which constitutes the point of application of the drawing force where the temperature of the yarn reaches the glass transition temperature. The modulus decreases sharply, and the striction occurs. The macromolecular orientation and the crystallization which occurs during drawing, are still insufficient to lower the thermal contraction sufficiently. A supplement to crystallization is obtained through heat treatment, possibly accompanied by relaxation, which is carried out on the drawing device itself. This results in the disorientation of the amorphous phases. The macromolecules tend to return to the shapes of disorientated balls, which are thermodynamically more stable. This complementary heat treatment is typically carried out between 130°C and 180°C for polyethylene terephthalate (Devaux, 2014).

3.2. Melt Blowing Process

Melt blown materials are nonwoven textiles made by a process in which the web is prepared as the fibers are being formed from a molten pellet/resin. It is an integrated, one-step nonwoven process beginning with a polymer resin and ending with a finished, self-bonded fabric. The process may be similar to the spunbonded process, but melt blown filaments are much finer.

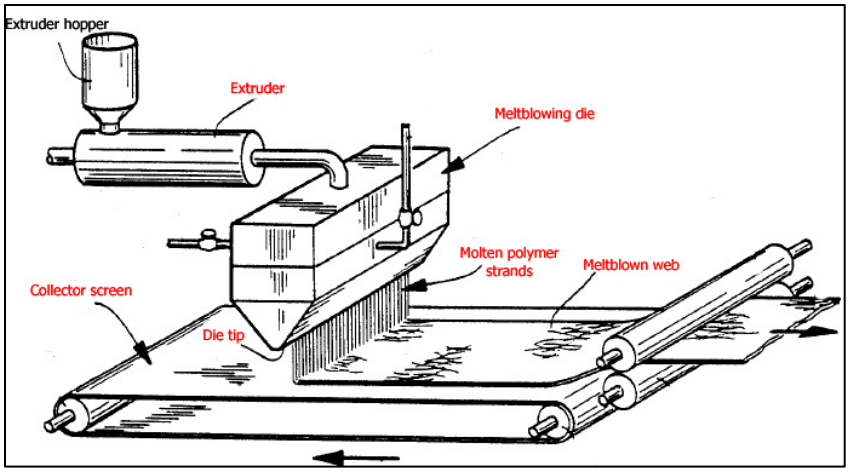

Figure 8. Meltblowing process.

3.2.1. History of Meltblown Technology

The melt-blown technology was first demonstrated in the mid-1950s by the Naval Research Laboratories. They were intent on developing extremely fine denier fiber for use in high altitude atmospheric research. Conceptually, this process was very similar to a 1940's Owens-Corning development of producing micro denier fiberglass. In the Owens-Corning process, glass fibers of 1 mm diameter were melt-drawn by a jet flame to a diameter of 0.5 microns. The line was semi-commercial but used primarily by ExxonMobil to further research and develop the melt-blown technology. It was ExxonMobil's decision not to commercialize the technology, but instead, license the process to other companies (Butler, 1999). The average melt blown line produces filaments in the 2-5 micron range. The web's uniformity and micro-porous nature make this technology attractive for a variety of end products. Melt blown fabrics' first significant commercial successes were monolithic filtration media, sorbents, and battery separator materials. There has been a considerable success with melt-blown laminates and composites. Kimberly-Clark, an early licensee, contributed many innovations to the technology with their development of the spunbonded/melt-blown and other melt-blown composite technologies (Butler, 1999).

Table 2. Major market and Product Examples for Meltblown Fabrics.

Filtration	Medical	Sorbents & Wipes	Hygiene	Industrial	Other
Air	Surgical gowns	Household wipes	Feminine hygiene products	Protective apparel	**Electronics**
Clean rooms	Surgical face masks	Industrial clean up wipes	Diapers (cover stock, waist and leg reinforcement)	Face masks	Battery separators
Heating	Surgical drapes	Oil clean up (oil booms)	Incontinence products		Cable wraps
Ventilation		Food fat absorption			**Adhesives**
Air conditioning (HVAC)					Hot-melt adhesives
Face masks					**Insulators**
Respirators					Apparel thermal insulator (3M Thinsulate®)
Gas masks					Acoustic insulation (appliances, automotive)
Vacuum cleaner					
Room air cleaners					
Liquid					
Water					
Food & beverage					
Chemicals & solvents					
Blood					

3.2.2. Production Process

In general, the meltblown process comprises five major components – the extruder, metering pump, die assembly, web formation, and winding (Dutton, 2008).

The polymer resin is fed into the extruder. It is then heated and melted until the appropriate temperature and viscosity are reached. The molten polymer is further fed to the metering pump, which ensures uniform polymer feed to the die assembly. The microfibers are formed when the molten polymer exiting the die is hit with hot, high-velocity air. The microfibers are collected on a moving screen (or a drum), where the self-bonded web is formed. A moving screen is used in a vertical setup, and a drum is used in a horizontal set up. The web is then wound up and prepared for finishing if required (Dutton, 2008).

3.2.2.1. Extruder

The extruder is similar to the ones used in the melt spinning, as well as the spunbonding process. It is a heated barrel with a rotating screw that is responsible for melting as well as feeding the polymer to the metering pump. The polymer, typically in the form of resins, chips or granules, is gravity fed from the hopper into the extruder. The polymer may be mixed with additives to improve web performance as well (Dutton, 2008). The extruder has three different zones, which are the feed zone, the transition zone, and the metering zone. The polymer mixture is preheated in the feed zone. The melted polymer is then pushed forward to the transition zone, where it is compressed and homogenized. Finally, the polymer is taken to the metering zone, where the polymer pressure is highest, to push polymer to the metering pump (Malkan & Wadsworth, 1993). A filter near the end of the screw extruder helps control the pressure, remove dirt, foreign and metal particles, and polymer lumps.

3.2.2.2. Metering Pump

A metering pump, also known as the gear pump, helps to maintain the required pressure in the extruder. This ensures that the molten polymer is delivered uniformly and consistently to the die assembly under various process variations (Dutton, 2008).

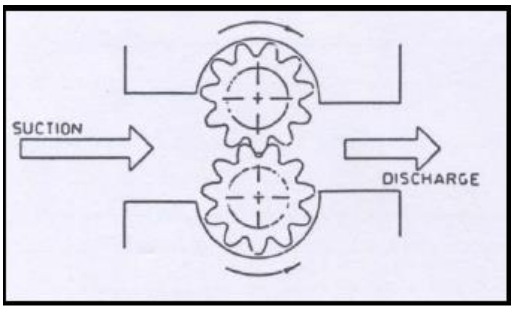

Figure 9. Schematic of a metering pump.

3.2.2.3. Die Assembly

The extruder and the metering pump are similar to the spunbond system, but the die assembly is entirely different. It is responsible for the production of quality and fine fibers. The die assembly consists of three components, which are 1) the polymer feed distribution plate, 2) the die nosepiece and, 3) the air manifolds. All of them are kept at a temperature of 215°C to 340°C (and also depends on the polymer type).

The feed distribution plates help create an even polymer flow across the place. The shape of the feed distribution is also crucial as it influences the distribution of the polymer. The die nosepiece, or die tip, is the critical component and mostly responsible for fiber diameter and quality, uniform webs. Hence, the design and fabrication of the die tip is critical and requires precise measurement. The air manifold is responsible for supplying the high-velocity air, known as primary air. This attenuates or draws, the polymer to form microfibers. Generally, the manifold is located on the sides of the die tip and hits the polymer with hot, high-velocity air as it exits the tip (Dutton, 2008).

3.2.2.4. Process Variables

The meltblown process appears simple; however, the number of variables and the interaction among the process variables make the process very complicated. The process consists of two types of variables: operational, or machine variables, and materials variables. Operational variables are also referred to as machine variables or parameters, including on-line and off-line variables. On-line parameters can be adjusted while the machine is in operation while off-line parameters can only be fixed when the machine is not operating (Dutton, 2008).

Table 3. Operational Variables.

On-line Variables	Off-line Variables
Polymer throughput rate	Die hole size
Air throughput rate	Die set-back
Polymer Temperatures	Air gap
Die temperatures	Air angle
Air temperature	Web collection type
Die-to-collector distance	Polymer/air distribution

The option of using a variety of polymers and polymer blends is an advantage of the meltblown process. A low molecular weight polymer is desired in the process. It indicates a low melt viscosity, or high melt flow index (MFI), which produces a more uniform web. Using a higher MFI and low operating temperature increases the throughput rate and decreases manufacturing costs (Malkan & Wadsworth, 1993).

Table 4. Material Variables.

Material Variables
Polymer type
Molecular weight
Molecular-weight distribution
Melt flow rate (MFR)/Melt flow index (MFI)
Melt viscosity
Polymer additives
Polymer degradation
Polymer forms (pellets, granules, chips)

3.2.2.5. Web Formation and Characteristics

Uniformity is essential in web characteristics, which is affected by the uniformity of fiber distribution in the air stream and the vacuum levels. The melt-blown process creates a web with a wide range of characteristics, as seen below.

Table 5. Meltblown web characteristics.

Web Characteristics	
Smooth surface texture	Low to moderate web strength
Favorable hand and drape	Highly opaque web (high cover factor)
Low abrasion resistance	Random fiber orientation
High surface area (good filtration, insulation, & absorption)	Wide range of fiber diameter
	Difficulty distinguishing fiber length (sometimes considered continuous)

Three significant defects can develop during production – shots, roping, and fly. A shot is a small, round clump of polymer in the web that can be caused by excessively high temperatures, low molecular weight polymer, or inadequate equipment hygiene (Gahan & Zguris, 2000). Roping is a long, thick "streak" of polymer in the web caused by turbulence in the airstream or fiber movement during and after lay down (Vargas, 1993). Fly is a collection of very short, fine fibers that do not collect on the screen, or drum. However, they contaminate the surroundings. Extreme and excessive blowing conditions cause it. A fourth defect is known as fiber splitting, branching, or bundling. Fiber branching typically occurs when fibers collide in the air stream near the die tip and fragment the filaments (Dutton, 2008).

3.3. Spunbond Process

Spun bond nonwoven fabrics are made of continuous filaments produced by an integrated fiber spinning, web formation, and bonding process. As it eliminates some intermediate steps, it is the shortest textile route from polymer to fabrics in one stage, providing opportunities for increased production and reduction of cost (Midha & Dakuri, 2017). The spunbonded technology, developed only in the mid-1960s, has emerged as the most crucial nonwoven technology. It has some advantages, not the least being the fabric's durability and lower cost in comparison to other nonwovens and conventional woven and knitted fabrics. Spunbonded fabrics are found in many disposable markets, such as diapers, sanitary napkins, and medical. Major durable end markets include bedding and home furnishings, agriculture, carpeting, and house construction (Butler, 1999).

3.3.1. History of Spunbond Technology

The early spunbonded systems were massive, expensive, and required a large amount of energy to operate. Because of the high capital costs and associated technical risks, only a few larger companies had the resources to develop the technology. From a global perspective, spunbonded has grown to be the dominant nonwoven technology and is amongst the fastest growing nonwoven technologies (Butler, 1999). The combination of lower manufacturing costs and products with superior strength and good web uniformity relative to alternatives gave this technology a significant competitive edge in many markets.

The largest producing regions of spunbonded materials are North America, Europe, and Japan. Together these regions produce and consume about 80% of the world's spunbonded materials. The increasing demand by absorbent (cover stock), disposable medical, home furnishing, and bedding industries in these markets is a driving force for spunbonded material

growth. The growth rates vary by region, depending upon the level of development of the nonwovens industry in the various countries. The emerging markets include Mexico, South America, China, Southern Africa, India, and other Pacific Rim. By far, most spunbonded materials produced in these markets are made from polypropylene resin (Butler, 1999).

3.3.2. Production Process

In the traditional manufacturing of spunbonded materials, a polymer is heated until the viscosity is appropriate for extruding the material (through a spinning process). Air is introduced to allow cooling of molten filaments. At the same time, the filaments are drawn to the specified diameter. The cooled loose filaments are deposited onto a moving conveyor and transported to a bonding device. The web of loose filaments can be thermally, mechanically, or chemically bonded. The integrated technology of producing fiber and textiles in one process is the most economical method of making fabric. Figure 10 is a simplified drawing of the spunbonded process (Butler, 1999):

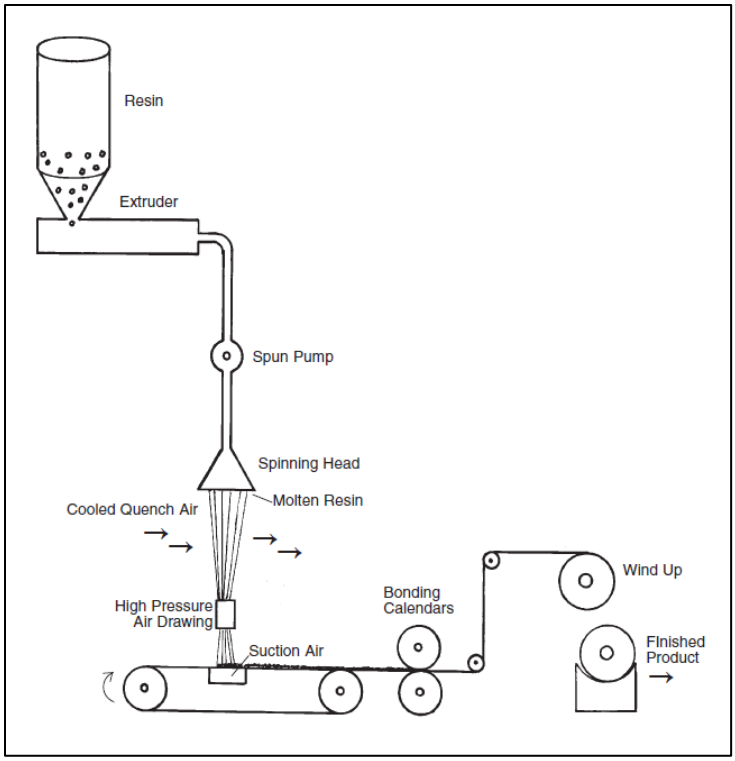

Figure 10. Spunbond Line.

The production process involves four simultaneous and integrated operations viz. filament spinning, drawing, lay down, and bonding. The first three operations are directly adopted from conventional fiber spinning. Melt spinning is most widely used because of its simplicity and economics. The primary function of this system is to solidify, draw, and deposit the extruded filaments onto a conveyor belt. The last operation is web consolidation, whereby strength is provided to the web through various mechanical, chemical, or thermal bonding methods. The following figure shows the various steps involved in the spun bonding process (Midha & Dakuri, 2017; Bhat & Kotra, 2008).

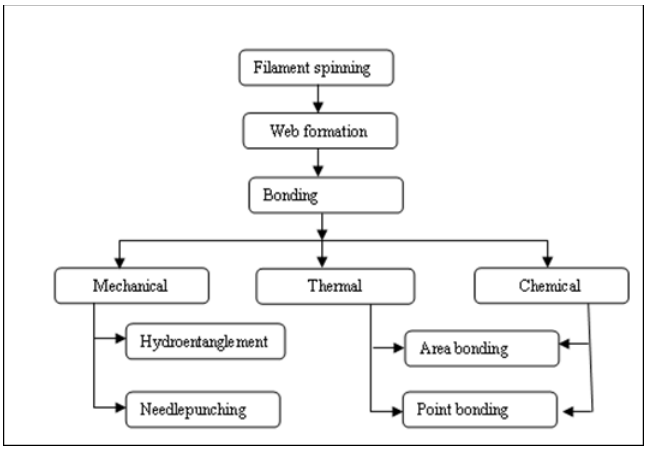

Figure 11. Steps in a spunbond process.

The key components of the spun bonding line are an extruder, filter, metering pump, spinning block, quenching, drawing, web forming, bonding, and winding. The barrel, screw, and the channel comprise the extruder. The screw helps to guide the molten melt homogeneously into the gear pump through filters. Different kinds of screws are available, but the single screw is commonly used. Twin-screw extruder shows excellent mixing capabilities for polymer additives and offers plant flexibility. There is a minimal amount of polymer in the barrel, and hence, it is easy to change the line from one polymer to another. The typical operation spinning speed is 4700-5000 m/min for polyester (Bhat & Kotra, 2008).

Filtration of the polymer melt is vital for high-quality filaments and fabrics besides a continuous and trouble-free production. The selection of the filter must be such that it does not damage the melt or interrupt the melt flow. The polymer melt is gradually driven into the spinning block with the help of a metering pump. For bicomponent fibers, two independently driven metering pumps are used (Kunze, 1998).

The spinning block consists of a spin block body, spin pack, and spinneret. The spinneret is a single block of metal having thousands of drilled orifices on it. Several spinnerets are placed side by side to produce the broader webs—design of spinneret influences web quality. The emitted

filaments solidify on being subjected to cool air. Crossflow or inflow systems are used to supply conditioned air to the filaments. Simple quench air box, multi-zone quench airbox, and quench airbox for air-conditioned zones are used as quench systems. Reifenhauser Reicofil spun bonding uses a low-pressure air system for processing polypropylene, polyethylene, polyester, and polyamides (Kunze, 1998).

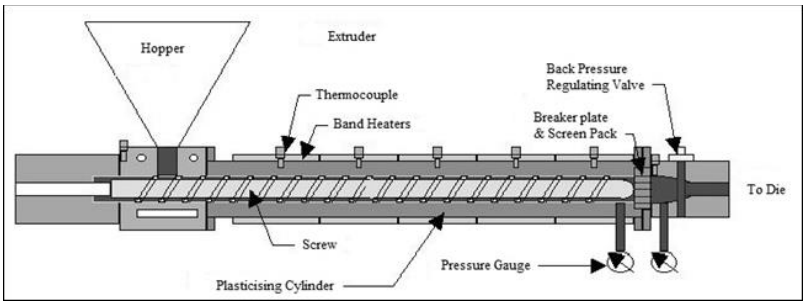

Figure 12. Extruder.

Several bonding methods, like thermal, chemical/adhesive, needling, and hydroentanglement, available for staple fiber fabrics, have been successfully adapted for continuous filaments. Higher production rates and flexibility have increased the use of needle-punched fabrics, particularly in geotextiles. Thermal bonding is common and more economical than chemical bonding (Midha & Kothari, 2004). Depending on the end-use, a variety of finishes such as embossing, resin treatment, flame retardancy, dyeing, and antistatic finishes can be applied to the bonded fabric (Lim, 2010).

Although all types of polymer can be used in the spun bonding process, polymers with high molecular weight and high molecular weight distribution like polypropylene, polyester, polyamides are commonly used for the production of spun-bond fabrics. Polyester (PET) is used in some commercial spun-bond products and offers certain advantages over polypropylene. Unlike polypropylene, polyester scrap is not readily recycled in spun-bond manufacturing. Tensile strength, modulus, and heat stability of polyester fabrics are superior to those of polypropylene

fabrics. Polyester fabrics are easily dyed and printed with conventional equipment. However, polyester fibers have lagged in their popularity due to economics and processing concerns. Polyester fibers are extruded at a relatively higher temperature, and the resin should be dry before melting and extrusion (Bhat & Kotra, 2008).

3.3.3. Polyester in Spunbond

Polyester spunbonded materials have higher strength relative to spunbonded polypropylene. However, it is more energy-intensive than polypropylene due to a higher melting point. Spunbonded polyester's higher melting point and moldable properties make this material attractive to the carpet backing, roofing substrate, and specific filtration end-use where heat is involved. Polyester is also insensitive to many acids, salts, and other corrosive materials.

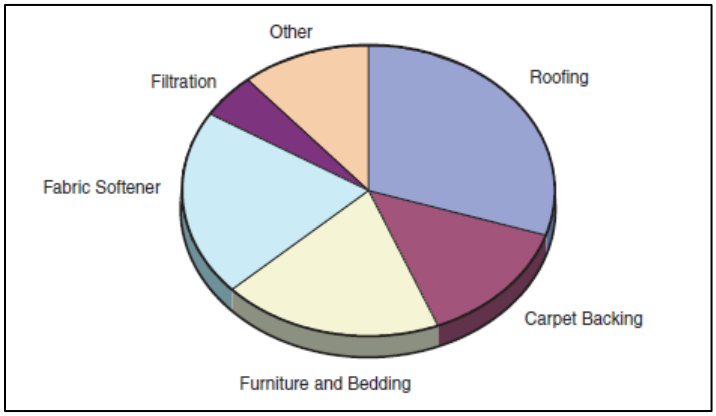

Figure 13. Spunbond PET by end-use.

Several manufacturers produce spunbonded fabrics from bicomponent fibers. Bicomponent fibers are used to combine the strong attributes of each polymer or improve the web's strength. In the spunbonded process, bicomponent fibers will usually have a polyester core with an outer sheath of some other polymer. The sheath is a lower melting point resin-like nylon 6 or polyethylene. The web is bonded by calendaring or heating to soften the sheath, which fuses the web's filaments at the cross-over points. Spunbonded webs using a polyester/ nylon 6 bicomponent

are isotropic, moldable, and have excellent dimensional stability. Spunbonded with a polyethylene sheath, they are soft and drapable and resistant to many acids and alkalis.

3.3.4. Influence of Properties

There are several factors that influence the physical and aesthetic properties of a spunbonded material (Butler, 1999). The significant variables that affect the physical properties of a spunbonded web are:

- type of resin or polymer used
- filament variables: thickness or diameter, crimp, fiber cross-section, filament drawing system
- bonding method: needle punched, the degree of point bonding or addition of a bonding resin or binder fibers
- web properties: fiber orientation, web uniformity

3.3.4.1. Resin Types

Polypropylene (PP) is the dominant resin accounting for two-thirds of total spunbonded products. PP is also the fastest-growing polymer because of its wide acceptance in several applications, e.g., absorbent products' cover stock, medical, and several durable end markets, which are growing faster than the industry.

Polyester and polyester bicomponent are the second most important resins with about a quarter of spunbonded production. The growth of polyester spunbonded production has been lower than polypropylene as most of these materials are sold to durable end markets where polyester has already captured a significant market share. The consumption of spunbonded polyester and polyester bicomponent is expected to rise by about 6% annually over the next several years.

3.3.4.2. Filament Variables

Denier is a unit of measurement that is used to determine the fiber thickness of individual threads or filaments. Fabrics with a high denier count tend to be thick, sturdy, and durable, while fabrics with a low denier count tend to be sheer, soft, and silky (Standard Textiles, 2020). Coarse denier (10-15 denier) spunbonded fabrics are often stiff and rough feeling and are generally produced for durable end markets. In contrast, spunbonded web of fine denier (1.5-3 denier) filaments will have higher web uniformity, softer hand, and draping qualities. Most fine denier spunbonded fabrics are found in consumer and disposable products, such as cover stock, fabric softener substrate, and apparel items.

3.3.4.3. Bonding Variables

Point bond calendaring is one of the most common methods for bonding spunbonded webs. The filaments in the web are fused by heat and pressure at all points where the calendar meets the web. The ratio of the bonded area to the unbonded area affects many of the web's physical properties, e.g., higher the ratio, stiffer the finished fabric. Needle punching a spunbonded web yields a higher strength fabric that resists distortion.

3.3.4.4. Web Properties

The distribution of individual filaments in a finished web is a critical parameter to determine the physical and performance characteristics of spunbonded materials. Non-uniform filament distribution, bundled fibers, and filament separation are factors that will negatively affect the fabric's performance and aesthetic qualities.

3.4. Challenges with PET (plastics)

Plastics have become quite prevalent in today's society. There are numerous disposal problems such as health hazards, littering problems, fire hazards, and energy shortages associated with the manufacture and usage of polyesters/plastics (University of Calgary, 2020).

3.4.1. Plasticizers and Health Hazards

Certain types of plastics, like polyvinyl chloride (PVC), when mixed with plasticizers, helps to soften the plastic so that it is more pliable. Some of the plasticizers used in vinyl plastics are phthalate esters. These esters are volatile compounds of low molecular weight. Phthalate esters may constitute a health hazard. Sometimes vinyl containers, which incorporate phthalate plasticizers, are used to store blood. The esters are leached from blood bags made of PVC, and they may be partly responsible for shock lung (a condition that sometimes leads to death during a blood transfusion). The long-term effects of these plasticizers are, however, not well-known. Other types of plasticizers that were once used were polychlorinated biphenyls (PCB) (University of Calgary, 2020).

3.4.2. Disposal Issues

One of the most common approaches is to bury the garbage in landfills. However, as we run out of places to bury, incineration appears to be an attractive method for solving the solid waste problem. It is estimated that about 64,000,000,000 kg of plastics are discarded per year in the United States: over 270 kg per person. About 80% of this plastic ends up in landfill sites; plastics account for about 25% of the volume of landfill refuse. One possible solution to reduce landfill waste is to combust the plastics which burn readily. The new high-temperature incinerators are efficient and can be operated with a minimum amount of air pollution. It could be possible to burn

our garbage, generate electrical power from it, albeit with the production of carbon dioxide, a critical greenhouse gas (University of Calgary, 2020).

We should either recycle all our effluent waste or not produce it at all. The plastic waste consists of nearly 55% Polyethylene (PE) and PP, 20% Polystyrene (PS), and 11% PVC. All these polymers are thermoplastics that can be recycled. They can be softened and remolded into new products. Unfortunately, thermosetting plastics or cross-linked polymers, cannot be remelted since they degrade and decompose at high temperatures. It is therefore advised to avoid using thermosetting plastics for 'disposable' purposes. Alternative techniques to simple reforming are de-polymerization, which allows us to recover the monomers for purification and potential re-polymerization (University of Calgary, 2020).

3.4.3. Littering

Plastics will not corrode or rust, if well-made, and they last almost indefinitely. Unfortunately, these desirable properties also pose a problem when plastics are buried in a landfill or thrown on the landscape. They do not decompose (University of Calgary, 2020).

3.4.4. Fire Hazards and Energy Shortage

Injuries are not uncommon or unheard of clothing made of polymers, in particular, children's clothing. Many of these organic fibers readily burn. To tackle this problem, chemists have developed flame-retardant fabrics. Toxic gasses are liberated when plastics burn. One example could be of hydrogen chloride generation when PVC is burned, and hydrogen cyanide when polyacrylonitriles are burned (University of Calgary, 2020).

The demand for renewable, clean energy has increased at an alarming rate and also led to an energy crisis. The production process of polymers requires petroleum as a raw material as well as a source of energy to conduct manufacturing. Now, fossil fuels are a non-renewable resource,

so as their availability decreases, we have a more significant problem. Natural substances, such as cotton, are renewable resources; perhaps for specific applications, they would be better and less costly than the synthesized polymers (University of Calgary, 2020).

With this project, we divided the research into a three-fold approach, trying to answer our research questions of:

i) *What:* Identify the challenges and shortcomings of the recycled material for fiber extrusion

ii) *Why:* Determine the cause for failure in fiber formation and establish limits for impurities

iii) *How:* Optimization of material and process parameters

In the next few chapters, we shall discuss in detail the experimental work conducted in answering these questions.

4. Chapter 4: Experimental Part 1 – Thermal Characterization

4.1. Materials

A total of 7 different grades of recycled PET materials have been studied. They were recycled PET grade 1 resins (/pellets), supplied by Wellman as well as commercial virgin PET from Eastman and Indorama Ventures. The recycled PET grade 1 contained 15-20% impurities in the form of PP and $CaCO_3$ (or industrially referred to as *ash*). Circular Polymers supplied the recycled PET grade 2 and 4 resins; grade 2 contained 5-6% of ash and ~20% of PP, while grade 4 contained 2-3% ash, 12% PP in the form of impurities and ~22% PTT (Polytrimethylene terephthalate) discovered during FTIR testing. The recycled PET grade 3 resins were supplied by Avanti Environmental Group, which comprised 2% ash and 2% PP. Recycled PET grade 5 resins were supplied by Bro-Tex Inc., which contained a negligible amount of ash and PP. Recycled PET grades 6 and 7 were supplied by California suppliers, and pelletized by Poly Quest; grade 6 had 5% ash and 3-5% PP, while grade 7 had 3% ash and 3% PP.

4.2. Methods

Thermogravimetric analysis (TGA) and Differential Scanning Calorimetry (DSC) are two favored thermal analysis techniques. TGA measures the mass changes of a sample with a simultaneous increase in temperature in a controlled atmosphere. In DSC, the polymer pellet sample is placed in an aluminum pan and run versus an empty reference pan. The subsequent heat flow curve obtained during heating is analyzed to obtain transition temperature and quantitative heats involved in the reactions.

4.2.1. Thermogravimetric Analysis (TGA)

Results are recorded as weight loss – time (for isothermal analysis) or mass loss temperature (for analysis made with a constant heating speed). The instrument used for

Thermogravimetric analysis was Discovery series TGA, the melting crucible was made of platinum, with the temperature range of 25-800°C, flowing 20cc/minute nitrogen atmosphere and the heating speed was of 20°C/min.

4.2.2. Differential Scanning Calorimetry (DSC)

The instrument used for Differential Scanning Calorimetry was Discover Series DSC. In this study, polymers at temperatures between 300°C and 350°C were evaluated while heating at 10°C/minute in a flowing 50cc/minute nitrogen atmosphere. The polymers were also equilibrated at 25°C.

4.3. Results and Discussion

The thermal properties of the Recycled PET pellets, such as the crystallization temperature (T_c), melting temperature (T_m), enthalpy of crystallization (ΔH_c), enthalpy of melting (ΔH_m), and enthalpy of cold-crystallization temperature (ΔT_{cc}) were calculated from the DSC curves. The degradation temperature was noted from the TGA results. The percentage of apparent crystallinity (X_c) was calculated using the equation below:

$$X_c\% = \left(\frac{\Delta H_m - \Delta H_{cc}}{\Delta H_m^0}\right) x\ 100$$

where ΔH_m^0 is the heat of fusion of a 100% crystalline PET sample and has a value of 140 J/g.

Table 6. Results of thermal analysis for PET polymer samples.

Polymer	**Onset T_d (°C)**	**Residue at 800 °C**	**T_m (°C)**
Eastman PET F61	378 °C	14.6%	252
Indorama PET Un-crystallized	370 °C	14.32%	258
Indorama Primary Crystallized	378 °C	12.3%	257
Indorama Secondary Crystallized	389 °C	13.34%	258
Rec PET grade 1	318 °C	15.5%	252
Rec PET grade 2	353 °C	15.62%	252
Rec PET grade 3	383 °C	4.79%	252
Rec PET grade 4	377 °C	5.26%	246
Rec PET grade 5	386 °C	13.88%	249
Rec PET grade 6	374 °C	17.19%	252
Rec PET grade 7	381 °C	17.69%	251

The TGA and DSC tests concluded that there was a certain extent of molecular degradation, which lowered the degradation temperature of Rec PET grade 1 to 318°C. The molecular degradation can be accounted to thermal changes in the previous processing of the polymer. All other grades of Rec PET had thermal properties similar to commercial virgin PETs, with the lowest amount of residue present in Rec PET grade 3 and 4.

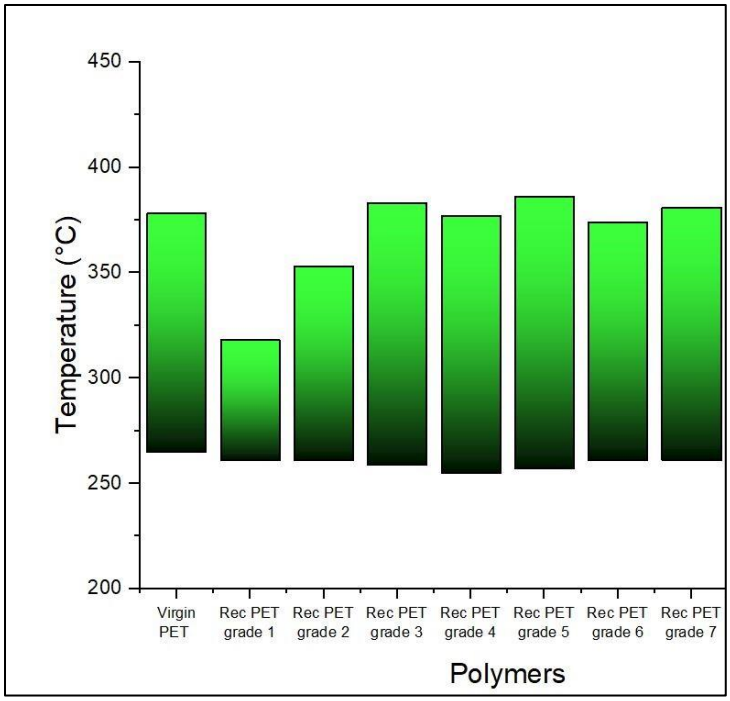

Figure 14. Processing window temperature range for PET polymers.

With the degradation temperature (obtained from TGA) and end-melting temperature (obtained from DSC), we were able to note down the operating range for each polymer. It indicates the temperature ranges, which shall be optimum for processing for multi-filament spinning or melt-blowing of webs. The typical processing temperature for multi-filament spinning is 280-300°C, while the melt-blowing of PET webs typically occurs at 315°C.

As seen in figure 14, even though Rec PET grade 1 has a narrow processing range, compared to the other grades, it was still within the processing temperature for multi-filament spinning.

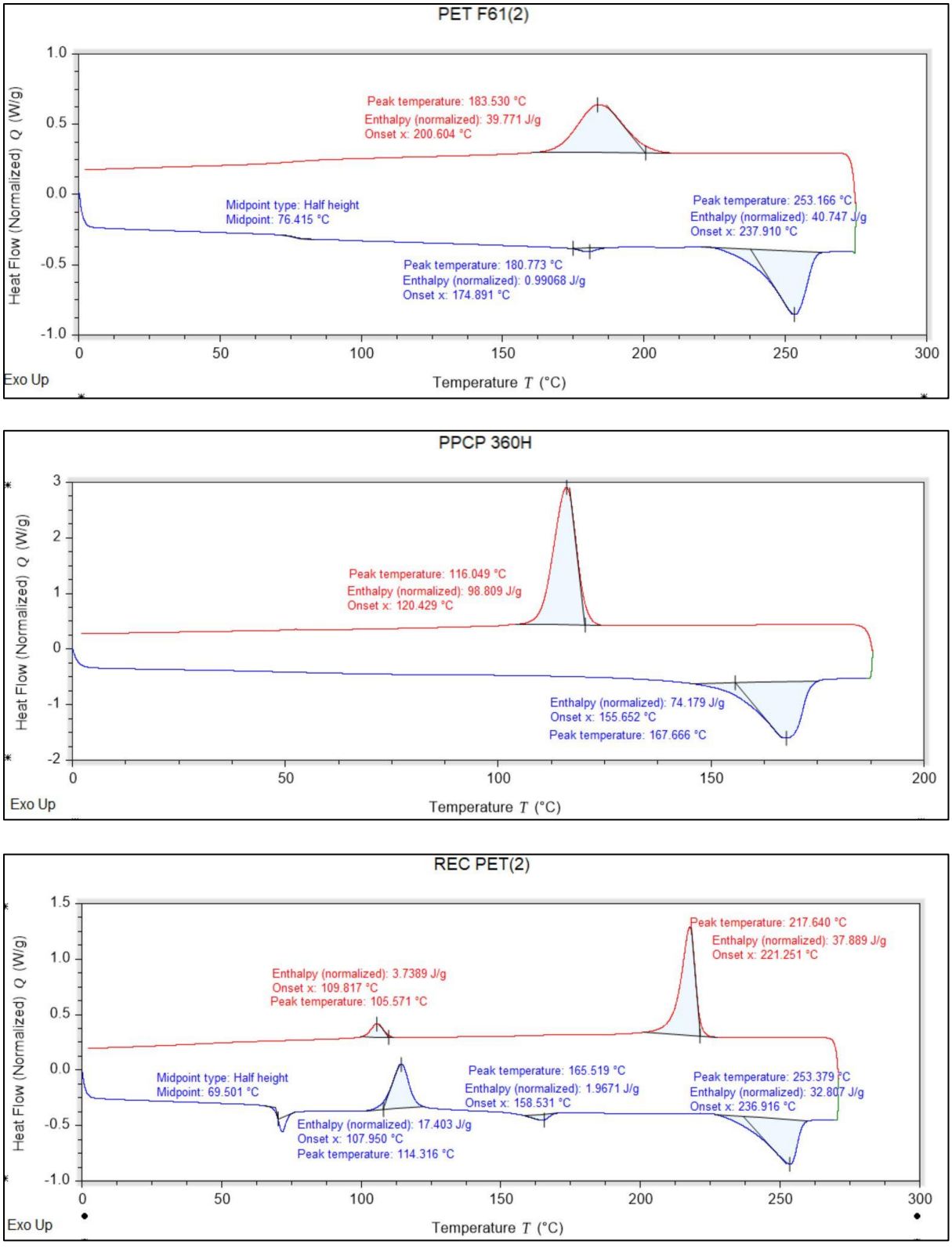

Figure 15. DSC curves for comparison - virgin PET, virgin PP and Rec PET grade 2 (heating and cooling).

According to the DSC heat curve for Rec PET grade 2 (Figure 15), we noticed there were two melting peaks, i.e., at ~166°C and ~253°C. The first peak corresponded to Polypropylene (PP), which was present as an impurity, while the second peak depicted the melting of the PET component. The thermodynamic incompatibility of the two different polymers is borne out by the existence of two melting peaks, the temperatures of which correspond to the melting temperatures of the initial components. This applies in particular to the case where there are comparable quantities of the two polymers. The higher the content of PET in the blend, the higher is the melting temperature of the polymer, and the greater its specific heat. The polymer pellet was not crystallized during testing, and so we notice a cold crystallization peak at around 114°C.

What is interesting to note, as seen in figure 16, grades 3 and 5 do not indicate the presence of PP as we see an absence of the melting peak—seen in grades 1, 2, and 4 around 160°C. The amount of PP was extremely low and therefore, could not be seen during the DSC analysis, or we can speculate the only impurity present within these grades was ash.

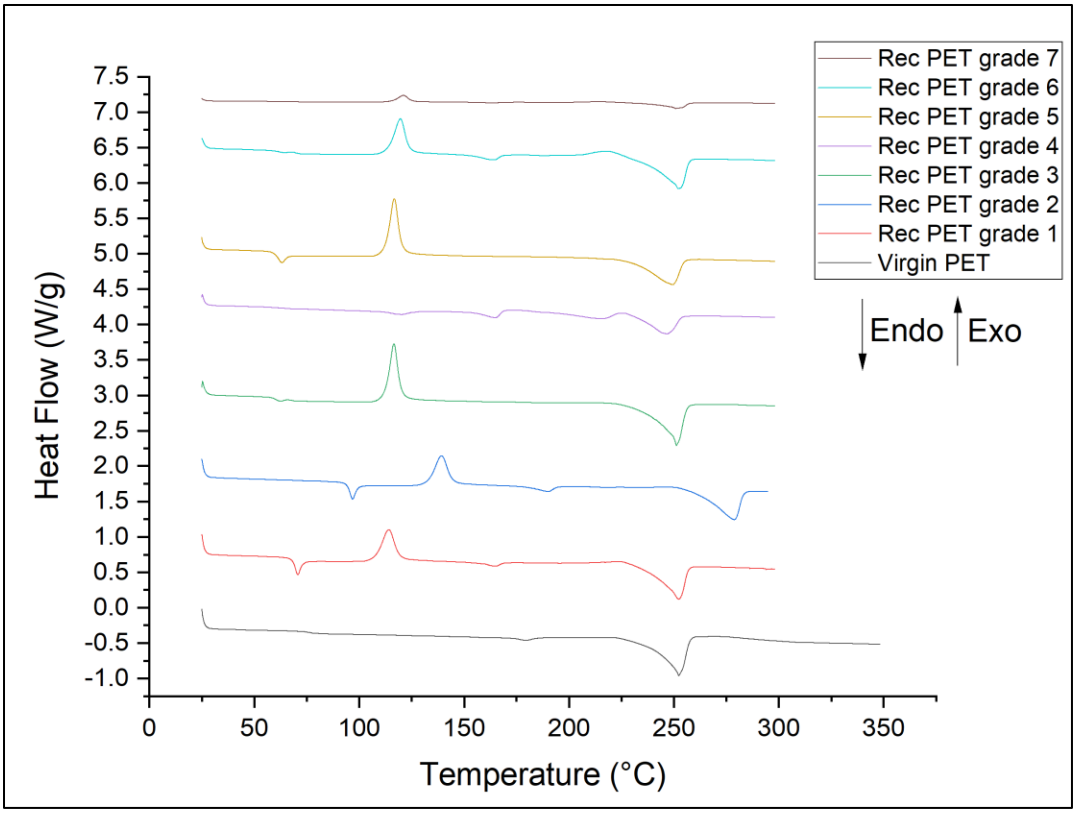

Figure 16. DSC peaks for carpet Rec PET grades 1-7.

Crystalline regions have denser chain packing than amorphous material, with higher elastic modulus and tensile strength. Because of the geometry of chain folding (which usually requires amorphous regions between crystalline regions), the maximum amount of crystallinity does not typically exceed about 80% (Materials Engineering, 2018). Also, with a high amount of chain folding, it will require a high amount of energy and temperature to convert the crystalline regions into amorphous.

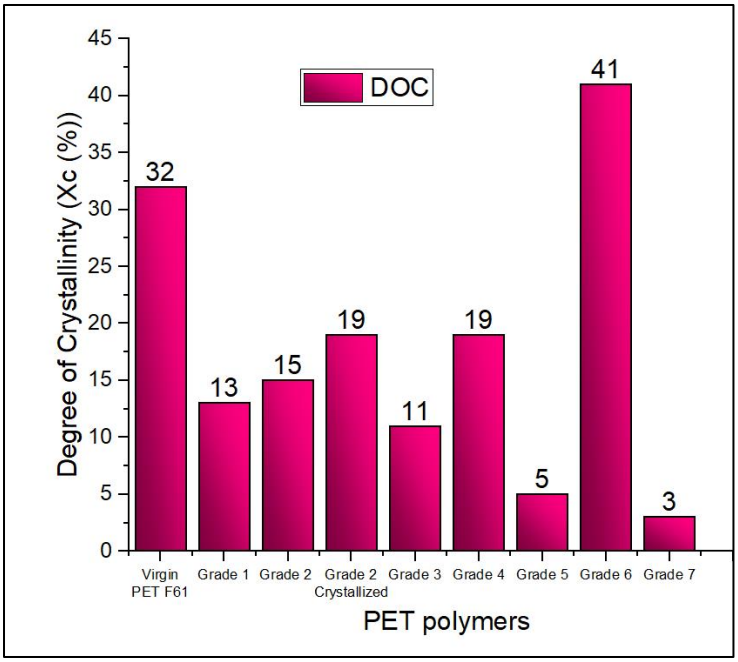

Figure 17. Degree of Crystallinity of PET polymers (first heating cycle).

Due to previous processing and expected low molecular weight of the recycled PET polymers, we notice a decrease in the degree of crystallinity (X_c%). Rec PET grade 1-4 were found to be between 11-19% (Figure 17). After crystallization, grade 2 X_c% barely increased by 4%. Rec PET grade 6 had a relatively high X_c% (41%). Rec PET Grades 5 and 7 had a significantly lower X_c% at 5% and 3%, respectively.

4.4. Conclusion

The material inherently must possess good thermal properties that will aid in ensuring fiber formation during melt spinning or melt-blowing nonwoven fabrics. With the material composition of carpet recycled PET containing impurities of PP and $CaCO_3$, the thermal properties were bound to be affected as was observed with the highest amount of impurities (grade 1), but less so with other samples such as Rec PET grades 2-7.

5. Chapter 5: Experimental Part 2 – Rheology Study

5.1. Approach

Polymer rheology testing is the study of how stress in material or any force applied is related to deformation and flow of the material (Intertek, 2018). Rheology studies, such as measuring melt flow rate, measures the rate of extrusion of thermoplastics through an orifice at a given temperature and load. It provides a means of measuring the flow of a melted material, which can be used to differentiate grades as with polyethylene or determine the extent of degradation of the plastic as a result of molding. Degraded materials would generally flow more as a result of reduced molecular weight and could exhibit reduced physical properties (Intertek, 2018). During the melt reprocessing of any PET, the polymer undergoes chemical, mechanical, thermal, and oxidative degradation that reduces its molar mass and, consequently, its viscosity, melt strength, and mechanical properties and limits its usefulness for many applications. This can be determined with rheology studies, as mentioned below.

Unfortunately, due to an insufficient amount of Rec PET grades 1 and 3, we were unable to test grade 1 for its intrinsic viscosity and grade 3 for its melt volume flow rate.

5.2. Methods

5.2.1. Moisture Analysis

PET is highly hygroscopic and absorbs moisture from the atmosphere. Any small amount of moisture will hydrolyze PET in the melt phase, reducing molecular weight. PET must be dry just before processing, and amorphous PET requires crystallizing before drying so that the particles do not stick together as they go through the glass transition. The polymer pellets were dried at 120°C to measure the moisture content with Radwag Moisture Analyzer.

5.2.2. Melt Flow Rate

The Melt Flow Rate is a measure of the ease of flow of melted plastic, and it represents a typical index for Quality Control of thermoplastics. Initially called Melt Flow Index or Melt Index, the standard designation today is Melt Mass-Flow Rate or MFR, expressed (SI units) in g/10min. An alternative quantity is the volume flow expressed (SI units) in cm^3/10min, called Melt Volume-Flow Rate or MVR. MVR multiplied by the melt density (i.e., the density of the material in the molten state) gives MFR (Instron, 2018).

5.2.3. Gel Time

Using a rotational rheometer (TA Instruments Discovery HR-3), the polymer pellet sample was placed on the plate, maintaining a gap of 1000 micron between the two plates. At 290°C, a shear rate of 100 s^{-1} was applied for 1 hour under nitrogen (N_2) environment. In this study, the gelation behavior is typically observed by studying storage modulus (G') vs. time at a constant frequency.

5.2.4. Inherent Viscosity and Intrinsic Viscosity

This test method ASTM D4603-03 was used for the determination of the inherent viscosity of PET, soluble at 0.50 % concentration in a 60/40 (or 50/50) phenol/1,1,2,2-tetrachloroethane solution using a glass capillary viscometer. The inherent viscosity is determined by measuring the flow time of a solution of known polymer concentration and the flow time of the pure solvent in a capillary viscometer at a fixed temperature. Billmeyer's relationship can help us calculate the intrinsic viscosity with this test method. The intrinsic viscosity is relatable to the composition and molecular weight of the polyester resin (ASTM, 2011).

5.3. Results and Discussion

Hydrolysis can occur due to moisture, which can often be seen as a reduction of molecular weight and intrinsic viscosity (IV) as well. It is imperative to note moisture content in PET before processing to ensure no oxidative degradation in the machine. The moisture content for PET typically must be less than 50ppm for melt spinning.

We conducted a before and after drying test on the moisture analyzer, and the results are as shown in Figure 18. One of the probable reasons for higher moisture content, post-drying, was the insufficient drying temperature in the oven. Therefore, we increased the drying temperature from 225F (107°C) to 248F (120°C), and we notice 0 ppm moisture content after drying.

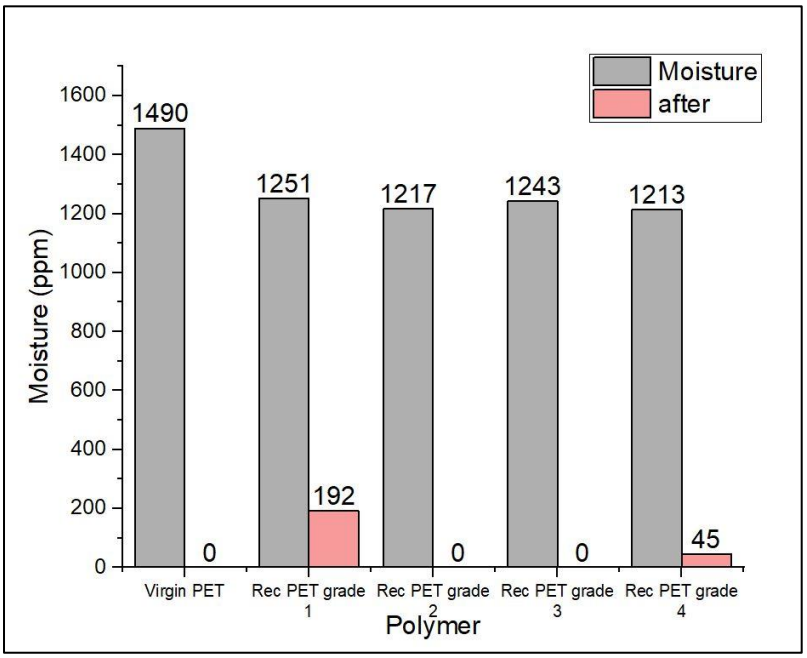

Figure 18. Moisture Analysis before and after drying (grades 1-4).

In Figure 19, we notice that all the grades of recycled PET had a higher MVR than other commercial virgin PETs, thereby concluding that it will flow easily. The melt density at 290°C for grade 1 was 1.37 g/cc, while grade 2 had 1.11 g/cc, grade 4 had 0.98 g/cc, grade 5 had 0.3 g/cc, grade 6 had 0.73 g/cc, and grade 7 had 2.04 g/cc. At 10°C lower, i.e., at 280°C, grades 1 and 2 did

not show any significant difference in melt densities; however, for grades 4-7, there was a slight increase in their melt densities.

Viscosity and MVR are inversely proportional to each other. With a high MVR result, we found that the viscosity was low. In polymer processing of fillers, the finest portion of fillers in the total range is critical to the polymer viscosity (US Patent No. US20120238175A1, 2010; US Patent No. US6797377B1, 2004; US Patent No. US8106121B2, 2012). The lower 10% of particle size also has to be strictly controlled (US Patent No. US20120238175A1, 2010). Because of the agglomeration tendency of those fillers due to large surface area, McAmish claimed that particle size distribution of the filler less than 5% of total particles should be less than about 0.5μm to avoid agglomeration (US Patent No. US20110059287A1, 2011).

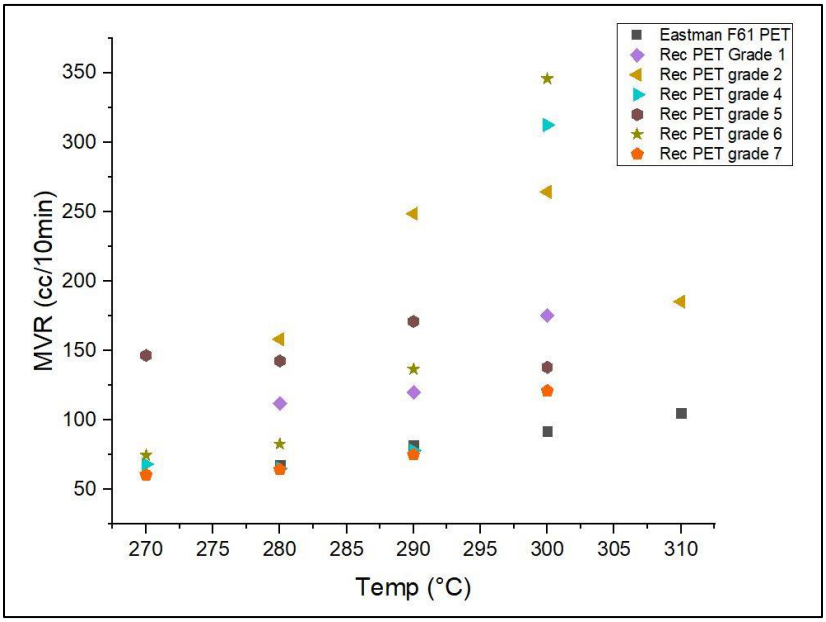

Figure 19. MVR vs. Temperature profile for PET polymers.

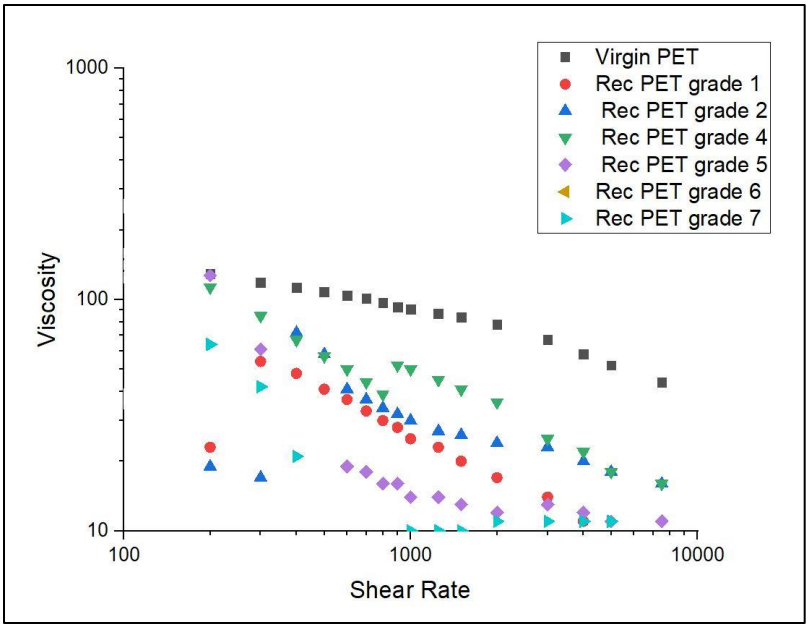

Figure 20. Viscosity vs. Shear rate plot of PET polymers.

Shear-thinning behavior, in which viscosity varies inversely to shear rate, is one of the most remarkable properties of polymeric materials. When the shear rate, i.e., the rate of extrusion through a die is increased, the viscosity will decrease because molecular disentanglement and alignments of the polymer chains will occur. The higher the shear rate, the greater the force required to push the polymer melt through a die. The rheology of a material is more sensitive to the structural aspects of the materials (Dupuis D. , 2009). Shear stress imposed on a polymer/filler blend primarily align polymer by melt extrusion from capillary. The morphology of fibers becomes unstable, and the reason that fiber property highly depends on filler loading is that the melt viscosity dominates over the polymer extrusion and structure solidification (Wei W. , 2015).

The gel-time study is one of the shorter routes to understanding the behavior of the polymer during processing. The most common residence time for a polymer in an extruder is around 10 minutes. We are, therefore, faced with a dilemma where, on the one hand, we want to push the polymer quickly through the extruder with a high throughput but end up with shear-thinning behavior of the polymer. But if we go slower, we may end up with a cross-linked material.

Crosslinked PET has higher tensile strength, and melting temperature, but is less flexible. With this test, we can observe some presence of crosslinking and degradation. As seen in figure 21, there is a slight peak in viscosity in grades 1 and 2 of recycled PET. There may have been experimental artifacts as we do not see a monotonic increase in the graph. The shearing may be preventing the crosslinking after some time and needs to be investigated with dynamic rheology experiments and comparison with grades 3-7 as well.

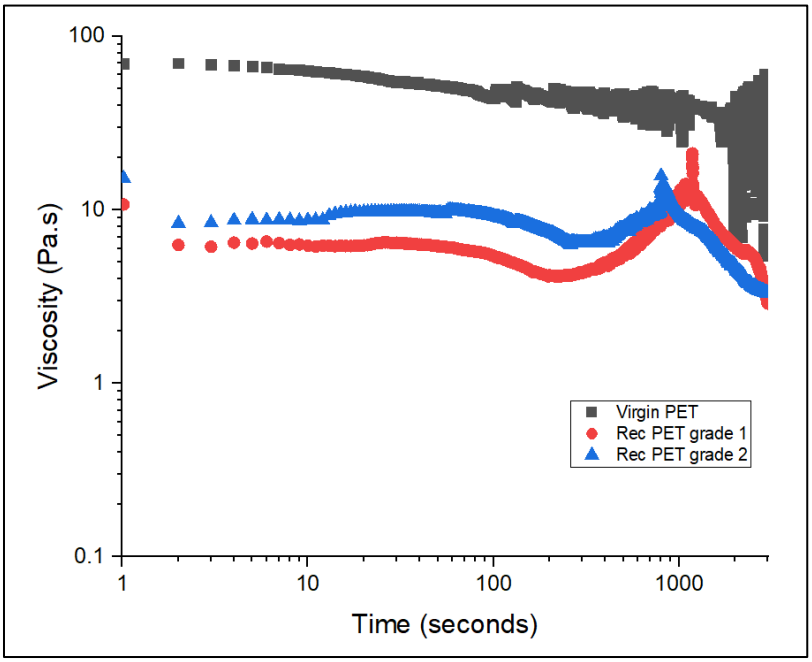

Figure 21. Viscosity vs. Time logarithmic plot for PET polymers.

According to ASTM D4603 (ASTM, 2011) method, from the experimental procedure, we determine the inherent viscosity as follows:

$$\eta_{inh}{}_{0.5\ \%}^{30°C} = \frac{\ln \eta_r}{C}$$

where

$\eta_{inh}{}_{0.5\ \%}^{30°C}$ = inherent viscosity at 30°C (86F) and at a polymer concentration of 0.5 g/dL (dimensions of inherent viscosity are dL/g)

η_r = relative viscosity which is t/t_o

t =average solution flow time (s)

t_o = average solvent flow time (s)

C = polymer solution concentration (g/dL)

An alternative means for calculating intrinsic viscosity [η], from a single measurement of the relative viscosity is by using Billmeyer's relationship:

$$[\eta] = 0.25\ (\eta_r - 1 + 3ln\eta_r)/C$$

The [η] results were found to be as follows:

Table 7. Intrinsic Viscosity results of PET polymers.

Polymer	**[η] (dL/g)**	**M_v (Da)**
Virgin PET (Eastman F61)	0.61	31371.73
Virgin PET (Indorama)	0.66	35427.29
Rec PET grade 2	0.54	25992.43
Rec PET grade 3	0.49	22373.43
Rec PET grade 4 (crystallized)	0.68	37097.59
Rec PET grade 5	0.56	27492.92
Rec PET grade 6	0.58	29022.8
Rec PET grade 7	0.6	30581.61

As expected, due to melt reprocessing and the presence of ash and PP, the [η] was lower than virgin PET for most carpet recycled grades. In grade 4, we denoted the presence of PTT (polytrimethylene terephthalate) and its [η] ~0.9 dL/g, which may explain the higher value for grade 4. Typically, a larger [η] value indicates a higher molecular weight and long-chain length in

a polymer. Intrinsic viscosity to the average molecular weight of a polymer sample can be calculated using the Mark-Houwink Equation:

$$[\eta] = KM_v^a$$

However, to use this equation, one must know the exact values of "*K*" and "*a*"; they are specific for fixed conditions of a polymer type, solvent, and temperature. Viscosity average molecular weight of the samples can be calculated using the above equation where $K = 7.44x10^{-4}$ *dL/g* and $a = 0.648$ (Pirzadeh, Zadhoush, & Haghighat, 2007). The viscosity average molecular weights of the recycled PET grades 2, 3, 5, 6, and 7 were 17%, 29%, 12%, 7%, and 2% respectively lower than virgin PET (Eastman F61). Grade 4, which was crystallized and had a possible presence of PTT, had a higher M_v by 15%. The presence of smaller polymer chains, due to degradation, may cause decrement in crystallinity, which can also influence mechanical and rheological properties (Tapia-Picazo C. , et al., 2014). For the condition of PET, which is solubilized in 60/40 phenol/1,1,2,2-tetrachloroethane at 25°C, the following relations can also be found in the literature (Gupta & Bashir, 2005; Jabarin, Crystallization kinetics of polyethylene I. Isothermal crystallization from the melt, 1987; Jabarin, Crystallization kinetics of polyethylene II. Dynamic crystallization of PET, 1987):

$$\eta = 3.72 \times 10^{-4} (\overline{M}_n)^{0.73}$$

$$\eta = 4.68 \times 10^{-4} (\overline{M}_w)^{0.68}$$

To calculate the molecular weights of the PET polymers using the equations mentioned above, the intrinsic viscosity value for each sample is calculated using the average between the values obtained by two other methods – ASTM D 2857 and the Schulz–Blaschke equation method. For ensuring replication of results with the suppliers, these methods were not tested.

5.4. Conclusion

Since Polyester is hygroscopic, it is quite vital to ensure proper drying. Before extrusion trials, we had to increase the drying temperature to remove moisture from the PET pellets. There is a negligible amount of moisture in the recycled pellets after drying at 248F (120°C). The recycled pellets also have a higher MVR that translates to low viscosity. We found intrinsic viscosity for carpet recycled PET grade 3 to be lower than commercial virgin PET, and other grades of recycled PET. Grade 4 had [η] at 0.68 due to the presence of PTT that typically has [η] of 0.9. Viscosity average molecular weight was calculated with the help of Mark-Houwink's equation. Intrinsic Viscosity reflects the polymer molecular weight, and other properties such as tensile strength, crystallinity, and melting point, we also observed that a low intrinsic viscosity might result in lower molecular weight and could cause issues during processing as well.

6. Chapter 6: Experimental Part 3 – Chemical Analysis

6.1. Approach

While considering some application areas of recycled PET, it has been observed that fiber, yarn, and fabric forms can be used, respectively. Especially, morphological structures, common characteristics, and differences in physical and chemical properties by changing production parameters of recycled PET and virgin PET fibers were investigated before (He, We, Liu, & Xue, 2014; Tapia-Picazo C. , et al., 2014). Material properties affect the final product, be it fiber, yarn, or fabric. Many researchers have studied at different recycling methods, different spinning speeds, and blend ratios of recycled PET yarns to investigate their physical properties (Telli & Özdil, 2013; Abbasi, Mojtahedi, & Khosroshahi, 2007; Lee, Won, Yoo, Hahm, & Lee, 2012). Moreover, chemical analysis becomes an integral part of the polymer investigation to get composition information and other chemical properties.

6.2. Methods

6.2.1. Scanning Electron Microscopy (SEM-EDS) Analysis

SEM-EDS analysis provides valuable information for metallurgical testing and composition analysis. It is also useful for investigating material failures since it can reveal where a fracture started, how fast it propagated, and whether the fracture mode was ductile or brittle. During SEM-EDS analysis, an electron beam is scanned across a sample's surface, as electrons strike and stimulate the sample. Almost instantaneously, when each element returns to its original energy state, it emits X-rays of specific energies. These X-rays are at different wavelengths, characteristic of the element. The identification of the elements is done by matching the peak values (that are on the x-axis) with known wavelengths for each element to reveal the sample's elemental composition (L.T., 2018).

6.2.2. Fourier Transform Infrared Spectroscopy (FTIR) Analysis

FTIR Spectroscopy/Analysis is an analytical technique used to identify organic, polymeric, and, in some cases, inorganic materials. The method uses infrared light to scan test samples and observe chemical properties. The FTIR instrument directs infrared radiation of about 10,000 to 100 cm^{-1} through a sample; some radiation is absorbed, and some pass through. The absorbed radiation is converted into rotational or vibrational energy by the sample molecules. The resulting signal at the detector presents it as a spectrum, typically from 4000 cm^{-1} to 400cm^{-1}, representing a *molecular fingerprint* of the sample. Each molecule or chemical structure will produce a unique spectral fingerprint, thus making the FTIR analysis an excellent tool for chemical identification (RTI Laboratories, 2019). However, it must be noted that FTIR is a "bulk" analytical technique. Little information can be gained from trace or small concentrations of material in a sample (typically greater than 5% constituent). FTIR was recorded on the Thermo Scientific iS50 bench with built-in diamond crystal, and a resolution of 4 cm^{-1}, 32 scans per sample.

6.3. Results and Discussion

The SEM-EDS analysis was carried out on the Phenom XL SEM machine. The Rec PET grade 2 pellet was sputter-coated with Gold (Au) and Palladium (Pd) before setting it on the mold for analysis. Upon completion, there were no metallic trace elements found in the pellet and confirmed the PET components of Carbon (C) and Oxygen (O) in the following amounts:

Table 8. Results of Analysis with SEM-EDS.

Element Number	Element Symbol	Element Name	Atomic Conc.	Weight Conc.
6	C	Carbon	76.37	70.81
8	O	Oxygen	23.63	29.19

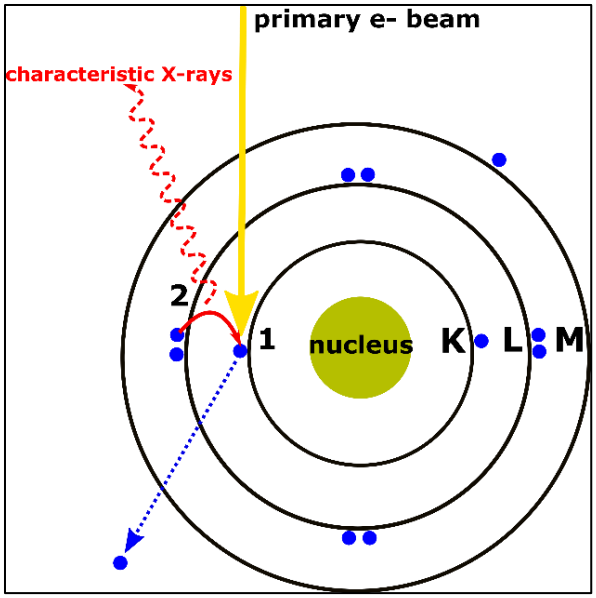

Figure 22. X-rays generated using EDS.

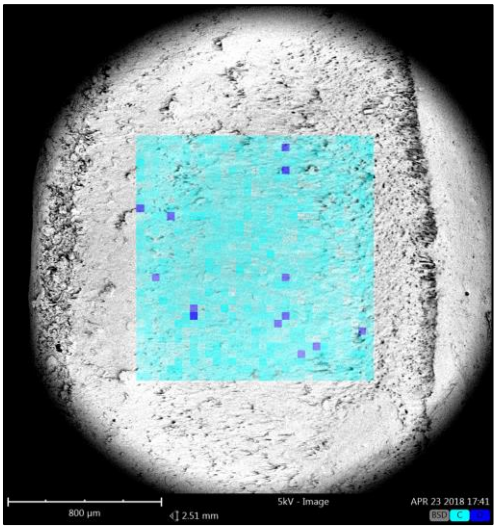

Figure 23. SEM-EDS analysis snapshot.

EDS can not routinely analyze light elements (Z < 11). Hydrogen (Z = 1) and He (Z = 2) do not have Characteristic X-rays and are of too low energy to be detected by EDS.

An FTIR scan can identify different functional group molecules present in a sample.

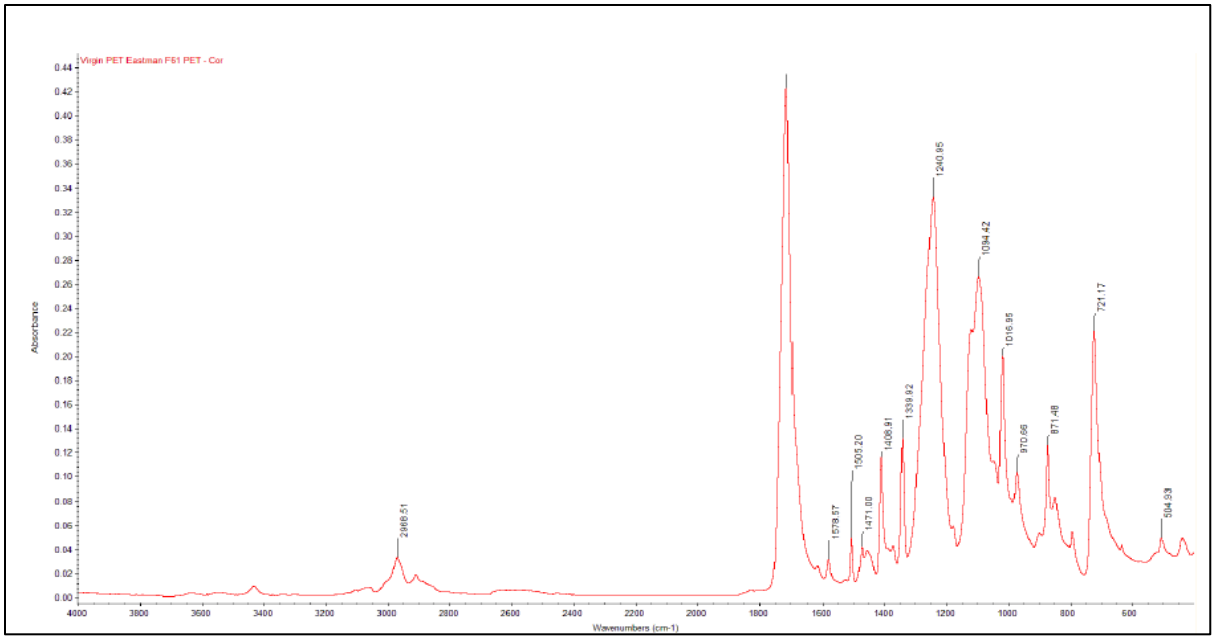

Figure 24. FTIR result of virgin PET.

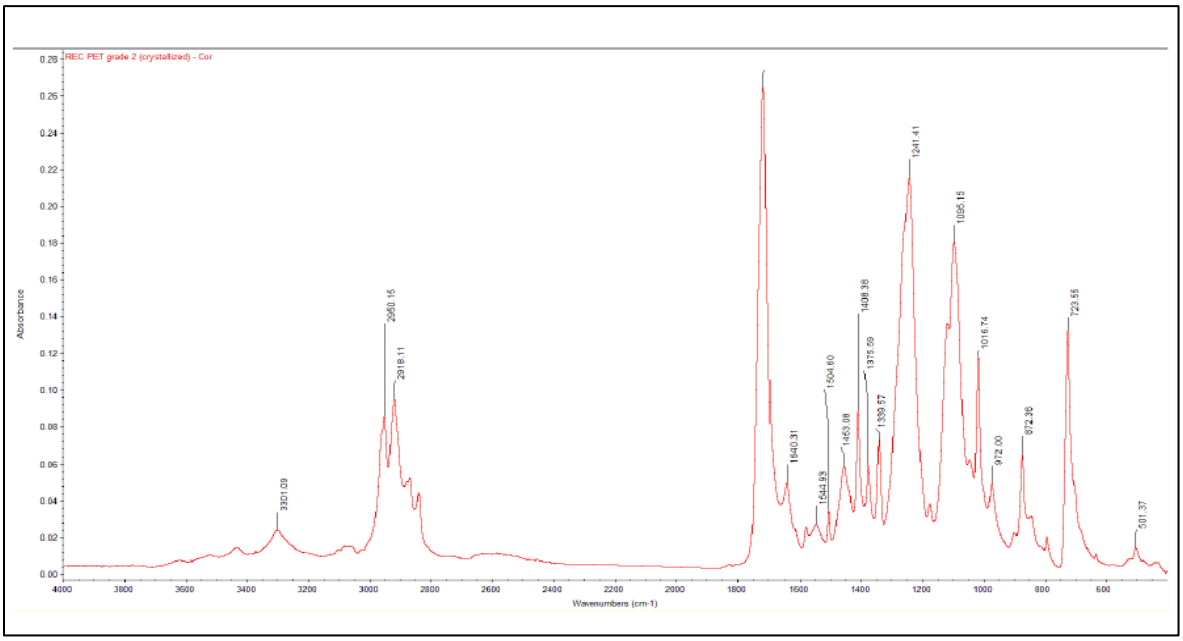

Figure 25. FTIR result of Rec PET grade 2.

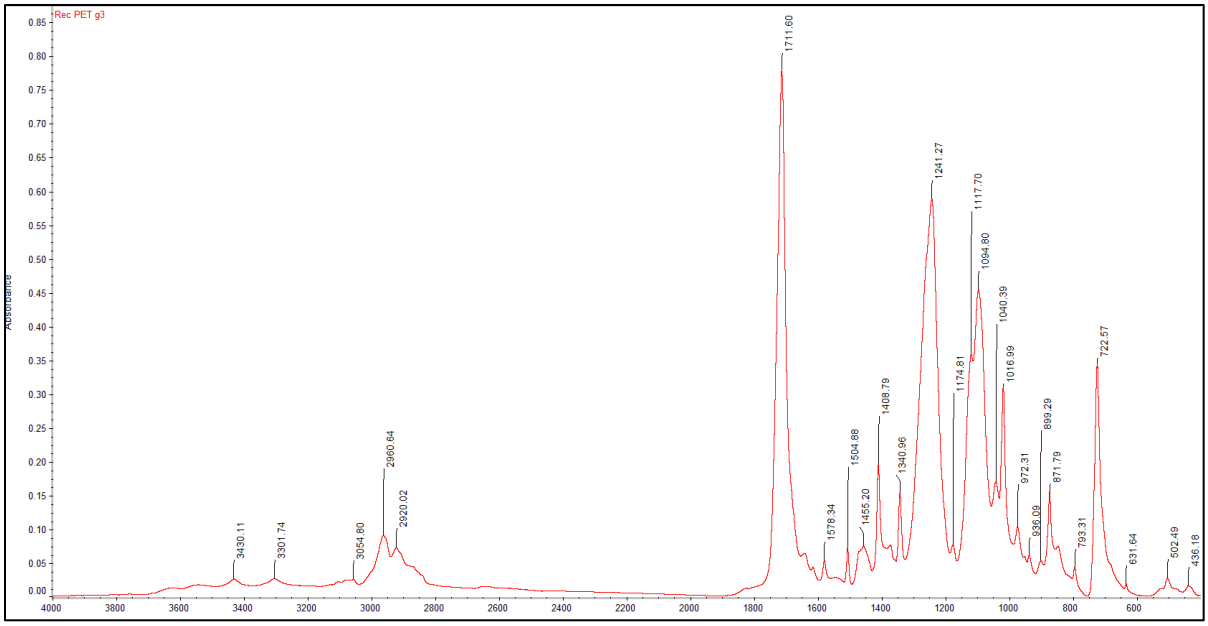

Figure 26. FTIR result of Rec PET grade 3.

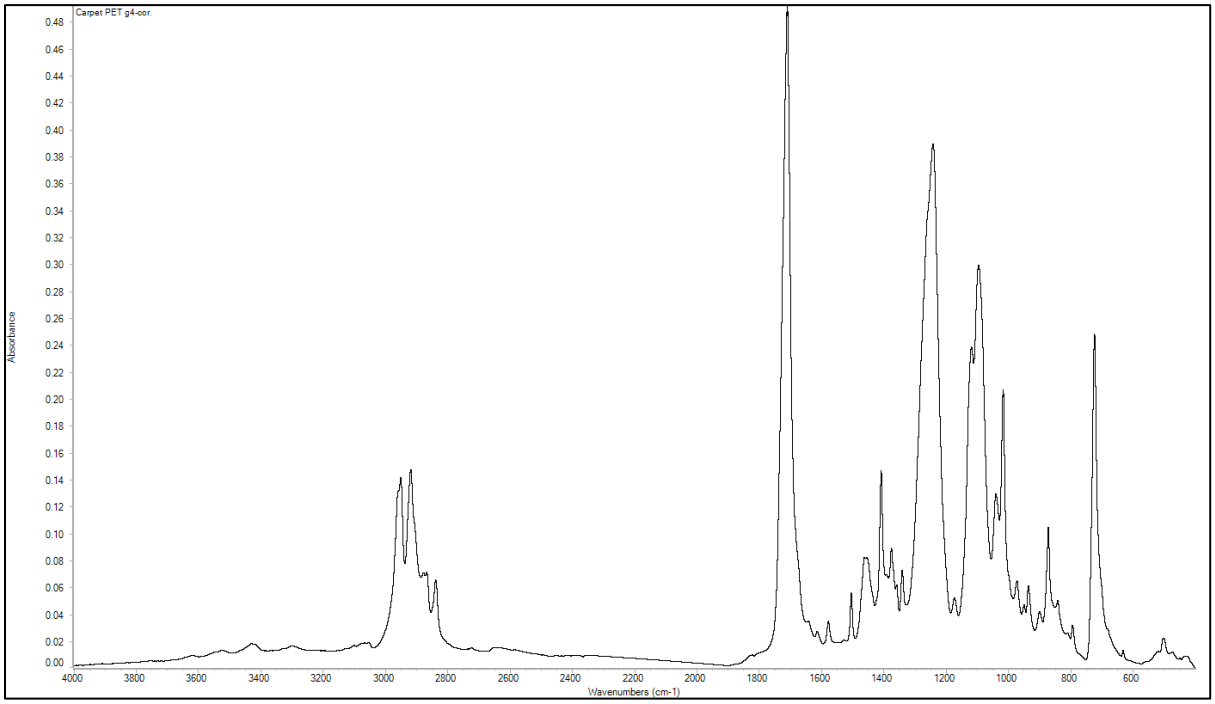

Figure 27. FTIR result of Rec PET grade 4.

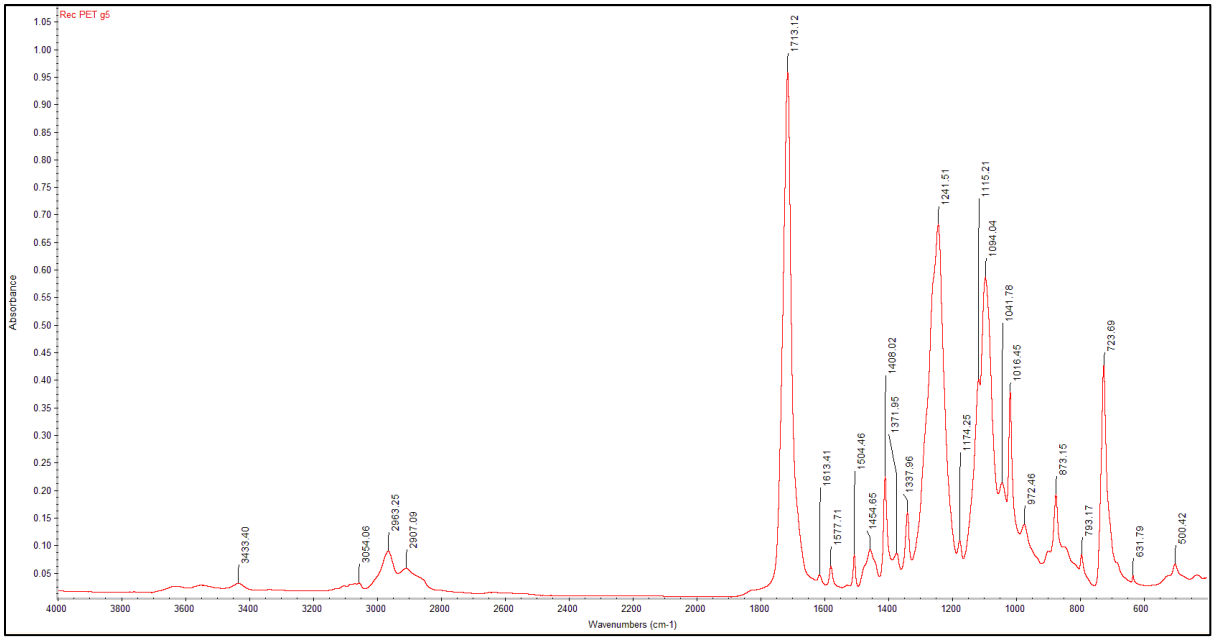

Figure 28. FTIR results of Rec PET grade 5.

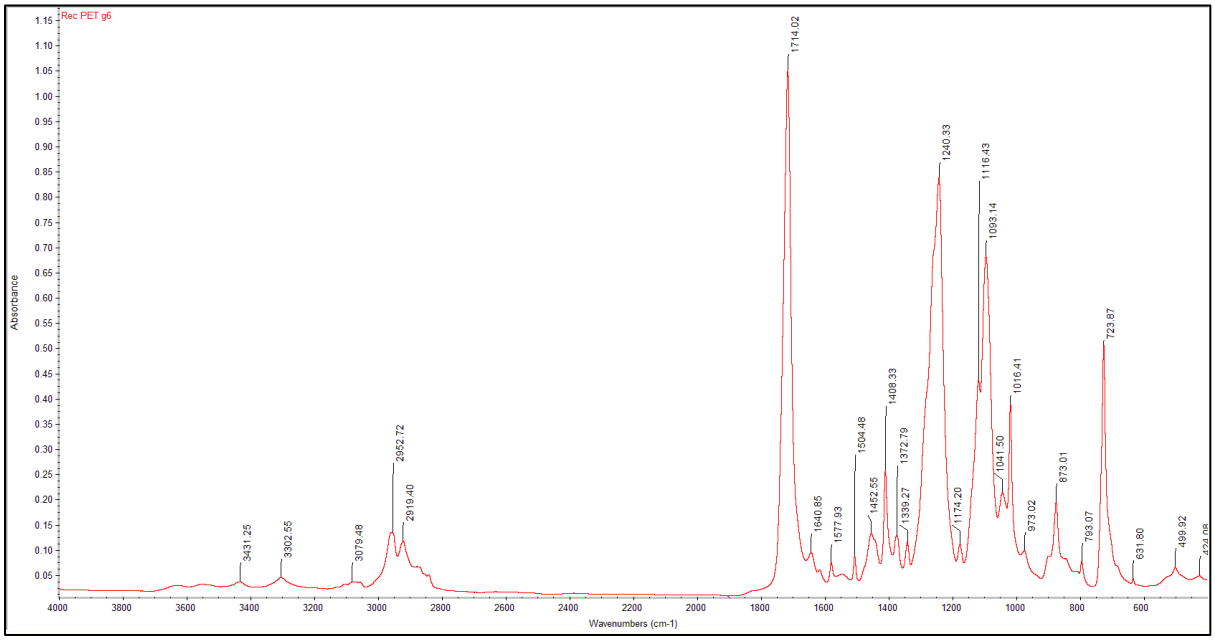

Figure 29. FTIR results of Rec PET grade 6.

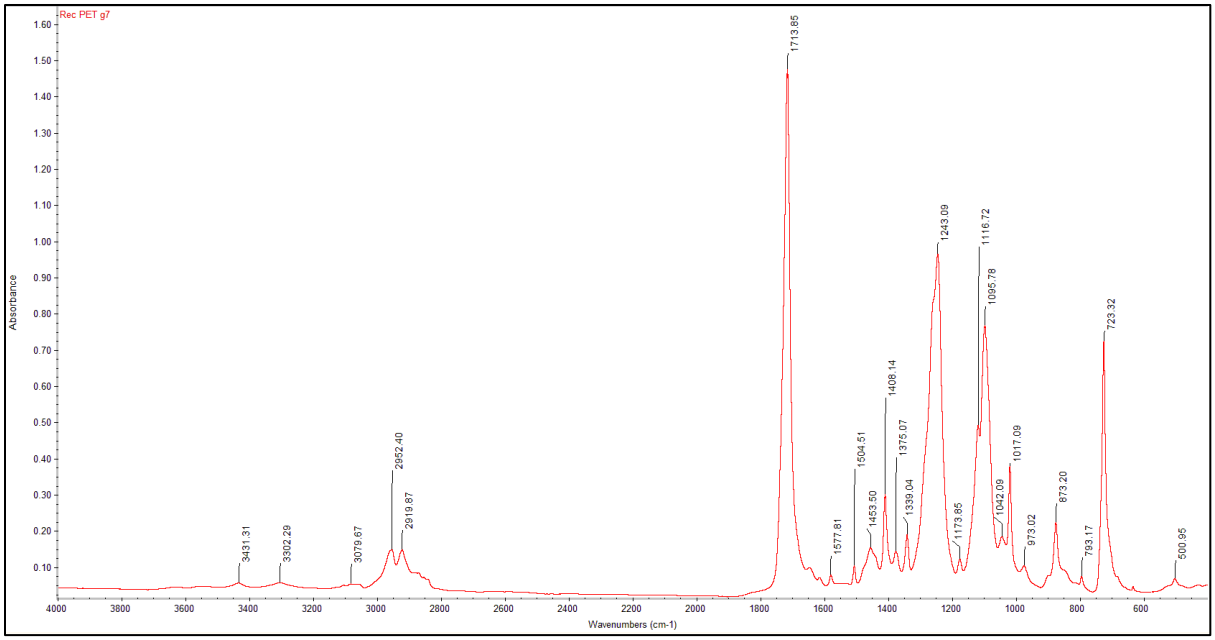

Figure 30. FTIR results of Rec PET grade 7.

The total absorbance can be related to the concentration of the species associated with the peak through the Lambert-Beer equation:

$$A_{tot} = l\varepsilon_p[S]$$

where A_{tot} represents the total area below the peak, l is the sample thickness, ε_p represents the molar absorptivity of the various band components, and $[S]$ represents the molar concentration of the different species. They can be further characterized, as seen in the tables below:

Table 9. Virgin PET functional groups.

Polymer	**Functional Group**	**Wave Number (cm^{-1})**	**Description**
Virgin PET Eastman F61	C=O (Ester)	1750	Stretch
	C-O (Ester)	1000-1300	Two bands or more
	C=C (Aromatic)	1400-1600	Medium-weak, multiple bands

Table 9 (continued)**.**

Polymer	Functional Group	Wave Number (cm^{-1})	Description
Virgin PET Eastman F61	C-H (Alkane)	1350-1480	Bending, variable
	C-H (Aromatic)	2969	Medium

Table 10. Recycled PET grades 2 and 4 functional groups

Polymer	Functional Group	Wave Number (cm^{-1})	Description
Rec PET grade 2 and grade 4	O-H (Oligomers)	2900-3000	Carboxylic Acids/Alcohol end-groups; broad and variable
	C=O (Ester)	1711 1750-1690	Stretch in crystalline Stretch in amorphous (PTT)
	C-O (Ester)	1017-1241	Two bands or more
	C=C (Aromatic)	1408-1545	Medium-weak, multiple bands
	C-H (Alkane)	2850-3000	Medium stretch
	C-H (Alkane)	1350-1480 842-790	Bending, variable Gauche CH_2 rocking in amorphous (PTT)
	C-H (Aromatic)	3301	Medium

Table 11. Recycled PET grades 3, 6, and 7 functional groups.

Polymer	Functional Group	Wave Number (cm^{-1})	Description
Rec PET grade 3, 6, 7	N-H	3100-3500	Unsubstituted with two bands
	O-H (Oligomers)	2900-3000	Carboxylic Acids/Alcohol end-groups; broad and variable

Table 11 (continued)**.**

Polymer	**Functional Group**	**Wave Number (cm^{-1})**	**Description**
Rec PET grade 3, 6, 7	C=O (Ester)	1711-1714	Stretch, strong
	C-O (Ester)	1016-1243	Two bands or more
	C=C (Aromatic)	1408-1578	Medium-weak, multiple bands
	C-H (Alkane)	2850-3000	Stretch
	C-H (Alkane)	1455	Bending, variable
	C-H (Aromatic)	3300-3303	Medium

Table 12. Recycled PET grade 5 functional groups.

Polymer	**Functional Group**	**Wave Number (cm^{-1})**	**Description**
Rec PET grade 5	N-H	3100-3500	Unsubstituted with two bands
	O-H (Oligomers)	2900-3000	Carboxylic Acids/Alcohol end-groups
	C=O (Ester)	1713	Stretch, strong
	C-O (Ester)	1094-1241	Two bands or more
	C=C (Aromatic)	1408-1577	Medium-weak, multiple bands
	C-H (Alkane)	1350-1460	Bending, variable
	C-H (Aromatic)	2963	Medium

The integrated absorbance of the peak at 1710-1750 cm^{-1} was representative of the concentration of the ester group in polyesters (as seen in Figures 24-30). The presence of a broader

and distinct peak at 2900 cm^{-1} in Rec PET grade 2 and grade 4 may be characteristic of short-chain molecules or *oligomers*, that may have led to cleavage of polymer chains. There is a small, broad peak seen in Rec PET grades 3, 5, 6, and 7 as well. In grade 4, we found the peaks characteristic of Polytrimethylene terephthalate (PTT) or Triexta (Zhen & ShouKe, 2013; Simons, 2020). In their studies (2013), Zhen & ShouKe found an enlarged region of 1750-1690 cm^{-1} generated by C=O stretching vibration and region of 842-790 cm^{-1} generated by CH_2 trans rocking vibration in amorphous phase respectively.

PTT belongs to the family of polyesters and has certain advantages over PET, especially in the carpet industry. It has been recognized to be more durable and resilient than conventional PET. Its appearance is similar to nylon giving it a more matte finish. It is also environmentally friendly. DuPont exclusively produces PTT as Sorona with a biotechnology process based on the fermentation of corn glucose. PTT also has better elastic recovery than PET due to its structure. As PTT fiber has excellent stretch recovery, stain resistance, and chemical stability, all these characteristics make PTT make a prominent polymer in the carpet industry (Yinyuda, 2020).

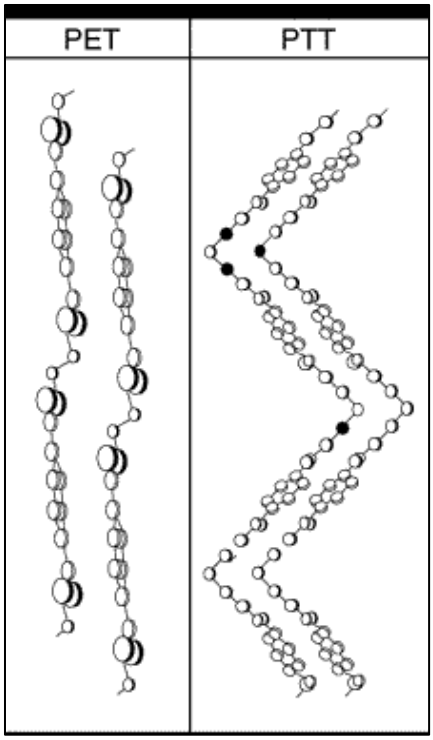

Figure 31. Structures of PET and PTT.

PET fibers can contain up to 4-5% cyclic oligomers, which makes it difficult to dye, finish, and process them. Oligomers are typically present in the bulk of the polymer and have almost no effect on properties; if they are present on the surface, it may negatively affect properties and processing of dyed polyester fiber. The carpet pellets received were from dyed PET carpets. In the course of hydrothermal treatments to the material, the oligomers could have migrated to the surface, thus affecting the eventual processes of the material. Functional oligomers (e.g., PET acrylate – to increase wetting) can be used to decrease viscosity and volatile organic compounds (VOC) in the material (Vavilova, Prorokova, & Kalinnikov, 2003).

6.4. Conclusion

We did not observe the presence of any metallic impurities in the carpet recycled PET. However, with the results of the FTIR analysis, we were able to detect the presence of short-chain molecules (*oligomers*) in Rec PET grades 2 and 4. An intrinsic viscosity around 0.5 (for grades 2

and 3), as opposed to 0.61 of virgin PET seen in the rheology studies, may also lead us to a conclusion of molecular degradation in the recycled polymer pellets. Gel Permeation Chromatography (GPC) analysis can help us confirm the degradation and measure the weight average molecular weight, which shall be studied in the next chapter.

7. Chapter 7: Experimental Part 4 – Molecular Weight Analysis by GPC

7.1. Approach

Standardized molecular weight analysis methods, like the Gel Permeation Chromatography (GPC), calculate the values through a comparison between the retention times of samples of unknown molecular weight with those of standards of known molecular weight. This method assumes that if two molecules are of the same size in solution, then they are the same molecular weight. The accuracy of this assumption is directly dependent upon the similarity between the hydrodynamic volume of the standards and that of the sample for a given molecular weight (Jordi Labs, 2018). Factors which are essential in determining the hydrodynamic volume of a polymer include the polarity and rigidity of a polymer, as well as the presence of charged functional groups incorporated into the polymer. It is therefore desired to keep the chemistry of the standards (a charge, polarity, chain stiffness) as similar as possible to that of the samples.

7.2. Method

7.2.1. Gel Permeation Chromatography

Gel Permeation Chromatography (GPC), also known as Size Exclusion Chromatography (SEC), is an analytical methodology that separates dissolved macromolecules based on size and their elution from columns. The columns are filled with a porous gel. GPC can be coupled with other techniques such as light scattering, viscometer, and concentration detectors (known as triple detection). When coupled, measurement of properties like absolute molecular weight, size, and intrinsic viscosity, as well as the generation of information on macromolecular structure, the conformation, and branching become easy (Malvern, 2018).

Typically, polymers do not have a single molecular weight but rather a range of values. Thus, to describe the range of molecular weights of a polymer, a molecular weight distribution

curve displaying the fraction of a sample with a given molecular weight is commonly used. The molecular weight distribution curve is, therefore, a graphical representation of the range of the molecular weights of the sample. The width of the distribution curve reflects the polydispersity of the sample, the narrower the distribution, the lower the polydispersity (Jordi Labs, 2018).

To describe the molecular weight distribution of a polymer numerically, three different molecular weight averages are commonly used. They are the number average molecular weight (M_n), the weight average molecular weight (M_w), and the *Z* average molecular weight (M_z). M_n provides information about the lowest molecular weight portion of the sample. M_w is the average closest to the center of the curve, and M_z represents the highest molecular weight portion of the sample (Jordi Labs, 2018). They are calculated according to the equations below, where M_i is the molecular weight, N_i is the fraction of the molecular with a molecular weight of M_i.

$$Number\ average\ Molecular\ Weight: M_n = \frac{\Sigma M_i N_i}{\Sigma N_i}$$

$$Weight\ average\ Molecular\ Weight: M_w = \frac{\Sigma M_i^2 N_i}{\Sigma N_i}$$

$$Z - average\ Molecular\ Weight: M_z = \frac{\Sigma M_i^3 N_i}{\Sigma N_i}$$

Therefore, a molecular weight distribution curve can be derived, given all M_i and N_i.

7.3. Results and Discussion

Virgin PET pellets (Eastman F61), as well as Recycled grade 2 PET pellets, were shipped to Jordi Labs, based in Boston, MA. Samples were dissolved for eight hours in hexafluoroisopropanol (HFIP) at room temperature with gentle agitation, yielding clear solutions with a small amount of insoluble material. Samples were filtered with 0.2 μm PTFE filters before injection. A filtered blank injection was analyzed along with the samples in order to identify any peaks that were potentially introduced during the filtration process. Samples were monitored using

a Schambeck RI 2012 refractive index detector. Data acquisition and handling were made with Jordi GPC software.

SOLVENT	Hexafluoroisopropanol with 0.01M Sodium trifluoroacetate
FLOW RATE	1.0 mL/min
INJECTION VOLUME	50 µL for sample, 50 µL for standards
COLUMN TEMPERATURE	40 °C
CONCENTRATION	~1.25 mg/mL for sample, 0.5 mg/mL for standards
COLUMN	Jordi Resolve X-Stream Mixed Bed (7.8 x 300mm)
RUN TIME	20 minutes
SAMPLE PREP CONDITIONS	8 hours at RTP with orbital shaking. Filtered with 0.2µm PTFE.
STANDARDS	Polystyrene: 675.5K, 320K, 121.6K, 66.65K, 26.08K, 10.64K, 4.64K, 1.95K & 960 Da

Figure 32. Conditions utilized for GPC testing.

Table 1
Average Molecular Weight
Relative to polymethyl methacrylate standards

Sample ID	Run	M_n	Avg.	M_w	Avg.	M_z	Avg.	M_w/M_n	Avg.
Green Pellets-Carpet Recycled Polyester	1	18,958	18,689	35,462	35,406	59,151	59,157	1.87	1.89
	2	18,421		35,351		59,163		1.92	
White Pellets-Virgin Polyester	1	28,092	27,921	49,963	49,824	81,451	81,678	1.78	1.78
	2	27,750		49,684		81,904		1.79	

Figure 33. Average Molecular Weight results.

The goal of the analysis was to determine and compare the relative molecular weight distributions of the samples. The carpet recycled PET (Rec PET grade 2) exhibits an average M_w of approximately 35 kDa, while virgin PET (Eastman F61) exhibits an average M_w of 50 kDa. The expected variability of a standard GPC test method is 10%. The M_w values for the two samples differ by 29%. This is per the assumption of degraded polymer chains in the carpet recycled PET due to prior processing. Torres, Robin, & Boutevin (2000) investigated the effect of molecular weight and intrinsic viscosity on molecular degradation. Their results showed that recycled PET

was more sensitive to thermal and hydrolytic degradation than virgin PET. This could be due to traces of moisture and impurities. They induce chain scission processes that lead to a reduction in intrinsic viscosity and molecular weight of recycled resins (Torres, Robin, & Boutevin, 2000). The results of this analysis also helped confirm the intrinsic viscosity to be lower for Rec PET grade 2 due to the reduction in molecular weight. In chapter 3, we were able to calculate the viscosity average molecular weight (M_v) for Rec PET grade 2 and virgin PET. These values slightly differ from the weight average molecular weight of the polymer. The principle of M_w is based on the fact that a bigger molecular contains more of the total mass of the polymer sample than the small molecules. In M_v, bigger molecules make the solution more viscous than the smaller ones (How Polymers Work, 2020). Higher the molecular weight, more viscous is the solution. When the polymer has a higher molecular weight, it has a more significant hydrodynamic volume. This is the volume that the coiled up polymer takes up in the solution. As it is larger, the polymer molecular can block more motion of the solvent molecules, thus, slowing them down.

7.4. Conclusion

The weight average molecular weight was measured with the help of GPC. Rec PET grade 2 was found to have 29% lower M_w than virgin PET. During recycling and reprocessing of the carpet recycled PETs, the chemical reactions result in cleavage of the polymer backbone (or main-chain bonds), thus producing the short-chain *oligomers* or monomers or low molecular weight degradation products. It was observed in chapters 5 and 6, that we were able to detect the presence of *oligomers* in the recycled PETs, and also study the effect of degradation on its intrinsic viscosity, and molecular weight. The next chapter will determine further effects and issues seen during extrusion.

8. Chapter 8: Initial Fiber Spinning Trials

8.1. Approach

The Hills line includes a multi-component spin-beam with independent temperature control for each polymer system. The design allows all multicomponent fibers to be commercialized with conventional downstream equipment (quench, take-up, etc.). It allows a much shorter polymer residence time in the spin-beam and the spin-pack. This short residence time allows for much higher temperature separation between the multi-polymers and between any polymer and the process equipment. The Homocomponent Hills line present in the Fiber Science Lab was a single-screw extruder design with three different screws: 1) General purpose screw, 2) Mixing screw and, 3) Polyester screw. The difference in the screws was the designs and the depth of the grooves. For the Bicomponent spinning, the line comprised of two extruders, each equipped with a single-screw and conventional downstream design as well. Bicomponent fibers have the additional advantage of being able to utilize the functionality of two or more components.

Meltblown systems transform polymers or solutions into very fine fibers and convert them into fibrous nonwoven roll goods in one step. Each section is equipped with its gear pump. The pump controls polymer flow to ensure uniform basis weights (weight per unit area). Each pump is also individually driven to allow maximum versatility. There is shorter exposure time to high temperatures that limits thermal degradation, producing stronger fiber, and higher yield of material (Biax Fiber-Film, 2018). Meltblown fabrics can be used in a variety of industries such as filtration, healthcare, hygiene, industrial, automotive, etc.

8.2. Trial Methods

8.2.1. Homocomponent (Hills) and Bicomponent Line

Before processing, the pellets were dried at 248F (120°C). The parameters for carrying out the Multi-filament spinning for Rec PET grade 1 were as follows:

Table 13. Parameters for Homocomponent Line – Rec PET grade 1

Start Throughout (g/hole/min)	**Temperature (°C)**	**Screw**	**Die (# of filaments)**	**Screen Size**
0.1-0.5	290	General Purpose	69 or 72	150

Since the ash ($CaCO_3$) content was deemed high, the particles clogged the screen, which eventually had to be removed. A standard 10% finish was applied while spinning. There was no fiber formation due to poor melt strength, and the Rec PET grade 1 dripped (as shown in Figure 34), which could not be spun. The next step was to try and mix virgin PET with grade 1. By taking a salt-pepper approach, we mixed different ratios of virgin PET (Eastman PET F61) with Rec PET grade 1. They were 50:50, 80:20, and 95:5, respectively. As the amount of virgin PET was increased, the dripping was reduced. However, due to the poor blending of the polymer melt, there was no fiber formation. This was the case with all throughputs, and both dies.

Figure 34. Rec PET grade 1 (left) and grade 2 in free fall (right) on Homocomponent Line (Hills system).

We tried to extrude Rec PET grade 2 on the Homocomponent line as well, with an absence of a screen. A standard 10% finish was applied to the polymer during spinning. The parameters for carrying out the Multi-filament spinning were as follows:

Table 14. Parameters for Homocomponent Line – Rec PET grade 2

Start Throughout (g/hole/min)	**Temperature (°C)**	**Screw**	**Die (# of filaments)**	**Speed (rpm)**	**Quench (°C)**
0.3-.07	270	General Purpose	72	1500	20

By increasing the throughput to 1 g/hole/min, we could see some amount of fiber formation. Compared to grade 1, grade 2 indicated a better potential for spinning as we were able

to make free fall samples (as shown in Figure 34). However, we were unable to wind-up and draw samples on the take-up rollers. The next step was to try and mix virgin PET (Eastman F61) with Rec PET grade 2. The ratios were 10:90, 20:80, 30:70, 50:50 and 90:10 respectively. The results did not change much as the melt strength did not improve due to the non-uniform and low mixing of Eastman F61 PET with Rec PET grade 2. Polymer melt contained filler particles have higher melt viscosity and low melt elasticity and inevitably retard the polymer chain coil-stretch property in polymer extrusion (US Patent No. US20120238175A1, 2010). With parameters similar to Rec PET grade 2, we tried to spin Rec PET grades 3 and 4 on the Hills line but with no success. A screen of 150 size was used, which got clogged, and the pressure on the extruder was quite high.

On the Bicomponent filament extrusion line, we found success with Rec PET grade 3. We were able to spin three samples in a 50:50 Sheath/Core (S/C) configuration: i) Grade 3 as the core, virgin Polyethylene (PE) as sheath, ii) Grade 3 as the core, virgin PET as sheath and, iii) control PE as the core, virgin PET as the sheath.

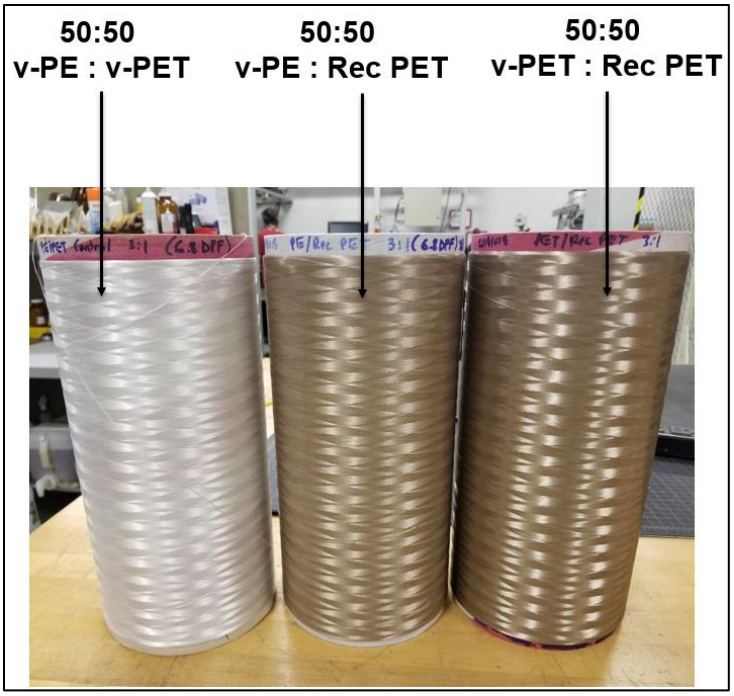

Figure 35. Bicomponent fibers with 6.8dpf.

The parameters were as follows:

Table 15. Parameters for Bicomponent Line – Rec PET grade 3

Pump speed (cc/rev)	Temperature (°C)	Screen	Die (# of filaments)	Quench (°C)	Denier and draw
0.66	275	250	72	15	6.8 dpf 3:1

Fiber tensile properties were measured on MTS Instron tensile tester. The crosshead speed was initially set at 300 mm/min, and the sample length was 20 mm.

Within the recycled polymer pellet, there is a non-homogeneity in the system due to possible phase separation. The formation of a two-phase structure is induced by a difference in temperatures or the molecular weight of the polymer. Because PET is a polar polymer and PP is non-polar, their blends are immiscible (Khonakdar, et al., 2013). Kusuktham (2011) conducted a

study with PET fibers containing ash. The fibers were found to exhibit brittle properties and had coarse denier. Incorporation of calcium carbonate in PET also decreased its mechanical properties as it inhibited the flow direction and orientation of the polymer melt. Even at 1% and above, the polymer melt could not flow easily through the spinneret. The addition of polymer modifiers such as chain-extenders or compatibilizers might help maintain the integrity of the polymer blends as fibers/web; it may also improve the melt strength of the polymer due to degradation or presence of PP (Tavares, et al., 2016; Körmendy, 2005).

The tensile strength results were found as follows:

Table 16. Tensile Strength results.

Sample	**Peak Load (lbf)**	**Strain at break (%)**
Control PE/PET	1.7334	196.3376
v-PE/r-PET (g3)	0.9742	80.9332
v-PET/r-PET (g3)	1.4996	98.9384

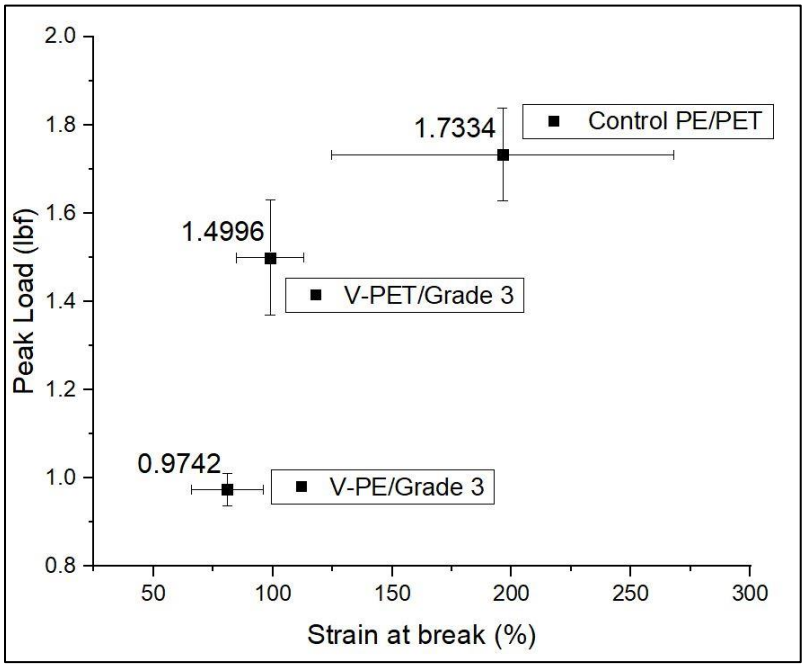

Figure 36. *Tensile Strength results for Bi-co trial.*

The maximum peak load observed for v-PET/r-PET (g3) was 1.4996 lbf, which was comparable to the control sample (v-PE/v-PET) peak load of 1.7334 lbf. PET overall, had higher strength and elastic limit than PE. The stress-strain curve revealed a uniformity in stress up to 20% in strain, and from this point, the stress increased linearly. According to Pierce weak-link, fiber strength is equal to the segment within fiber material when its breaking stress is lower than other segments (Naito, Yang, Tanaka, & Kagawa, 2012). Based on this theory, the strength of one fiber or yarn is equal to the lowest strength linking in the fiber. Such weak spots, if contained with $CaCO_3$ particulates, can be regarded as cross-sectional linkages within the fiber structure that forms an initiator at organic/inorganic interfaces. Stress could propagate from a pin crack around the particulate periphery region while radially expanding to the adjacent semi-crystalline region, eventually rupturing the fiber sample as drawing force exceeds the weak link strength (Pukanszky, Belina, Rockenbauer, & Maurer, 1994; Weiner & Addadi, 1997). We suspect the presence of ash

in Rec PET grade 3 and its irregular particle size could have increased the chance of an unavoidable agglomeration surrounded by voids in the polymer matrix, which eventually led to breakage.

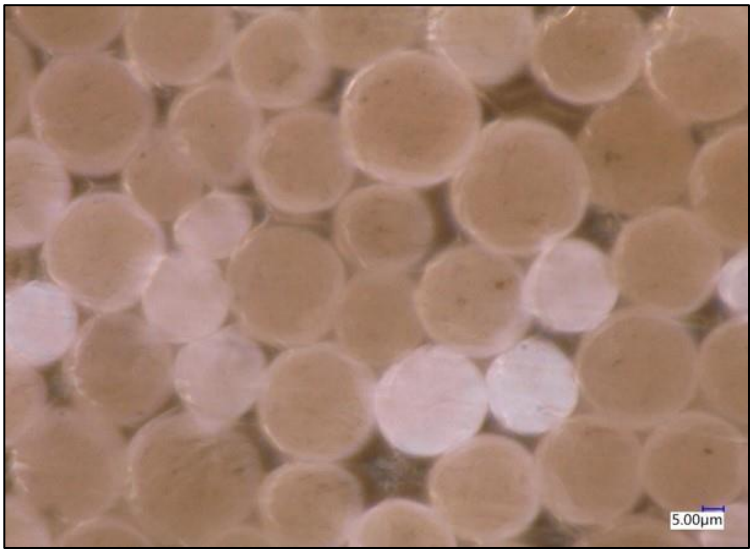

Figure 37. 50:50 virgin PET: Rec PET grade 3 bicomponent S/C configuration.

The fundamental sheath/core (S/C) structure is useful in many applications demanding engineering polymers, and the applications depend entirely on the surface properties of the outer polymer. In this case, the fiber's core can be made with a suitable lower-cost polymer that can provide properties of flexibility and tensile strength. In figure 37, we do observe the spilling of the core into the sheath. It may denote the difference in melt viscosities and solidification temperatures, which affected the interaction of the two components. As the two polymers traverse the capillary, they will spontaneously rearrange themselves until the configuration that produces the least amount of resistance to flow is obtained. The material of lower viscosity will move to regions of higher shear, near the walls, leading to the encapsulation effect (Mukhopadhyay, 2014). These factors also affected the spinline stresses acting on each component and change their thermal histories (Dasdemir, Maze, Anantharamaiah, & Pourdeyhimi, 2012). Besides this, it has also been previously shown that the diameter of bicomponent fibers is larger if the core has some fillers

present, also depicting a correlation of increase in diameter with an increase in the concentration of fillers (Wei W. , 2015).

Polymer viscosities, rates of cooling, and surface tensions of the two components are critical for the formation and properties of bicomponent fibers (Khatwani & Yardi, 2003; Jeffries, 1971). Polymer viscosities of each component should be comparable at the spin pack along with the temperature to obtain desired cross-section (Cooke, High technology fibers, 1996; Khatwani & Yardi, 2003). Rates of cooling determine the orientation of each component, while the surface tensions determine the adhesion between two components and the final cross-sectional shape in the resultant bicomponent fiber.

8.2.2. Biax Line

Before processing, the pellets were dried at 248F (120°C). Due to the insufficient amount of Rec PET grade 1, we were unable to run a trial on the Biax line. 100% Rec PET grade 2 was meltblown, and the parameters were set as follows:

Table 17. Parameters for Biax Line – Rec PET grade 2

Die	Die Temperature (°C)	Air Temperature (°C)	Capillary Size	DCD (cm)	Throughput (rpm)
15”	285	295	0.02”	20	15

The Biax die has a total of 368 holes and 1128 air holes. The temperature was quite high, so we reduced it to 280°C and further down to 270°C. There was no consolidated web structure formed on the take-up roller. The next step was to meltblow at selected ratios of Eastman F61 PET with Rec PET grade 2. The different ratios were 90:10, 80:20, 70:30 and 50:50 respectively.

We also tried 100% Rec PET grade 3 on the Biax line and 50:50 virgin PET (Eastman F61): Rec PET grade 3. The parameters were optimized to be as follows:

Table 18. Parameters for Biax Line – Rec PET grade 3 and blends

Die	Die Temperature (°C)	Air Temperature (°C)	Capillary Size	DCD (cm)	Throughput (rpm)
15”	275	265	0.02”	20, 25	15

By lowering the temperature, DCD, and the presence of a lower amount of ash and PP in grade 3 material led to successful web formation.

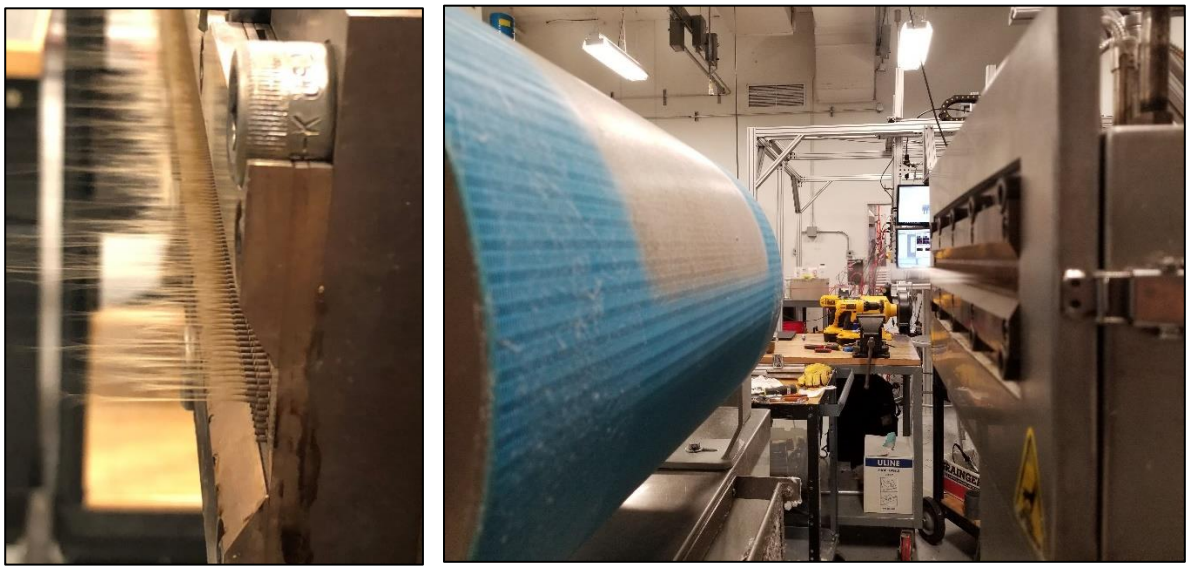

Figure 38. Melt blowing of 100% Rec PET grade 2 (left) and 3 (right) on the Biax line.

With Rec PET grade 4, we found similar success on the Biax line. We were also able to create a 100% recycled PET meltblown web with a 50:50 ratio of Rec PET grade 4: bottle grade PET. Although bottle grade PET had a higher melt flow, it was more forgiving on the Biax line to create strong webs with fine fibers. The texture of the material was similar to a 50:50 ratio of virgin PET: Rec PET grade 3 melt-blown web.

Table 19. Bottle grade PET properties.

Polymer	Onset Degradation	Residue at 800°C	Melting Temperature	Xc (%)	[η] (dL/g)
Bottle Grade PET	372°C	10.61%	259°C	24	0.69

The parameters were optimized to be as follows:

Table 20. Parameters for Biax Line – Rec PET grade 4 and blends

Die	Die Temperature (°C)	Air Temperature (°C)	Capillary Size	DCD (cm)	Throughput (rpm)
15”	270	260	0.02”	30	15

When the temperature was 280°C, the texture of the 100% Rec PET grade 4 webs were similar to grade 2 melt-blown webs. The higher IV and better melt flow of grade 4 and bottle grade PET, respectively, contributed to the formation of meltblown webs on the Biax line.

The meltblown samples were sputter-coated with a thin layer of gold and analyzed with a scanning electron microscope to examine the fiber morphology. A scanning electron microscope (SEM) scans a focused electron beam over a surface, thus creating an image. We can obtain information about the surface topography and composition. The instrument used was Phenom Pro desktop SEM with a resolution <8nm (SE) and <10nm (BSE), magnification up to 150,000x. Images were taken at 10,000-x under 5kV of an accelerating voltage for the electron beams. Fiber diameters were measured using the Phenom Suite Fiber Metric software. For each meltblown web, at least 100 individual fiber diameters were measured.

Upon SEM image analysis, we observed a non-uniform distribution of fiber sizes with thick and thin fibers. For 100% Rec PET grade 3, the mean fiber diameter was ~8µm, for 100% Rec PET grade 4, mean fiber diameter was 56 µm, while it was ~16 µm for 100% bottle grade PET. The average fiber diameter is typically affected by throughput rate, melt temperature, viscosity, and air temperature (Dutton, 2008). A decrease in the polymer molecular weight also leads to obtaining fibers a smaller diameter, which is beneficial for nonwoven properties (Lewandowski, Ziabicki, & Jarecki, 2007). Uniformity is essential and can be affected by the uniformity of fiber distribution in the air stream and the vacuum levels. Poor die design or non-uniform ambient air will negatively affect the air stream and fiber distribution resulting in a non-uniform web and diameter distribution. Polymer temperature may also affect the mean fiber diameter. An increase in temperature can decrease the mean fiber diameter. An increase in airflow rates decreases the mean fiber diameter (Dutton, 2008). The non-uniformity in fiber size distributions, seen in figures 38-40, could be the result of the complex interactions between the air stream and the polymer jet, as well as the melt viscosities of the three different grades of recycled PET. The substantial increase in fiber diameter of grade 4 can be suspected due to the presence of a high amount of calcium carbonate particles and PP. The average diameter of fiber increases with the loading concentration (Wei W. , 2015).

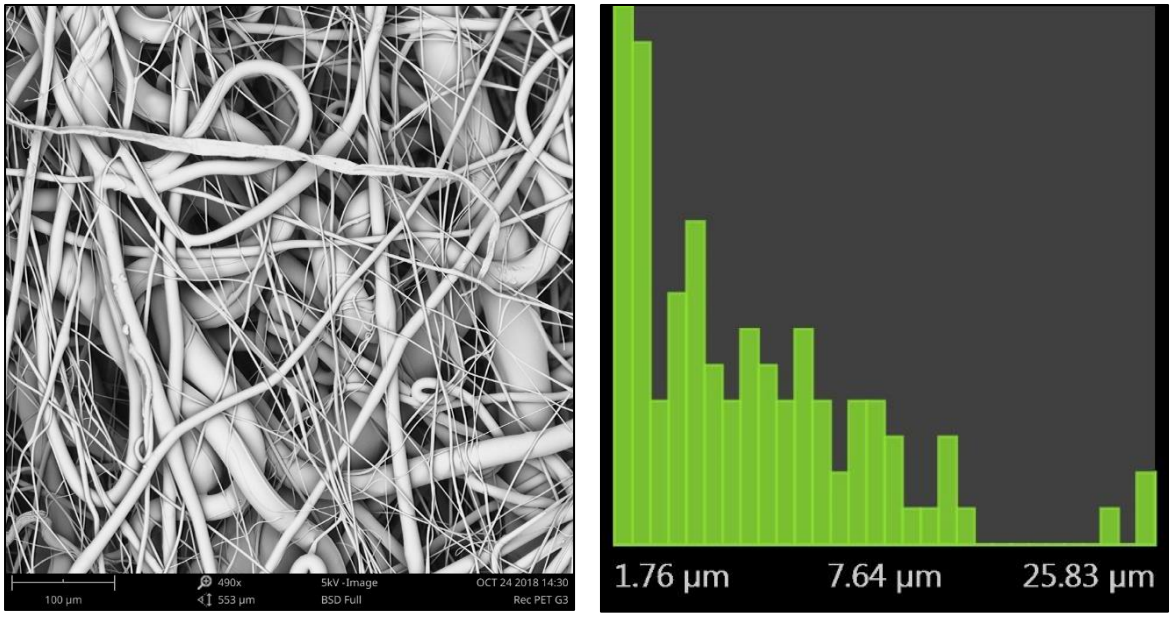

Figure 39. SEM image analysis of 100% Rec PET grade 3 fabric, 500x (zoom); fiber size distribution.

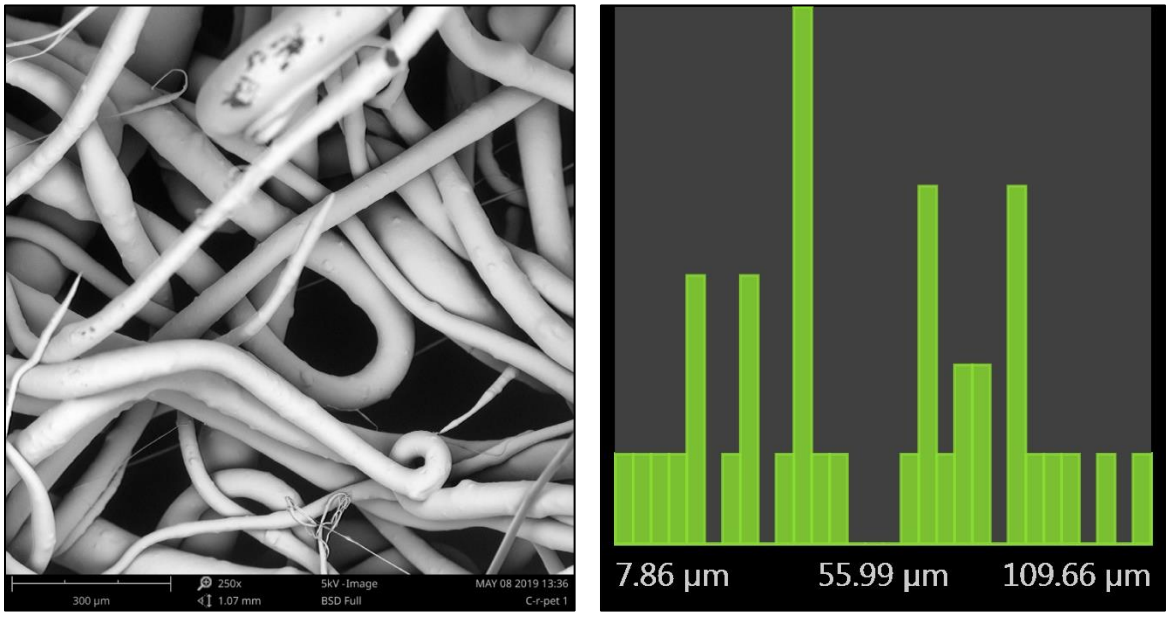

Figure 40. SEM image analysis of 100% Rec PET grade 4, 250x (zoom); fiber size distribution.

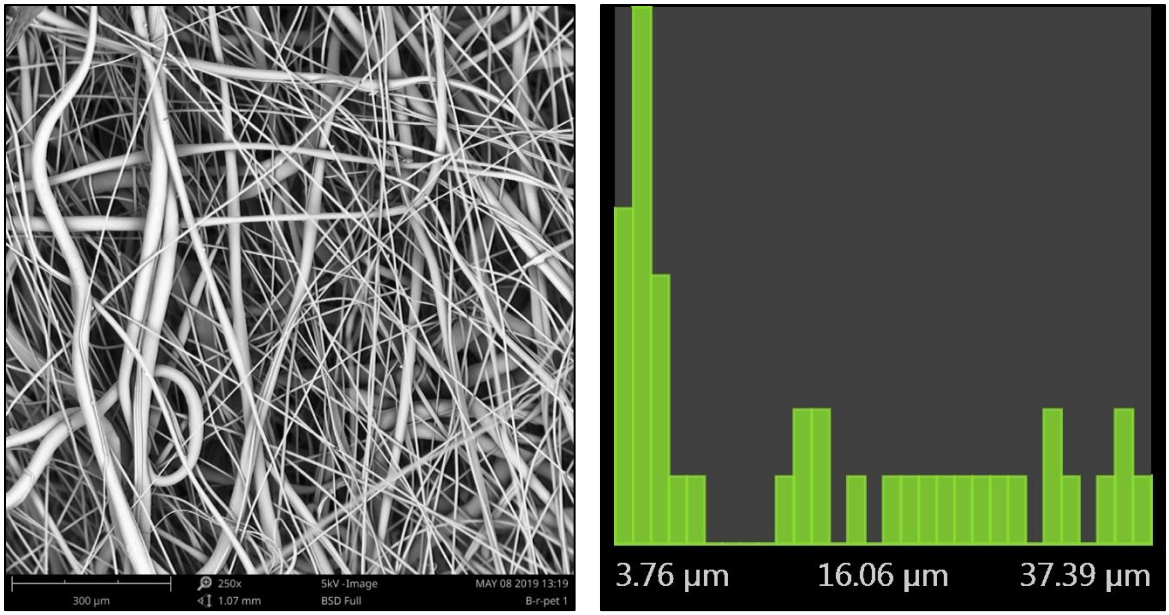

Figure 41. SEM image analysis of 100% Bottle grade PET fabric, 250x (zoom); fiber size distribution.

8.3. Conclusion

During our preliminary trials conducted on the Hills line (multi-filament spinning), we determined the five parameters that influenced the limited fiber formation of Rec PETs with poor melt strength:

1. *Crystallization of pellets:* The pellets were crystallized at 120°C before running through the Hills line.
2. *The temperature during processing:* Typically, the processing temperature for PET is 290-300°C. By lowering the temperature, we were able to achieve fiber formation to a certain extent.
3. *Medium-high throughput:* 0.1-0.3 g/hole/min was too low for strength to be imparted to the fiber integrity. By ensuring the throughout to be in the middle (~0.6-0.7 g/hole/min), we optimized control over the structure of the fiber as well as a natural drawing of the fiber.

4. *Quench conditions:* The grade 1 trial had an absence of quench conditions, and therefore, the fiber was not cooled enough during processing. By adding quench, we were able to ensure the spinning and formation of fibers.
5. *Thermal stability:* As seen during the thermal analysis, grades 2, 3, and 4 had higher thermal stability than grade 1, which helped it process better.
6. *Calcium Particulates:* Any agglomeration of fillers down the fiber spinning can weaken the fibers, but also cause spinneret capillary clogging issue (Verlag, 2001) as was observed with grade 3 extrusion.

During the meltblown web formation trials, we were able to form web structures at the following ratios:

Table 21. Meltblown web formation for carpet recycled PETs.

Polymer ratio	**Web formation**	**Parameters**
90:10 (Virgin PET: grade 2)	✓	T= 290°C, 15rpm
80:20 (Virgin PET: grade 2)	✓	T= 290°C, 15rpm
70:30 (Virgin PET: grade 2)	✓	T= 290°C, 15rpm
	✓	T= 290°C, 25rpm
100% grade 3	✓	T= 275°C, 15rpm
50:50 (Virgin PET: grade 3)	✓	T= 275°C, 20rpm
50:50 (Virgin PET: grade 3)	✓	T= 275°C, 25rpm
100% grade 4	✓	T= 270°C, 15rpm
50:50 (grade 4: bottle grade)	✓	T= 270°C, 15rpm
100% bottle grade	✓	T= 270°C, 15rpm

Figure 42. Meltblown webs of virgin PET: Rec PET grade 2 in 90:10 ratio (left) and 70:30 ratio (right).

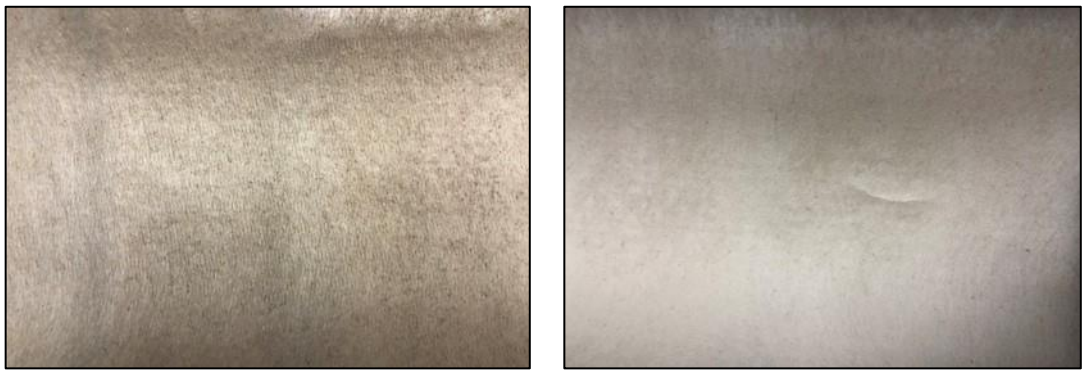

Figure 43. Meltblown webs of 100% Rec PET grade 3 (left) and 50:50 virgin PET: Rec PET grade 3 (right).

With the success of 100% Rec PET grade 3, we were able to prove that a significantly lower amount of impurities in the material can reduce the processing issues and allow the formation of melt-blown webs. With 100% Rec PET grade 4, the material had good rheological properties as compared to other grades, due to the presence of PTT.

Large particles in polymer melt may interrupt with the screen filter, which may cause clogging in the spin pack. Clogging of screen filters may cause long term running issues. Patents referred here indicate there is a limit for filler top cut in fiber spinning (US Patent No. US20120238175A1, 2010; US Patent No. US20110059287A1, 2011). Filler particles tend to form agglomerations by cohesion. In fibers, even a small portion of agglomeration influences fiber

structure continuity and uniformity. A weakness of fibers is caused by poor dispersion of fillers in the polymer during polymer extruding, mixing, and spinning (Wei W. , 2015).

We also concluded that the addition of polymer modifiers such as chain-extenders or compatibilizers might help maintain the integrity of the fibers and web as well as improve the melt strength of the polymer when the presence of ash and PP is high. During the chemical reprocessing of any PET, the polymer undergoes chemical, mechanical, thermal, and oxidative degradation that reduces its molar mass. This, consequently, affects the viscosity, melt strength, and mechanical properties, thereby limiting its usefulness for many applications. These flaws can be compensated for by introducing modifiers such as chain extenders or compatibilizers.

Chain extenders are general poly-functional compounds with thermal stability and have the ability of fast reaction with the hydroxyl or carboxyl end groups of PET. They do not prevent degradation but can balance the effects on the molar mass of the polymer. The most widely used chain extenders are di- and multi-functional epoxides (Demetris & George, 1996), di-isocyanates (Yang, He, & Liang, 2001; Torres, Robin, & Boutevin, Chemical modification of virgin and recycled poly(ethylene terephthalate) by adding of chain extenders during processing, 2001), dianhydrides (USA Patent No. US Patent 3 533 157, 1971), bis-oxazolines (Zhou, Ma, Pan, & Liang, 2002; Hiroo & Shunichi, 1986) and phosphates (USA Patent No. US Patent 4 468 720, 1986).

Another way to improve the processing would be to eliminate the phase separation issues caused by PP and PET incompatibility. Compatibilization is the modification of the interface in immiscible polymer blends in order to refine and stabilize the phase structure. The presence of a compatibilizer at the interface markedly affects the deformation behavior of the dispersed droplets during and after cessation of flow (Starý, Pemsel, Baldrian, & Münstedt, 2012). A suitable

compatibilizer not only improves the compatibility between PET and PP but also improves the characteristics of the resulting blends. Usually, the compatibilizer concentrates at interfaces during blending, and plays the role of reducing interfacial tension, preventing coalescence and strengthening interfacial adhesion. Such compatibilization often results in stabilized morphologies with a fine dispersion of the minor phase, which affects the macroscopic properties of the blends. The compatibilization of polymers has been extensively studied through the diminution of the interfacial tension of the polymers in the blend (Baccouch, Mbarek, & Jaziri, 2017).

9. Chapter 9: Understanding failures: Designer PET resin study

9.1. Approach

From the previous chapters, we learned that the presence of impurities such as ash ($CaCO_3$) and PP causes extrusion issues such as clogging up of the screens, dripping during melt spinning, and low melt flow for the carpet recycled polyester pellets. It was, therefore, necessary to understand the amount of impurities that could be present in the pellet for smooth processing. Our main objective was to identify component/s that led to the failure of fiber formation. We decided to create our own 'dirty' pellets and mimic the carpet recycled polyester that was received from the supplier. By accomplishing a limiting % of PP and ash, we would be able to relay the numbers back to the recycling facilities for better efficiency in extrusion.

9.2. Method

Virgin PET (Eastman F61), PP (MF 35), and $CaCO_3$ were sent to Techmer PM, Tennessee, for compounding the materials in different proportions. The virgin PET was compounded as follows:

Table 22. Creation of 'dirty' designer PET resins.

Virgin PET/PP (%)	Virgin PET/Calcium (%)	Virgin PET/(PP+Calcium) (%)
99.5/0.5*	99.5/0.5*	99.5/(0.37+0.10)*
99/1	99/1	99/(0.75+0.25)
98/2*	98/2*	98/(1.5/0.5)*
97/3*	97/3*	97/(2.25+0.75)*
95/5	95/5*	95(3.75+1.25)*
92.5/7.5	93/7	90/(7.5+2.5)

Table 22 (continued)**.**

Virgin PET/PP (%)	Virgin PET/Calcium (%)	Virgin PET/(PP+Calcium) (%)
90/10	-	85/(10+5)
85/15	-	80/(13+7)

*Samples taken for trial

The designer PETs were then characterized by solution viscometry for [η] and taken for trials on the homocomponent extrusion and melt-blowing system.

9.3. Results

Due to time constraints and previous success in recycled PET grades 3 and 4, we decided to select roughly 7-8 samples for trials and recognize the limits for allowing impurities in the PET. We wished to catalog the melt properties and fiber spinning options with these samples. The materials that we selected were in the range of the composition of recycled PET grade 3, as marked in table 22.

Table 23. Intrinsic viscosity results of designer PETs.

Polymer	[η] (dL/g)
Virgin PET (Eastman F61)	0.61
Virgin PET (Indorama)	0.66
3% $CaCO_3$ (ash)	0.41
3% PP	0.47
95% PET + 1.25% ash + 3.75% PP	0.44
98%PET + 0.5% ash + 1.5% PP	0.54

Before processing, the pellets were dried at 248F (120°C). For the melt-spinning homocomponent trials, the parameters were:

Table 24. Parameters for Homocomponent Line – Designer PET

Start Throughout (g/hole/min)	**Temperature (°C)**	**Screw**	**Die (# of filaments)**	**Speed (rpm)**	**Quench**
0.5	275	Mixing	72	500	10-0%

Due to clogging, the screen was eventually removed. A standard 10% finish was applied while spinning. For samples containing 0.5% and 3% PP, 0.5% and 3% $CaCO_3$, (0.37% PP + 0.13% $CaCO_3$), and (2.25% PP + 0.75% $CaCO_3$) we noticed slight dripping and brittle fiber formation. Inconsistency in the fiber formation and random fiber breaks led to an inability in drawing and a failure in fiber collection.

For the Biax melt-blown trials, the parameters were set to:

Table 25. Parameters for Biax Line – Designer PET

Die	**Die Temperature (°C)**	**Air Temperature (°C)**	**Capillary Size**	**DCD (cm)**	**Throughput (rpm)**
15”	280-290	270-280	0.02”	30	15

Table 26. Designer PETs meltblown trial summary.

Designer PET Polymer	Melt-blowing Biax Line	Comments
0.5% PP	Web formation	Successful at a lower pressure (8psi)
2% PP	Web formation	Higher airflow (13.9psi)
2% ash	Web formation	-
3% ash	Web formation	At higher airflow (13.9psi), finer fibers formed = better web
5% ash	Brittle web	Lower pressure (8psi)
1.5% PP + 0.5% ash	Web formation	-
2.25% PP + 0.75% ash	Web formation	Successful at higher pressure (14psi)
3.75% PP + 1.25% ash	Web formation	Difficulty in maintaining extruder pressure

9.4. Discussion

With the solution viscometry test, we found the [η] to be extremely poor. Intrinsic viscosity is typically not affected by fillers, in the case of ash, as it is only a function of molecular weight.

The longer the chain length, stiffer the material, and higher the intrinsic viscosity. From the results, we can infer that the designer PETs may have undergone hydrolysis due to insufficient drying, which resulted in a drop in molecular weight and, therefore, a reduction in [η].

Typically, at higher shear rates, the filler component (ash) does not affect shear viscosity. However, since the particles may have weak interfacial bonding with the polymer, a larger extension rate is applied which exceeds the maximum tensile strength of the fiber, it may encounter breaks in the spin-line (Haworth & Jumpa, 1999; Ariffin, Jikan, Samsudin, Ariff, & Ishak, 2006; McGenity, Hooper, Paynter, & al, 1992). White & Tanaka (1981) attempted to develop ideas on filament stability during melt spinning operations. Their investigations revealed that adding the filler (ash in this case), increased the spinline elongational viscosity and caused it to fall off more rapidly with deformation rate. This suggested spinline instability. It might be conjectured that segregated groups of particles could be "stress concentrators" (as discussed in chapter 8), which led to premature failure.

In the recycled material and the designer PETs, the PET component is more abundant than PP; therefore, the PET became a matrix, and PP was embedded in this system. The combination of PET and PP is a typical example of an immiscible blend, due to differences in polarity, chemical nature, and their processing temperature (Rudin, Loucks, & Goldwasser, 1980). The mixing of PET and PP, even with a low amount of PP, results in droplets of PP dispersed in the PET matrix. Without any compatibilizer, two distinct, incompatible phases can be observed, and the PP phase in the physical blend is easily identified. As expected, the interpenetration of chains from the two polymers at the interface can be deduced as weak, thus resulting in poor interfacial adhesion (Baccouch, Mbarek, & Jaziri, 2017). While the PET content enhances the stiffness of the blend, particularly at higher temperatures, the polyolefin facilitates the crystallization of PET by

heterogeneous nucleation, further raising the stiffness of the blend (Sia, Guoa, Wanga, & Lau, 2008; Yi, et al., 2010).

There is a body of literature dealing with the compatibilization of the PET/PP blends using different compatibilizers (Pang, Jia, Hu, Hourston, & Song, 2000; Chiu & Hsiao, 2006; Papadopoulou & Kalfoglou, 2000). For example, the effect of various kinds of PP-grafted compatibilizers on the final morphology of PET/PP blends was highlighted by Pang et al. (2000). The compatibilizing effects of the studied PP grafts were different and depended on the functional groups present. The results revealed that the compatibilizers with a long alkyl radical unit, due to their higher compatibility with PP than with PET, played an essential role in preventing coalescence. On the contrary, the compatibilizers with hydroxyl groups reacted with the PET phase to form graft copolymers of PP and PET at blends' interfaces, leading to the reduction of interfacial tension (Pang, Jia, Hu, Hourston, & Song, 2000).

9.5. New Carpet Recycled Grades

With the results obtained in the controlled trials conducted with varying amounts of PP and ash, we were able to relay the numbers back to the suppliers to improve recycling efficiency. By filtering out the component of ash with the help of coarse filters, the minimum amount of ash impurity was found to be present in Rec PET grade 5, 5% in grade 6, and 3% in grade 7 after recycling and pelletizing the materials. The minimum amount of PP was found in Rec PET grade 5, 3-5% in grade 6, and ~3% in grade 7. The availability of resources and material paired with the machine capabilities of the different suppliers led to a difference in the impurity content of the new carpet recycled grades.

With the initial trials and optimized parameters, by itself, the new recycled grades were unable to be processed on the Biax line nor the Bi-component extrusion line. The screen got

clogged that led to the extruder pressure shooting above the machine's limitations. Even with a negligible amount of impurity content, it was evident that the material required a modifier that would tackle the incompatibility of PP and PET, a coarse mesh for fine $CaCO_3$ particles, and a blend of virgin polymer to maintain viscosity during processing.

9.6. Conclusion

Whenever there have been talks and reports about recycled PET, they have usually referred to plastic bottle waste recycled PET. A crucial difference between carpets and the bottles is the composition and impurities found in carpet recycled PET. In terms of product applications, old carpets can go into products such as composite lumber, construction – roofing shingles, railroad ties, automotive parts, carpet cushion, stepping stones, etc. Most of these products last far longer than those they replace, thereby avoiding cutting down of trees or the use of chemicals as preservatives. Carpets can be kept out of landfills by requesting these products. Recovery of the energy content from old carpet, since it is made from crude oil as raw material, is also a vital outlet (CARE, 2019).

The presence of $CaCO_3$ (ash) and PP in the carpet recycled PET was established in the previous studies; it became essential to understand how these two components were affecting fiber extrusion. With the presence of ash, we realized that the screen size could be made bigger, or else the screen must be removed during extrusion. On an industrial scale, this is an unlikely scenario. Another conclusion that was realized was the application of this principle during recycling, where the carpet fluff can be filtered out with different screen sizes to ensure the amount of ash remains low. For the homocomponent spinning, there were drips during extrusion but stable fiber formation. Since PP and PET are incompatible, we would need a compatibilizer to ensure smooth processing. Drawing of fibers was not possible as they were brittle. Since we had the most success

on the melt-blowing system, we decided to conduct trials on the Biax line. For melt-blowing, the maximum limit (for impurities) that were found not to affect the set processing parameters were 2% ash and 2% PP and/or a total of 3% impurities. These numbers can change once the recycled pellet is compounded with the compatibilizer and further blended with virgin PET.

10. Chapter 10: Compatibilizer Study – Compounding with Rec PET Grades 2, and 6

10.1. Approach

Polymer blending is one of the most important and continuously growing sectors of polymer engineering. It is an economical method to produce new engineering materials as indicated by a large number of versatile polymer blends available in the market and number of patents of polymer blends registered annually (Pracella, Pazzagli, & Galeski, 2002; Thomas, Grohens, & Jyotishkumar, 2014; Utracki & Shi, 1992). Polyester has a wide application due to its thermal stability, transparency, clarity, high tensile, impact strength, and chemical resistance. PET is capable of both chemical reactions with polar polymers and polar interactions like hydrogen bonding because of the ester group (Razak, Inuwa, Hassan, & Samsudin, 2013). The polarity of these ester groups improves the interchain reaction of PET, resulting in excellent mechanical properties. These unique properties of PET are the basis for its broad application. However, considering the environmental issues such as contamination and specific processing problems, recycled PET has limited applications. R-PET also has poor mechanical properties and low molecular weight (Mariano, Federico, & Andrzej, 2002).

As reported previously in this study, carpet recycled PET primarily contained impurities in the form of PP and $CaCO_3$. PET and PP are immiscible owing to their different chemical natures and polarities. As a result, blends of these polymers exhibit phase separation, forming a continuous PET phase (matrix) and a discontinuous PP phase (dispersed phase) (Yong Wan, et al., 2018). Immiscibility in the polymers blends leads to poor interfacial bonding and poor physical and mechanical properties. The blending of recycled materials can be achieved if suitable compatibilization methods and processing technologies are used to enhance the phase dispersion and interfacial adhesion in the blends (Elabid, et al., 2016; Lepers, Favis, & Tabar, 1997).

Numerous studies have been focused on polymer blends containing compatibilizer to modify interfacial bonding and mechanical properties (Barlow & Paul, 1984; Khan, et al., 2019; Li & Xie, 2017). One way to improve the compatibility of immiscible polymeric blends is by utilizing graft or block copolymers as compatibilizers to improve the interfacial activity by reinforcing the interface. However, the major problem of this strategy is the highly controlled processability of graft copolymers used widely (Wei, et al., 2019; Deng, Bai, Liu, Zhang, & Fu, 2019; Liu, et al., 2019; Volokhova, Waugh, Arrington, & Matson, 2019; Tanrattanakul, Jaratrotkamjorn, & Juliwanlee, 2019).

Efforts to develop effective compatibilization of PET/polyolefin blends are mainly turned to reactive mixing processes through the addition of polyolefins bearing functional groups (anhydride, carboxyl, epoxy, etc.) in the chains, capable of giving rise to chemical reactions with the carboxyl and/or hydroxyl end-groups of PET during melt blending (*in situ* compatibilization) (Fu, Chen, Xu, Wang, & Wang, 2016; Si, Guo, Wang, & Lau, 2008; Inuwa, et al., 2014). The formation of graft copolymers contributes to a decrease in the interfacial tension as well as an increase in the adhesion between the phases (Bui, Nguyen, Ho, & Uong, 2016).

10.2. Methods

The most commonly used compatibilizers can be divided into PP-based polymers and copolymers. PP-based polymers include maleic anhydride-modified PP (PP-g-MAH) and glycidyl methacrylate-grafted PP (Papadopoulou & Kalfoglou, 2000; Calcagno, Mariani, Teixeira, & Mauler, 2008; Akbari, Zadhoush, & Haghighat, 2007), and typical copolymers are a hydrogenated styrene–butadiene–styrene block copolymer, a glycidyl–methacrylate-modified styrene-b-(ethylene-co-olefin) block copolymer, an n-butyl acrylate glycidyl methacrylate ethylene terpolymer, ethylene-glycidyl methacrylate copolymer, and poly(ethylene-comethyl acrylate-co-

glycidyl methacrylate) (Yong Wan, et al., 2018). Akbari, Zadhoush, & Haghighat (2007) observed that compatibilizing effects for PET/PP blends are dependent on the quantity of loading of PP-g-MAH into the blends. Papadopoulou & Kalfoglou (2000) reported that thermoplastic polyolefin alloy (TPO) with PP/ethylene-propylene copolymer enhanced compatibilizing efficiency. Overall, the literature review shows that compatibilizers play an essential role by enhancing the mechanical properties of miscible blends.

Considering the points mentioned above, in this experimental research, carpet recycled PET that contained varying amounts of PP were compounded with Vistamaxx^{TM} 6502 provided by ExxonMobil. It is an isotactic propylene repeat unit with random ethylene distribution compatibilizer, produced using their proprietary metallocene catalyst technology. Metallocenes are advantageous metal catalysts, which consist of minute particles of positively charged metal ions. These are sandwiched between two cyclopentadienyl anions having five atoms per ring. They are also known as single-site catalysts because they have only one active site per catalyst particle, of which, all are identical (Polymer Database, 2020). The metallocene-catalyzed polymerization has many advantages over traditional polymerization techniques; it results in very pure, and consistent resins with well-defined properties. Several derivatives of early metallocenes were active catalysts for olefin polymerization. Unlike traditional and still widely used heterogeneous Ziegler-Natta catalysts, metallocenes are homogeneous. The polymerization with metallocenes and other coordination catalysts involves the coordination of the monomer to the transition metal site before insertion at one end of the polymer chain. The coordination step is generally responsible for the versatility of these catalysts (Polymer Database, 2020).

10.2.1. Materials and Processing

Carpet Recycled grades 2 and 6 were used for the compatibilizer study. They were representative of the recycled materials that are readily supplied in the East and West coast. ExxonMobil provided us with Vistamaxx^{TM} 6502, which has a mass flow rate of 45 g/10min and 13 wt% ethylene content. First, the recycled blends were compounded with 3% and 7% of the compatibilizer. Techmer carried out the process of compounding in Tennessee. Then, the rec-PET/6502 materials were melt-blown to produce nonwoven webs.

Table 27. Properties of the carpet recycled PET pellets.

Polymer	**PET (wt%)**	**PP (wt%)**	**Ash (wt%)**	**T_m (°C)**	**[η] (dL/g)**
Virgin PET	100	-	-	252	0.61
Rec PET grade 2	74	20	6	252	0.54
Rec PET grade 6	90	5	5	252	0.58

Before processing, the pellets were dried at 248F (120°C). The compounded pellets were melt-blown on the Biax Line. The die temperature was maintained from 270-280°C, the extruder temperature at 290°C, extruder rpm at 25, the die air pressure was set at 13.9 psi (0.9 bar), and die-to-collector distance (DCD) at 15cm. Different blends of rec-PET/6502 with virgin PET were created. The weight ratio of the components in the blending is listed below in table 28. Since grade 2 pellets had a maximum of 20 wt.% of PP, two loadings of 6502 were utilized (3 wt.% and 7 wt. %). A blank control experiment with virgin PET was also carried out.

Table 28. The weight ratio of components in the blends.

Blends	PET (wt%)	PP (wt%)	Ash (wt%)	Vistamaxx 6502 (wt%)
G2-PET/PP/Ash	74	20	6	-
G2-PET/PP/Ash/3C	71	20	6	3
G2-PET/PP/Ash/7C	67	20	6	7
G6-PET/PP/Ash	90	5	5	-
G6-PET/PP/Ash/3C	87	5	5	3

10.2.2. Thermal Analysis

The instrument used for Differential Scanning Calorimetry was Discover Series DSC. In this study, the meltblown webs were evaluated while heating at 10°C/minute in a flowing 50cc/minute nitrogen atmosphere. The polymers were also equilibrated at 25°C. The thermal properties of the Recycled PET pellets, such as the crystallization temperature (T_c), melting temperature (T_m), enthalpy of crystallization (ΔH_c), enthalpy of melting (ΔH_m), and enthalpy of cold-crystallization temperature (ΔT_{cc}) can be calculated from the DSC curves. The percentage of apparent crystallinity (X_c) was calculated using the equation below:

$$X_c\% = \left(\frac{\Delta H_m - \Delta H_{cc}}{\Delta H_m^0}\right) x\ 100$$

where ΔH_m^0 is the heat of fusion of a 100% crystalline PET sample and has a value of 140 J/g, and for a 100% crystalline PP, it has a value of 207 J/g.

10.2.3. Optical Analysis

The meltblown samples were sputter-coated with a thin layer of gold and analyzed with a scanning electron microscope to examine the fiber morphology. A scanning electron

microscope (SEM) scans a focused electron beam over a surface, thus creating an image. We can obtain information about the surface topography and composition. The instrument used was Phenom Pro desktop SEM with a resolution <8nm (SE) and <10nm (BSE), magnification up to 150,000x. Images were taken at 10,000-x under 5kV of an accelerating voltage for the electron beams. Fiber diameters were measured using the Phenom Suite Fiber Metric software. For each meltblown web, at least 100 individual fiber diameters were measured.

10.3. Results and Discussion

10.3.1. Thermal Properties

Figures 43-47 show the DSC scans of compatibilized grade 2 pellets with a 3% and 7% loading of 6502, respectively. These have been blended with virgin PET at different ratios of 5:95, 10:90, 15:85, 20:80, 25:75, and 30:70. The crystallization could be observed in the cooling scan, and the melting process was recorded in the heating scan as well.

An exothermic peak known as “cold crystallization" (Cobbs & Burton, 1953) arises from the crystallization of the amorphous phase. This phenomenon is typical of polymers such as PET. This arises from the weak mobility of planar benzenic nuclei (sp^2 hybridization of carbon) and can easily be explained: chains being frozen, the heating involves critical mobility leading to the reorganization of the structure (Torres, Robin, & Boutevin, 2000).

The evident crystallization peak (T_c) of the polymer blends, observed in table 29, was closer to PET than the polyolefin. Noticeably, there is only one melting peak indicating the melting point of PET. The crystallization temperature of the blends was also lower than the uncompatibilized polymer (Rec PET grade 2). This might be ascribed to the plasticizing effect the compatibilizer may have on the PET/PP blend and the facilitation of crystallization. From these

results, it may be speculated that the PET/PP blends are materials that have a homogeneous structure (Wagner, et al., 2008; Chiu, Yen, & Lee, 2010).

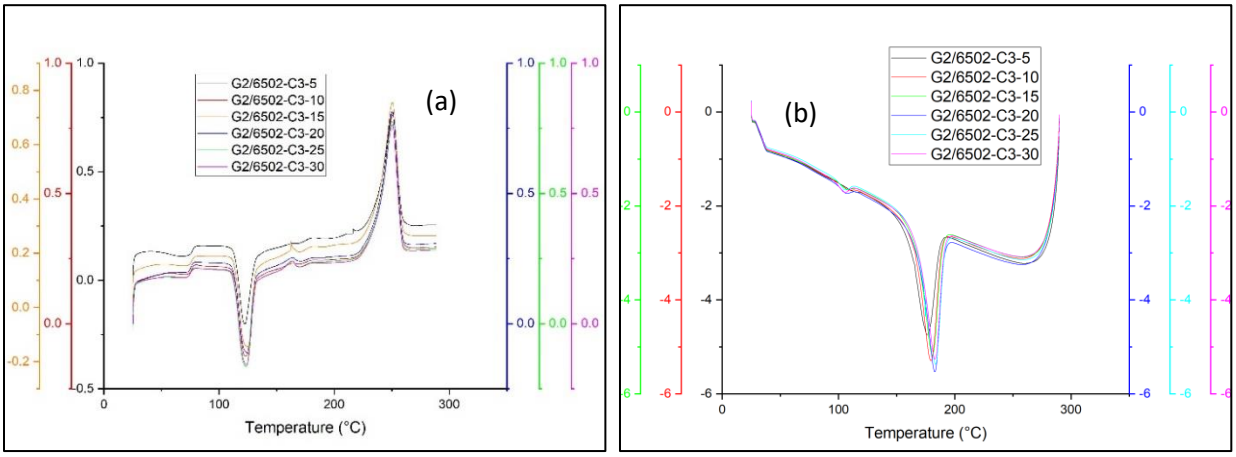

Figure 44. Heating (a) and cooling (b) DSC scans of Rec PET grade 2, compatibilized with 3% Vistamaxx 6502, and blended with virgin PET.

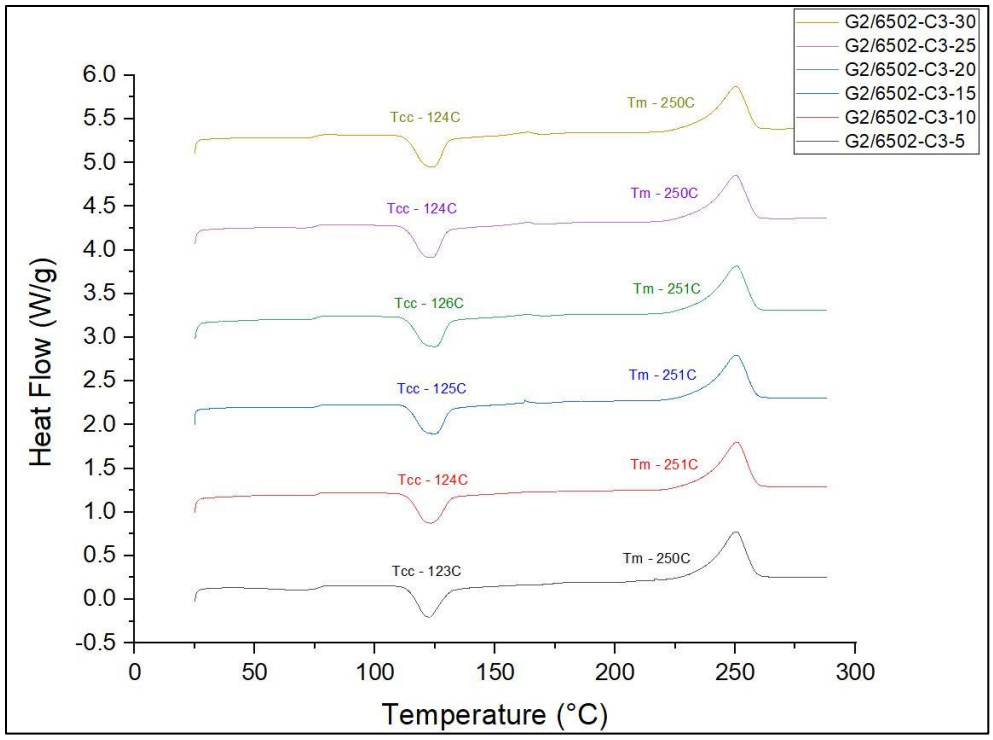

Figure 45. Heating DSC curves of Rec PET grade 2, compatibilized with 3% Vistamaxx 6502 and blended with virgin PET.

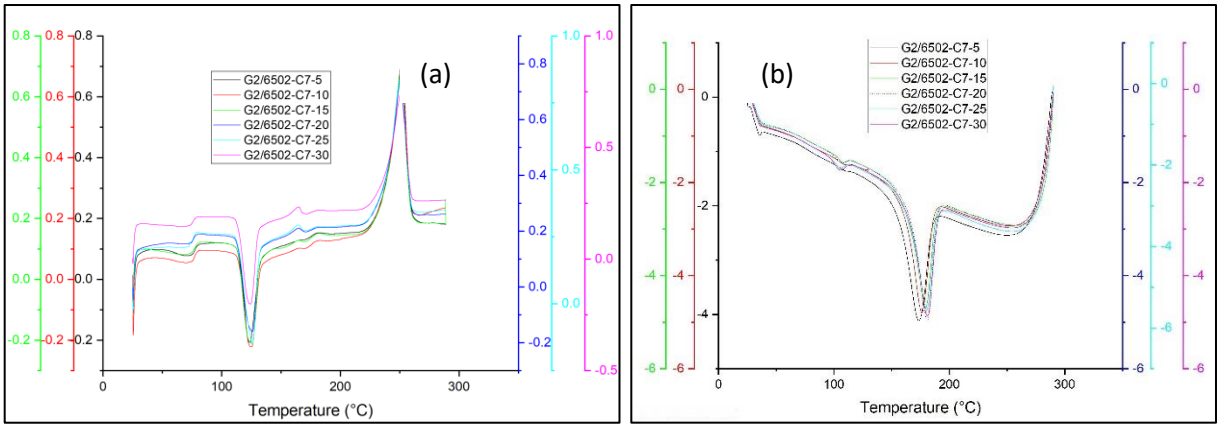

Figure 46. Heating (a) and cooling (b) DSC scans of Rec PET grade 2, compatibilized with 7% Vistamaxx 6502, and blended with virgin PET.

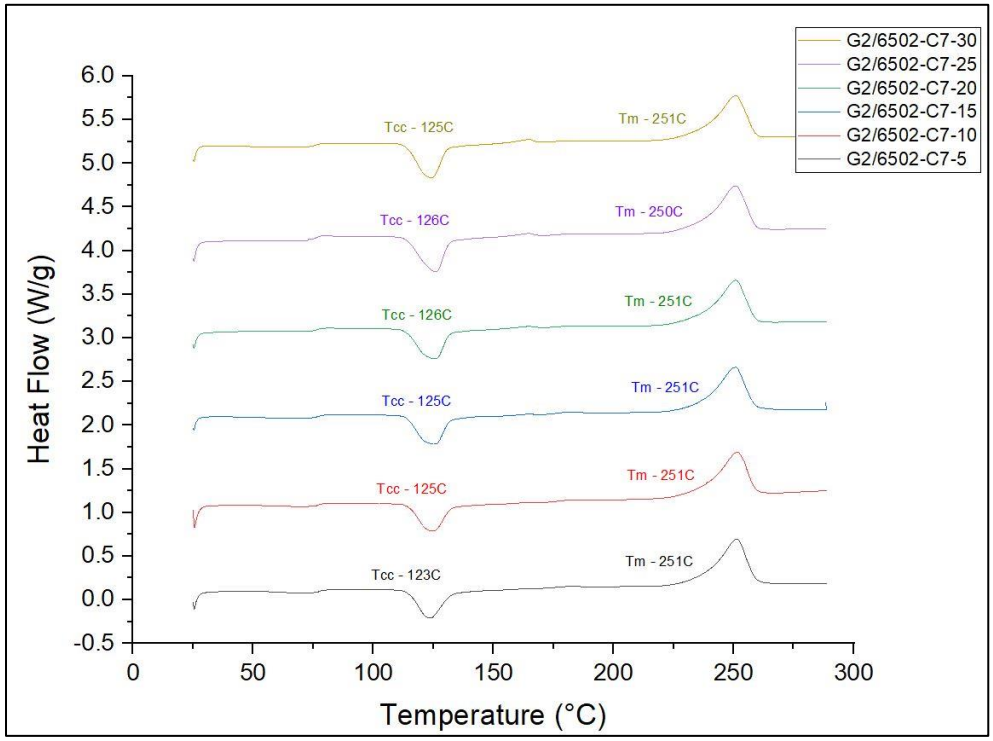

Figure 47. Heating DSC curves of Rec PET grade 2, compatibilized with 7% Vistamaxx 6502 and blended with virgin PET.

A miscible polymer blend is homogeneous down to the molecular level, and it constitutes a single-phase, over the full range of blend compositions, under specific conditions of pressure and temperature.

Thermodynamically speaking, the Gibbs free energy of mixing is given by the following equation:

$$\Delta G_m = \Delta H_m - T\Delta S_m$$

where ΔH_m is the enthalpy of mixing, and ΔS_m is the entropy of mixing. Full miscibility is achieved when two conditions are satisfied:

1. The Gibbs free energy of the system is negative (spontaneous process) (figure 48). A homogenous mixture on a concave curve has lower free energy than any mixture of two phases it could separate into, and therefore, is always in stable equilibrium (Polymer Database, n.d.)

2. The second derivative of the Gibbs free energy with respect to the volume fraction of a component in the blend is positive (phase stability).

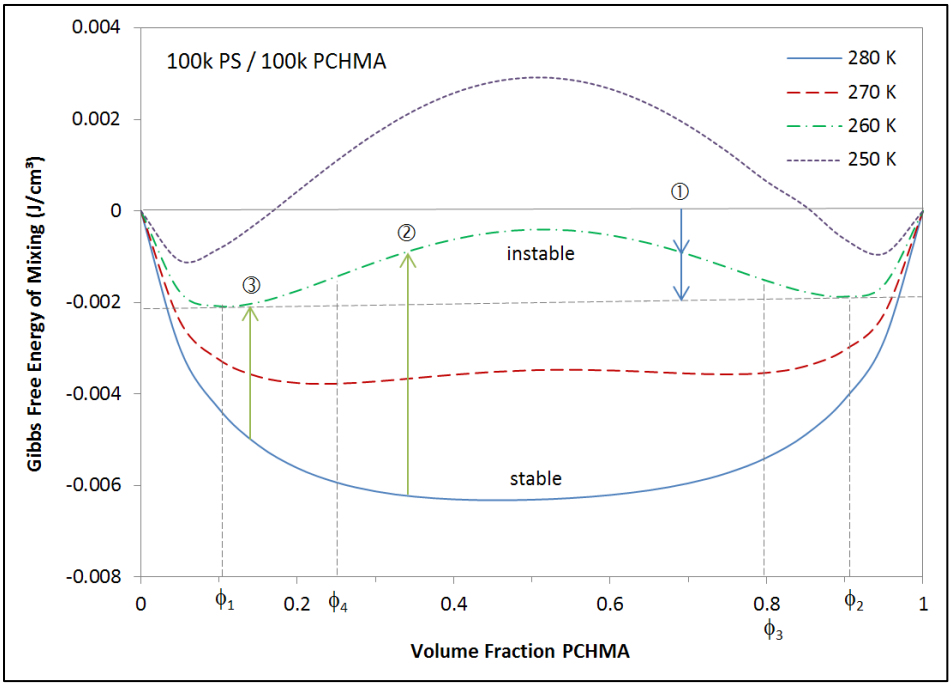

Figure 48. Example of Gibbs Free Energy curve.

It must be considered that ΔH_m refers to the interactions between the polymer chains. It is negative (exothermic) when attractive polar interactions (strong covalent and ionic, in the case of

bonding strong interactions, or dipole-dipole, hydrogen, etc., in the case of weak nonbonding interactions) are present. In contrast, it is positive (endothermic) when repulsive van der Waals interactions are present. ΔS_m is related to the degree of randomness, all the possible ways that the chain units can be arranged in space. A polymer blend made up of PET and PP is an entirely immiscible system, meaning that the two polymers are incompatible. This is because polymers with high molecular weight create a blend with limited possible arrangements; therefore, ΔS_m results to be minimal (Graziano, Jaffer, & Sain, 2019).

Moreover, PET and PP have no attractive polar interactions. Thus, ΔH_m is positive (endothermic), which leads to a positive ΔG_m. The thermodynamic differences, in the case of a PET/PP binary polymer system, hinder the overall properties of the final product, preventing it from being used for novel and high demanding commercial applications. The unbalanced thermodynamics between two immiscible polymers create excess energy at the interface between these two polymers. This is the interfacial tension (Graziano, Jaffer, & Sain, 2019).

Table 29. Crystallization and melting temperatures for the compatibilized Rec PET grade 2 blends.

Polymer	***Carpet Rec PET grade 2***							
	T_g (°C)	**T_{cc} (°C)**	**ΔH_{cc} (J/g)**	**T_c (°C)**	**ΔH_c (J/g)**	**T_m (°C)**	**ΔH_m (J/g)**	**X_c (%)**
Pure PET	76	-	-	184	39.77	253	43.67	31.1
Pure PP	-	-	-	116	98.8	168	84.24	41.2
G2-PET/PP/Ash	70	118	17.83	218	39.4	253	33.55	11.23

Table 29 (continued)**.**

Polymer	*Carpet Rec PET grade 2*							
	T_g (°C)	**T_{cc} (°C)**	**ΔH_{cc} (J/g)**	**T_c (°C)**	**ΔH_c (J/g)**	**T_m (°C)**	**ΔH_m (J/g)**	**X_c (%)**
G2-PET/PP/Ash /5-3C	77	123	29.6	175	52.16	250	54.2	17.6
G2-PET/PP/Ash /10-3C	76	124	31.3	180	38.21	251	49.67	13.12
G2-PET/PP/Ash /15-3C	77	125	26.16	180	57.85	251	49.54	16.7
G2-PET/PP/Ash /20-3C	76	126	33.76	183	38.8	251	49.33	11.12
G2-PET/PP/Ash /25-3C	76	124	28.42	183	53.73	250	48.88	14.6
G2-PET/PP/Ash /30-3C	76	124	28.2	183	36.94	250	48.46	14.47
G2-PET/PP/Ash /5-7C	78	123	27.54	173	35.06	251	48.84	15.2
G2-PET/PP/Ash /10-7C	77	125	28.34	176	43.66	251	49.34	15
G2-PET/PP/Ash /15-7C	76	125	35.72	183	37.29	251	48.3	9
G2-PET/PP/Ash /20-7C	76	126	33.1	181	35.45	251	47.64	10.3
G2-PET/PP/Ash /25-7C	75	126	36.93	181	47.94	250	49.58	9
G2-PET/PP/Ash /30-7C	76	125	37.52	181	34.96	251	46.68	6.54

The melting behaviour of pure PET or pure PP and the compatibilized blends did not significantly change. In the case of PET phase, with respect to uncompatibilized Rec PET grade 2, we observe a decrease in the crystallization temperatures (T_c) by almost 40°C.

We also noticed similar observations in the compatibilized grade 6 pellets with a 3% loading of Vistamaxx 6502. These were also blended with virgin PET in ratios of 5:95, 10:90, 15:85, 20:80, 25:75, and 30:70.

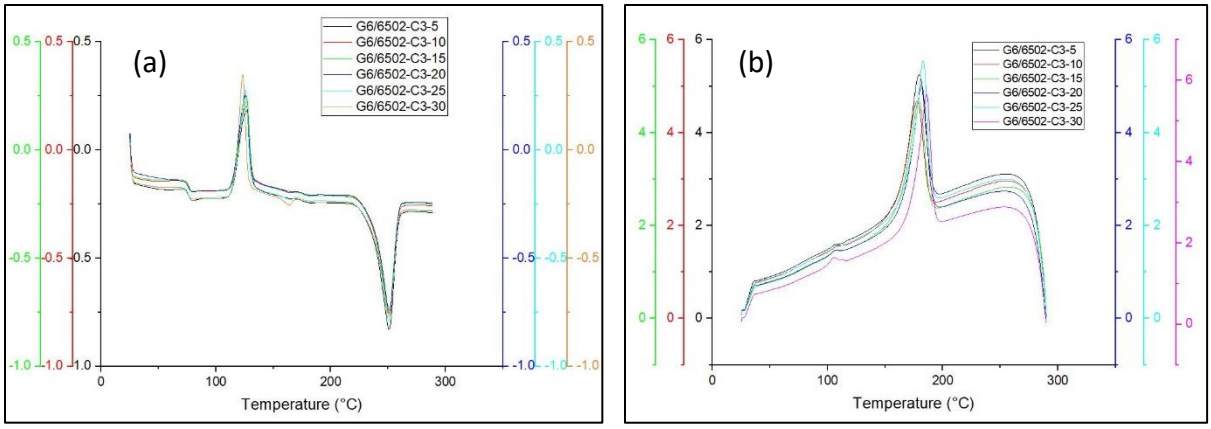

Figure 49. Heating (a) and cooling (b) DSC scans of Rec PET grade 6, compatibilized with 3% Vistamaxx 6502 and blended with virgin PET.

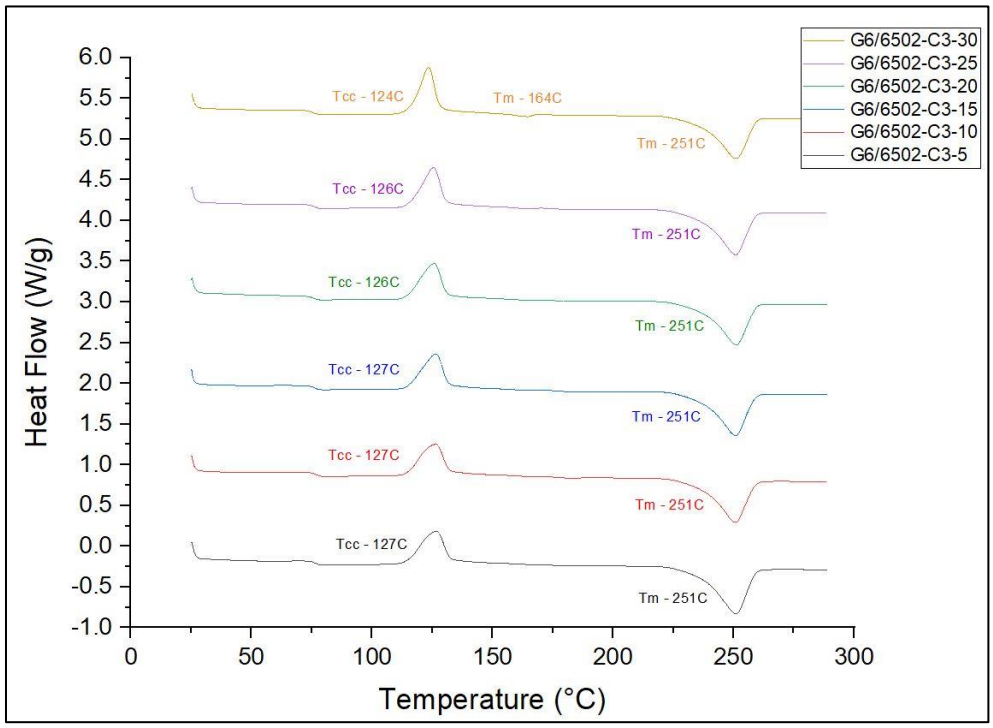

Figure 50. Heating DSC curves of Rec PET grade 6, compatibilized with 3% Vistamaxx 6502 and blended with virgin PET.

In Figure 50, we observe a single melt peak for blends 5:95, 10:90, 15:85, 20:80, and 25:75. However, for the 30:70 compatibilized blend, we can see two distinct melt peaks for both PP (164°C) and PET (251°C) components. It is a clear indication of insufficient compatibilization

between the Vistamaxx and the recycled polymer (at 30 wt.%). The melting behaviour of pure PET and the compatibilized blends did not significantly change.

Table 30. Cold crystallization and melting temperatures of compatibilized Rec PET grade 6 blends.

Polymer	***Carpet Rec PET grade 6***					
	T_g (°C)	**T_{cc} (°C)**	**ΔH_{cc} (J/g)**	**T_m (°C)**	**ΔH_m (J/g)**	**X_c (%)**
Pure PET	76	-	-	253	43.67	31.1
Pure PP	-	-	-	168	84.24	41.2
G6-PET/PP/Ash	70	120	2.80	252	40.28	26.77
G6-PET/PP/Ash /5-3C	77	127	32.43	251	52.63	14.42
G6-PET/PP/Ash /10-3C	76	126	31.3	251	48.29	12.13
G6-PET/PP/Ash /15-3C	77	127	31.88	251	49.49	12.57
G6-PET/PP/Ash /20-3C	76	126	32.46	251	47.63	10.83
G6-PET/PP/Ash /25-3C	76	126	33.89	251	49.97	11.48
G6-PET/PP/Ash /30-3C	76	124	28.59	251	48.3	14.15

In the cooling curves of the DSC scans (figures 44, 46, and 49), we observe the melt-crystallization peaks shift slightly to a lower temperature as the virgin PET content increased in the compatibilized blends. This could mean that the virgin PET component developed a crystalline structure more slowly, and their crystallization rate was lower than that of the recycled component.

An alternative explanation is that the thermal recycling process disentangles the polymer chains, thereby increasing the degree of crystallinity when the virgin PET is more (Lee, Lim, Hahm, & Kim, 2012).

10.3.2. Fiber Size Measurement

The compatibilized Rec PET grade 6 meltblown webs, blended with virgin PET, were analyzed on the SEM. With 250x magnification, we were able to observe the nonwoven structure in the meltblown webs. Figure 51 shows the average fiber diameter distribution histograms along with the optical images of the compatibilized blends. In general, we notice an increase in average fiber diameter as the recycled content increases in the compatibilized blends. At 5% grade 6 compatibilized with Vistamaxx 6502, the average fiber diameter was 8 μm whereas, at 30% grade 6 compatibilized with Vistamaxx 6502, it was 43 μm. The distribution of the meltblown fiber is log-normal for 5:95, 10:90, 15:85, and 20:80 ratios of the blends. This is quite common for meltblown structures. Hassan, Yeom, Wilkie, Pourdeyhimi, & Khan (2013) have reported an increase in fiber diameter as the throughput increased. Lowering polymer mass flow rate can decrease fiber diameter since the same drag force from the air jet is acting on a smaller polymer mass.

Figure 51. SEM images and fiber size distributions of meltblown webs - Grade 6 compatibilized with 3% Vistamaxx 6502, blended with virgin PET in ratios 5:95 (a), 10:90 (b), 15:85 (c), 20:80 (d), 25:75 (e), 30:70 (f), and 100% virgin PET (g).

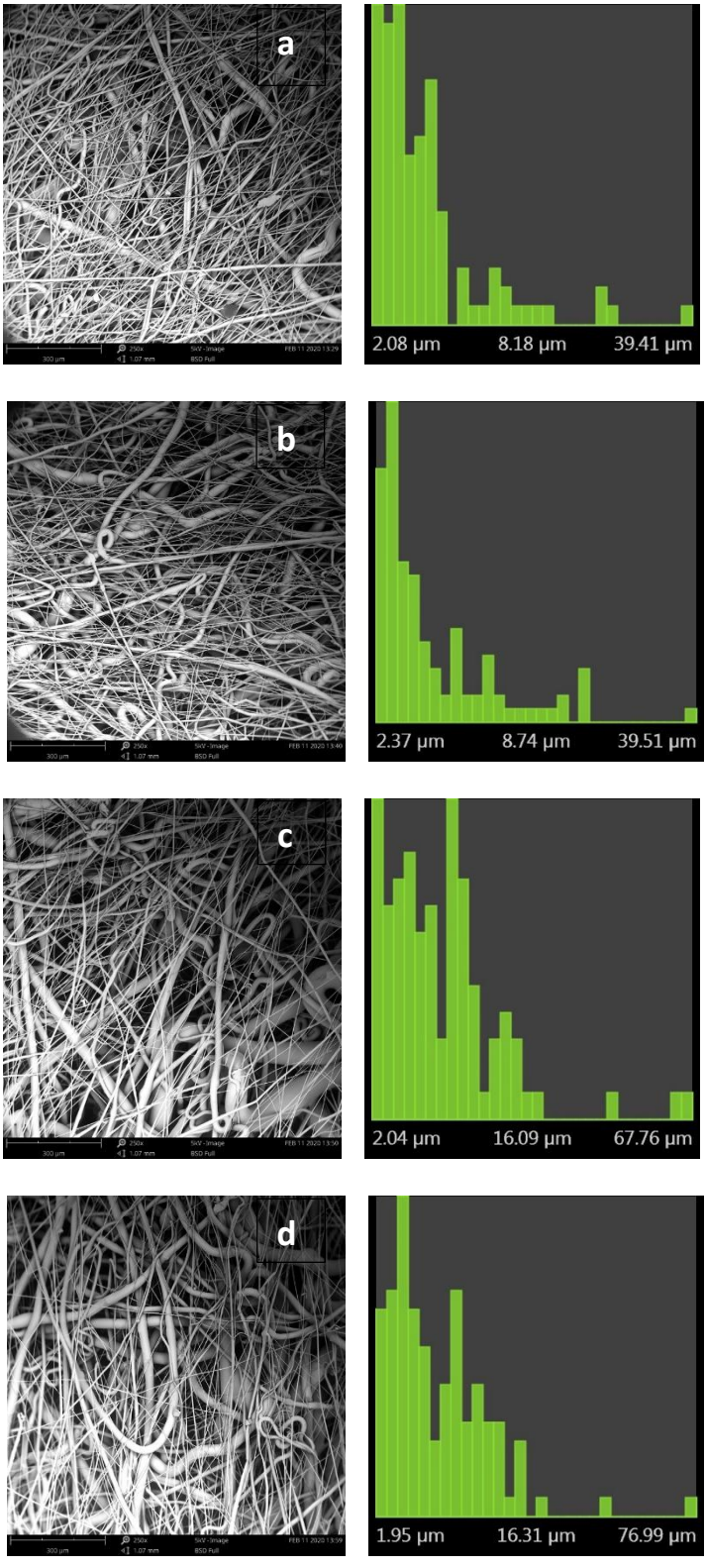
a
2.08 µm
8.18 µm
39.41 µm
b
2.37 µm
8.74 µm
39.51 µm
c
2.04 µm
16.09 µm
67.76 µm
d
1.95 µm
16.31 µm
76.99 µm

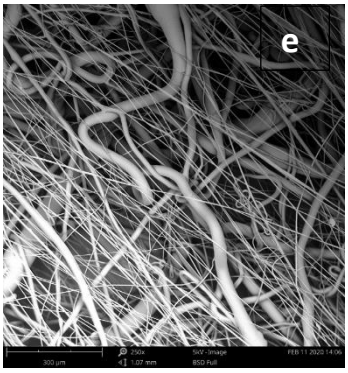
e

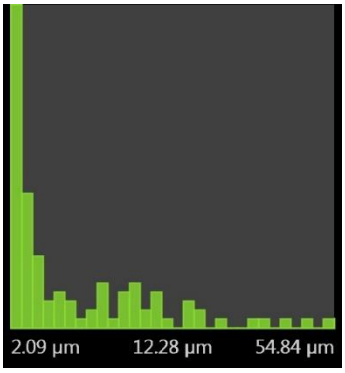
2.09 µm
12.28 µm
54.84 µm

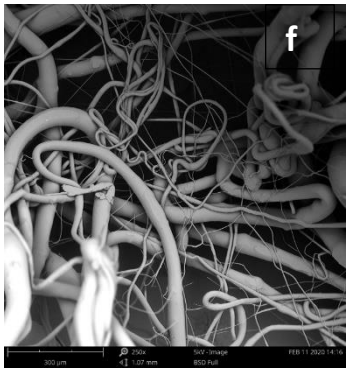
f

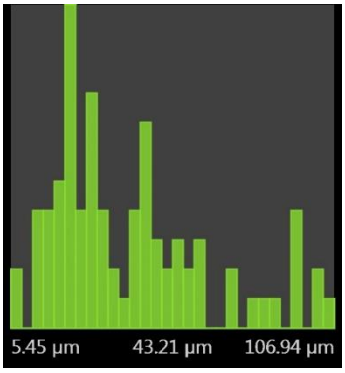
5.45 µm
43.21 µm
106.94 µm

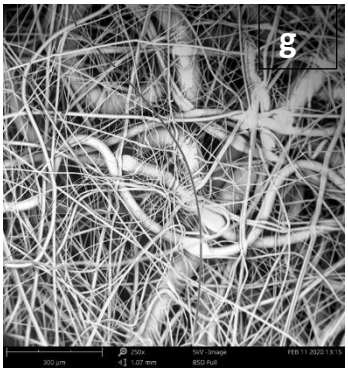
g

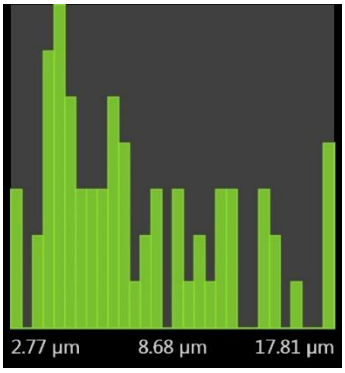
2.77 µm
8.68 µm
17.81 µm

The compatibilized Rec PET grade 2 meltblown webs (at 3 and 7% loading), blended with virgin PET, were analyzed on the SEM. With 250x magnification, we were able to observe the nonwoven structure in the meltblown webs. Figures 52-53 shows the average fiber diameter distribution histograms along with the optical images of the compatibilized blends. For 3% loading, the mean diameter is <10µm until 20% of the recycled content in the blend. At 30% recycled content, the mean diameter increased to 20 µm. For 7% loading, the mean diameter is ≤ 10µm until 30% of the recycled content in the blend. The distribution of the meltblown fiber is log-normal for 5:95, 10:90, 15:85, and 20:80 ratios of the blends at 3% loading, and log-normal for all blends at 7% loading of Vistamaxx 6502.

Figure 52. SEM images and fiber size distributions of meltblown webs - Grade 2 compatibilized with 3% Vistamaxx 6502, blended with virgin PET in ratios 5:95 (a), 10:90 (b), 15:85 (c), 20:80 (d), 25:75 (e), 30:70 (f).

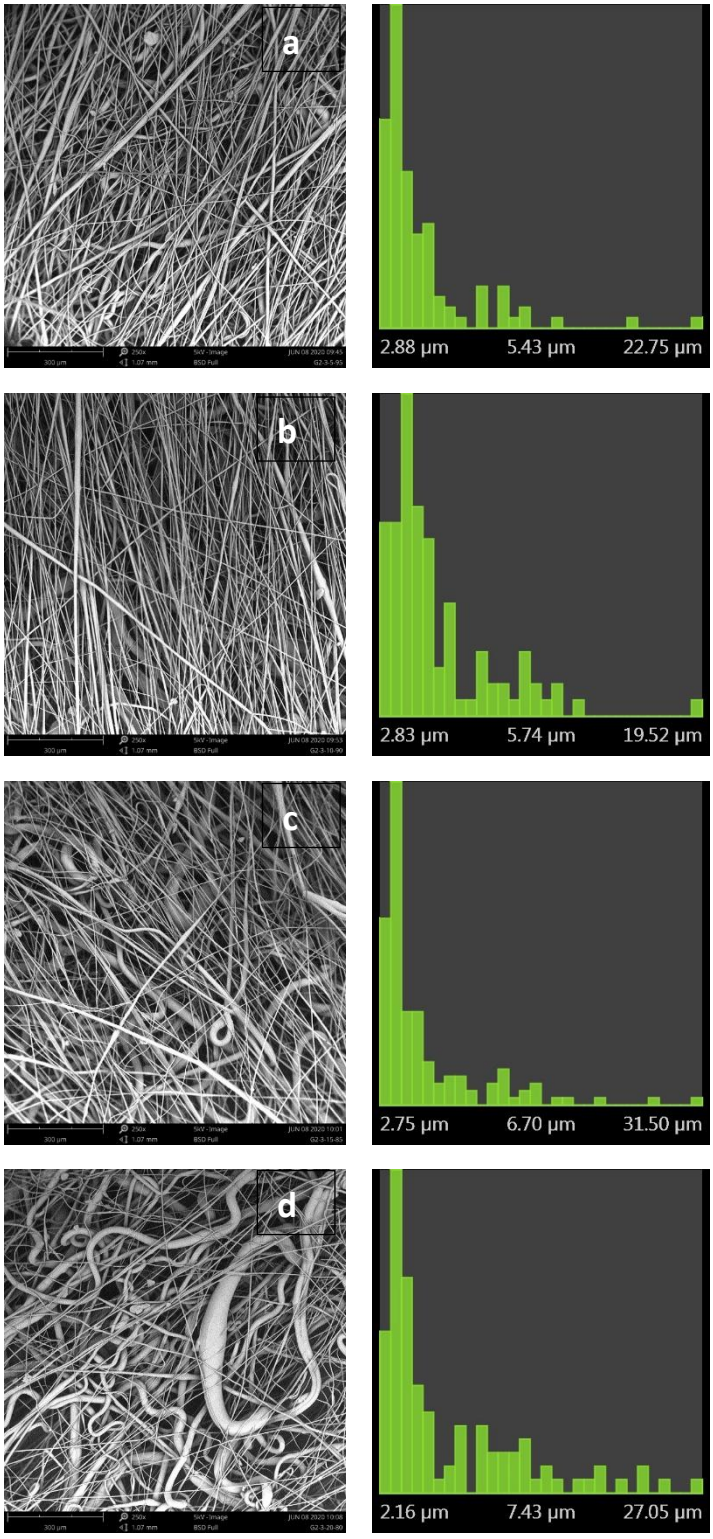
a
2.88 µm
5.43 µm
22.75 µm
b
2.83 µm
5.74 µm
19.52 µm
c
2.75 µm
6.70 µm
31.50 µm
d
2.16 µm
7.43 µm
27.05 µm

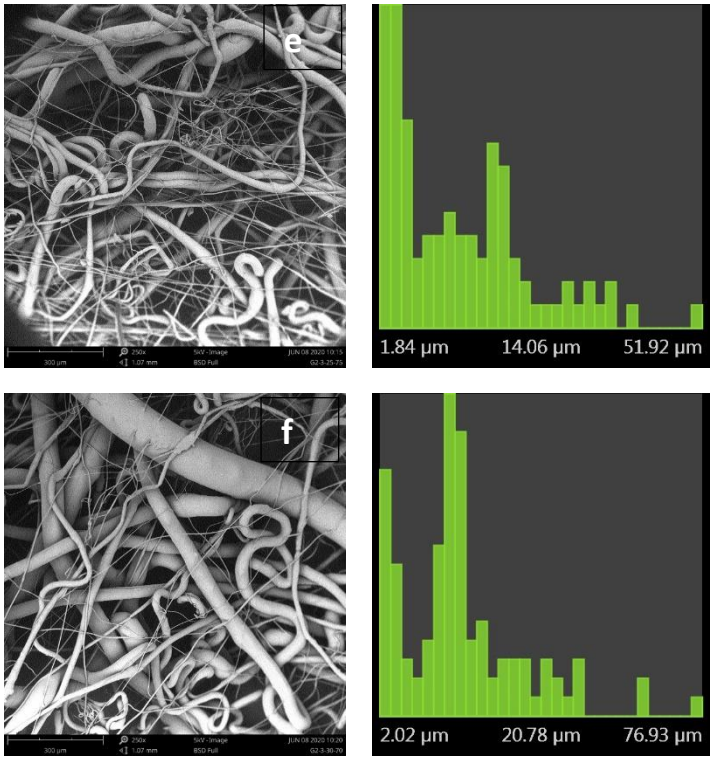
e
1.84 µm
14.06 µm
51.92 µm
f
2.02 µm
20.78 µm
76.93 µm

Figure 53. SEM images and fiber size distributions of meltblown webs - Grade 2 compatibilized with 7% Vistamaxx 6502, blended with virgin PET in ratios 5:95 (a), 10:90 (b), 15:85 (c), 20:80 (d), 25:75 (e), 30:70 (f).

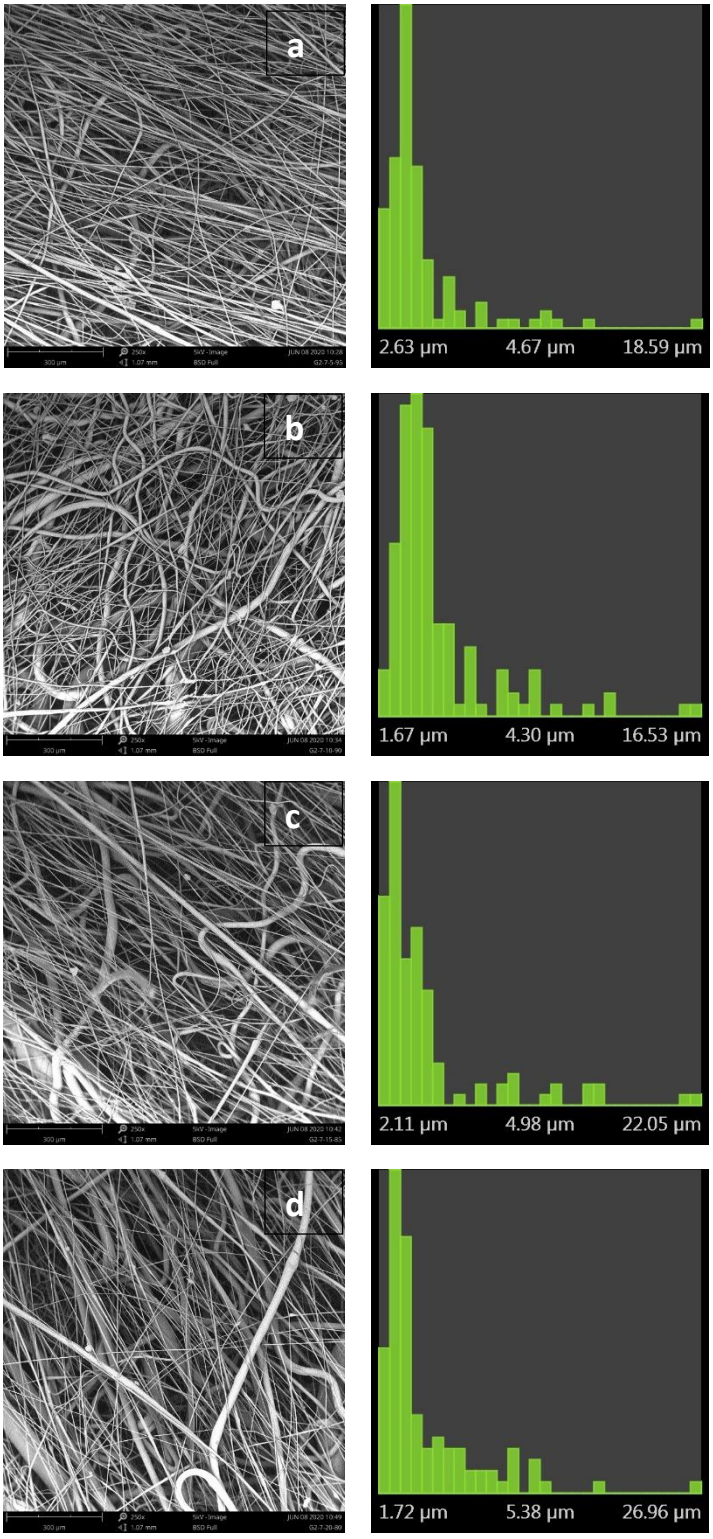
a
2.63 µm
4.67 µm
18.59 µm
b
1.67 µm
4.30 µm
16.53 µm
c
2.11 µm
4.98 µm
22.05 µm
d
1.72 µm
5.38 µm
26.96 µm

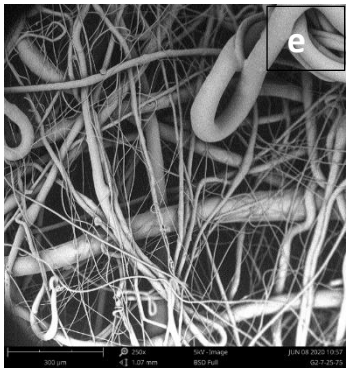
e

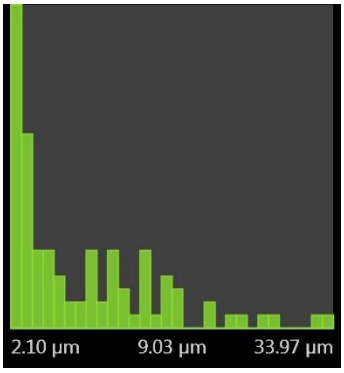
2.10 µm
9.03 µm
33.97 µm


f

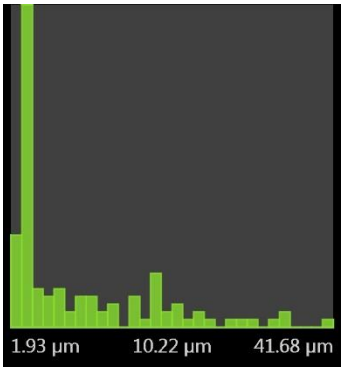
1.93 µm
10.22 µm
41.68 µm

Qin, Qu, Kaschta, & Schubert (2018) studied the effects of take-up pressure and temperature on melt-spun fiber diameters. For all PET materials, fiber diameter decreases with increasing take-up pressure independent of the processing temperature. At take-up pressures below 2 bar, the diameter of the fibers at 270°C was more significant than those at 280°C. This phenomenon can be explained with an understanding of rheology; a higher processing temperature only results in a lower melt viscosity, that enables the polymer to be extruded more easily. A better flowability of the PET melt ensures a yield of finer fibers due to localized drawing. We have also discussed in chapter 8 that the average fiber diameter can be affected by throughput rate, melt temperature, viscosity, and air temperature during processing. Further testing by SEM micrographs can help reveal the compatibilization of the carpet recycled grades of PET and its correlation to fiber diameter.

10.4. Conclusion

In this study, a compatibilizer was compounded with recycled PET and then further blended with virgin PET. Meltblown fabrics were produced to study their thermal properties and morphology. Vistamaxx 6502 was used at two different loadings (3% and 7%) for Rec PET grade 2, and 3% loading for Rec PET grade 6. These compatibilized grades were then mixed in a self-pepper approach to blend virgin PET at different ratios of 5-30 wt% recycled component. With grade 2 thermal results, we see the presence of a single melt peak in the DSC curves, indicative of a homogenous system of the polymer blend, for all ratios. The melting temperatures were closer to PET component than PP suggestive of compatibilization of the PP component and Vistamaxx 6502.

With grade 6 thermal results, there was a second distinctive exothermic peak near 165°C, which is the melting temperature of PP, for 30 wt% of the compatibilized blend. This could depict

a non-homogenous system of the polymer blend. Further, the degree of crystallization was higher when the virgin PET component was more abundant in the compatibilized blend. The crystallization rate of the recycled component was faster than the virgin component.

For the Rec PET grade 2 compatibilized blends of 3% loading, the fiber diameter was within the range of a meltblown fabric (≤ 10μm), until 20 wt% blend; for 7% loading, it was ≤ 10μm till 30 wt% blend. For the Rec PET grade 6 compatibilized blends, the fiber diameter was within the range of a meltblown fabric, except for 30 wt% blend. Analyzing the SEM micrographs can help us establish a relationship with the degree of compatibilization and diameter.

11. Summary and Future Work

This dissertation mainly explored the properties and extrusion parameters of carpet recycled PET. We initially received four different grades of carpet recycled PET. In the characterization studies, we were able to understand the thermal, rheological, and chemical properties. From the initial testing, it also became clear that a higher amount of PP or ash led to degradation in the carpet recycled PET pellets. The processing window for the recycled grades was well within the range for commercial virgin PET, except grade 1, which had the maximum impurities among all grades. It was found that the polymer composition content also affected the rheology of the polymer melt. All materials shear different, but recycled materials are sensitive to shear due to the presence of impurities in them. The carpet recycled polymers had poor viscosity and little to no melt strength, as was observed during extrusion trials. Most of the recycled grades also had oligomers present, which may explain the reduced molecular weight, and in turn, inferior properties and performance. Before the trials, we anticipated challenges during extrusion. Due to the high amount of impurities, there may be possible clogging of the screens. The presence of two immiscible polymers, PET and PP, would lead to phase separation, fiber breaks, and failure in fiber formation.

During the limited spinning and web formation trials, carpet recycled PET had poor melt strength due to low molar mass and degradation of the polymer. The mechanical strength of the undrawn fibers was low. The *salt-pepper* approach to the blending of virgin PET with recycled PET was unsuccessful and produced brittle fibers and webs. Moisture content and drying played an essential role before fiber extrusion, which was depicted during the trials on Rec PET grade 4. The presence of water and insufficient drying led to failure in fiber formation on the

homocomponent extrusion line. The first four recycled grades helped us understand the influence of PP and ash, which was analyzed in the designer PET study.

With the designer PETs, we wanted to establish the maximum amount of impurities that would be allowed for fiber spinning. By compounding virgin PET with varying amounts of PP and ash, we were able to note the limiting amount for stable formation of fibers and meltblown fabrics. A maximum of 3% of PP+ash led to stable formation on the Hills line and Biax line. Our most important learning of the study was that we could clean the material as thoroughly as possible during the recycling process. By removing all the dirt and calcium particles, we were left with a mix of polymers in the system, i.e., PET and PP.

By relaying these numbers and results to the suppliers, they were able to recycle the materials more efficiently and deliver three more grades – Rec PET grades 5, 6, and 7. The availability of resources and materials (carpets) paired with the machine capabilities present with the suppliers led to a difference in the impurity content of these grades. However, they were significantly lower than the previous four grades of carpet recycled PET. The new grades could not be melt-spun by themselves. It was evident that the material required a modifier to tackle the incompatibility of PET and PP, a coarse mesh for finer calcium particles, and a blend of virgin polymer to maintain viscosity during processing.

Usually, a compatibilizer concentrates at the interface during blending, and plays a vital role in reducing interfacial tension, preventing coalescence, and strengthening interfacial adhesion. Such compatibilizations often result in stabilized morphologies with a fine dispersion of the minor phase (PP) in the matrix (PET). ExxonMobil's Vistamaxx 6502 was compounded with Rec PET grades 2 and 6 at 3 and 7wt% loading and 3 wt% loading, respectively. The compatibilized polymers were then blended with virgin PET, in a *salt-pepper* approach, in ratios 5:95, 10:90,

15:85, 20:80, 25:75, and 30:70. Stable meltblowing of nonwoven fabrics were possible with the blends.

We were able to answer the "what" and "why" part of the research questions and moved on to answer, "how." At the end of this research, we hoped the results obtained could provide benchmark extrusion parameters and composition of modifiers in the recycled PET pellet, which was achieved in the three-year study. We suggest keeping the investigation ongoing by carrying out more tests on the compatibilized meltblown fabrics and compare the rheological properties and performance of the fabrics. The influence of calcium particles was seen during mechanical testing of the bicomponent fibers. The particles agglomerate and act as stress concentrators that led to eventual fiber breaks and relatively lower tensile strength. We suggest studying the calcium particles and figuring out the particle size to filter them out prior to processing. In the future, it may also help to study a variety of modifiers such as different compatibilizers, chain extenders or a combination, and their effects on the properties of the carpet recycled polymer.

There are also possible applications wherein meltblown polyester fabrics could be used – such as spunbond-meltblown-spunbond fabric (SMS) or produce laminated composites with other substrates. Utilizing these fabrics for products such as carpet cushions, insulation, fiberfill, geosynthetics, and geotextiles, wherein the appearance, feel, and texture will not be a priority, can be a viable option. Maintaining an eye on the economic value of the recycled polymer can also allow us to produce products with standard properties, lower prices, and better marketability. To solve the chemical affinity between the immiscible phases and modifier, while improving material properties, is the fundamental crux of the problem of carpet recycled polyester.

12. References

Abbasi, M., Mojtahedi, M. R., & Khosroshahi, A. (2007). Effect of spinning speed on the structure and physical properties of filament yarns produced from used PET bottles . *Appl Polym Sci*, 103; 3972-3975.

Aharoni, S., & Masilamani, D. (1986). *USA Patent No. US Patent 4 468 720.*

Akbari, M., Zadhoush, A., & Haghighat, M. (2007). *J. Appl. Polym. Sci.*, 104, 3986.

Al-Salem, S. (2009). Establishing an integrated databank for plastic manufacturers and converters in Kuwait. *Waste Management*, 479-484.

Al-Salem, S., Lettieri, J., & Baeyens, J. (2009). Recycling and recovery routes of plastic solid waste. *Waste Management*, 2625-2643.

Aoyama, M., & Tanaka, Y. (2016). History of Polyester Resin Development for Synthetic Fibers and Its Forefront. In T. S. Technology, *High-Performance and Specialty Fibers* (pp. 67-82). Japan: Springer.

Ariffin, A., Jikan, S., Samsudin, M., Ariff, Z., & Ishak, Z. (2006). Melt elasticity phenomenon of multicomponent (talc and calcium carbonate) filled polypropylene. *Journal of Reinforced Plastics and Composites*, 25(9), 913-923.

ASTM. (2011). *Standard Test Method for Determining Inherent Viscosity of Poly(Ethylene Terephthalate) (PET) by Glass Capillary Viscometer.* West Conshohocken, PA, USA: ASTM.

ASTM Standard. (2003). D4466 Standard Terminology for Multicomponent Textile Fibers. *ASTM International,*. Retrieved from www.astm.org.

Awaja, F., & Pavel, D. (2005). Statistical models for optimisation of properties of bottles produced using blends of reactive extruded recycled PET and virgin PET. *European Polymer Journal*, 2097-2106.

Baccouch, Z., Mbarek, S., & Jaziri, M. (2017). Experimental investigation of the effects of a compatibilizing agent on the properties of a recycled poly(ethylene terephthalate)/polypropylene blend. *Polym. Bull.*, 74, 839-856.

Barlow, J., & Paul, D. (1984). Mechanical compatibilization of immiscible blends. *Polym Eng Sci*, 24, 525–534.

Bhat, G., & Kotra, R. (2008). Development of structure and properties during spun bonding of metallocene catalysed polypropylene. *Polymer plastic Technology and Engg*, 47 (5), 542-549.

Biax Fiber-Film. (2018, April 26). *Spun-blown/Melt-blown systems*. Retrieved from Biax Fiber-film: http://www.biax-fiberfilm.com/spunblownmeltblown/

Bigham, K. (2018). *Drawn Fiber: Polymers, process, and properties.* Resinate.

Bork, J., SR, S. P., Schroeder, A., & Heise, W. (2014). *US Patent No. US8864057 B2*.

Bui, T. T., Nguyen, D. A., Ho, S. V., & Uong, H. T. (2016). *J. Appl. Polym. Sci.* , 133, 43920.

Burich, B., & Murdock, D. (2014). *US Patent No. US20140251545 A1*.

Butler, I. (1999). Introduction to spunbonded materials. In I. Butler, *The Spunbond and Melt Blown technology handbook* (pp. 1-20). Raleigh, North Carolina, USA: INDA, Printing by Design.

C.A.R.E. (2014, June 16). *A Look at the Current Challenges and Opportunities for PET Carpet*. Retrieved from Developing Market Based Solutions for the Recycling & Reuse of Post-Consumer Carpet: https://carpetrecovery.org/a-look-at-the-current-challenges-and-opportunities-for-pet-carpet/

Calcagno, C. I., Mariani, C. M., Teixeira, S. R., & Mauler, R. S. (2008). *Compos. Sci. Technol.* , 68, 2193.

CARE. (2018). *CARE Annual Report 2017*. CARE.

CARE. (2019, September 17). *About CARE*. Retrieved from CARE: https://carpetrecovery.org/about-care/faqs/

Chang, Y., Chen, H.-L., & Francis, S. (1999). Market Applications for Recycled Postconsumer Fibers. *Family and Consumer Sciences Research Journal*, 320-340.

Chiu, F., Yen, H., & Lee, C. (2010). Characterization of PP/HDPE blend-based nanocomposites using different maleated polyolefins as compatibilizers. *Polym. Test.*, 29, 397–406.

Chiu, H., & Hsiao, Y. (2006). Compatibilization of poly(ethylene terephthalate)/polypropylene blends with maleic anhydride grafted polyethylene-octene elastomer. *J Polym Res*, 13, 153–160.

Cobbs, W., & Burton, R. (1953). *J Polym Sci*, 10, 275.

Coca Cola. (2017, June 29). *Stages of PET Recycling*. Retrieved from Infineo: http://www.infineo-economiecirculaire.com/en/factory-tour/the-steps-of-pet-recycling-plastic..html

Cooke, T. (1996). Bicomponent Fiber. In L. M., & J. Preston (Eds.), *Handbook of Fiber Science and Technology: High Technology Fibers Part D; 14th ser. 3* (p. 264).

Cooke, T. (1996). *High technology fibers.* (M. Lewin, & J. Preston, Eds.) New York: Marcel Dekker Inc.

Dasdemir, M., Maze, B., Anantharamaiah, N., & Pourdeyhimi, B. (2012). Influence of polymer type, composition, and interface on the structural and mechanical properties of core/sheath type bicomponent nonwoven fibers. *Journal of Material Science*, 47:5955–5969.

DeLucia, M. L., & Hudson, R. L. (2004). *US Patent No. US6797377B1*.

Demetris, B., & George, K. (1996). Chain extension of polyesters PET and PBT with two new diimidodiepoxides. *II. J Polym Sci A Polym Chem*, 34(7):1337–42.

Deng, S., Bai, H., Liu, Z., Zhang, Q., & Fu, Q. (2019). Toward Supertough and heat-resistant stereocomplex-type polylactide/elastomer blends with impressive melt stability via in situ formation of graft copolymer during one-pot reactive melt blending. *Macromolecules*, 52, 1718–1730.

Devaux, E. (2014). Understanding the behaviour of synthetic polymer fibres during spinning. In A. i. polymers, *D. Zhang* (pp. 31-47). Woodhead Publishing.

Dijkstra AJ, G. I. (1971). *USA Patent No. US Patent 3 533 157.*

Dupuis, D. (2009). Textile processes: the importance of rheology . *Mecanique and Industries* , 10 (1). 21–25.

Dupuis, R., Nelson, D., & Soane, D. (1991). Evaluating thermal stability of nonwoven polyester. *International Symposium on Roofing Technology* (pp. 432-435).

Dutton, K. (2008). Overview and Analysis of the Meltbown Process and Parameters. *Journal of Textile and Apparel, Technology and Management*, 6(1), 1-25.

East, A. J. (2004). Polyester Fibres. In J. E. McIntyre, *Synthetic Fibres: Nylon, Polyester, Acrylic, Polyolefin* (pp. 95-166). Cambridge, England: Woodhead Publishing.

EcoGreen Equipment. (2017, July 5). *Secondary Recycling: What it is and why we need more of it*. Retrieved from EcoGreen Equipment: http://ecogreenequipment.com/secondary-recycling-what-it-is-and-why-we-need-more-of-it/

Elabid, A. E., Zhang, J., Shi, J., Guo, Y., Ding, K., & Zhang, J. (2016). *Appl. Surf. Sci.* , 375, 26.

Fibers., B. C. (18 Sept. 2002). *Patent No. EP1241284 A1*.

Fu, J. H., Chen, X. D., Xu, Q. J., Wang, R. Y., & Wang, X. J. (2016). *Polym. Compos.*, 37, 1167.

Gahan, R., & Zguris, C. (2000). A review of the melt blown process. *Battery Conference on Application and Advances* (pp. 145-149). The Fifth Annual.

Gaia. (2016). *Swept Under The Carpet: Exposing the greenwash of the U.S. Carpet Industry*. GAIA.

Garside, M. (2019, August 15). *Polyester fiber production globally 1975-2017*. Retrieved from Statista: https://www.statista.com/statistics/912301/polyester-fiber-production-worldwide/#:~:text=This%20statistic%20shows%20the%20production,to%2053.7%20million%20metric%20tons.

Geller, V. E. (2016). Similarities and differences in structure formation processes in polyester yarns during orientational drawing and high-speed spinning: A review. *Fibre Chemistry*, 47 (5), 433-445.

Graziano, A., Jaffer, S., & Sain, M. (2019). Review on modification strategies of polyethylene/polypropylene immiscible thermoplastic polymer blends for enhancing their mechanical behaviour. *Journal of Elastomers and Plastics*, 51(4), 291-336.

Gupta, V., & Bashir, Z. (2005). PET fibers, films, and bottles: sections 5–7. In *Handbook of Thermoplastic Polyesters*, (pp. 362–388.). Wiley-VCH, Verlag GmbH & Co.

Hassan, M. A., Yeom, B. Y., Wilkie, A., Pourdeyhimi, B., & Khan, S. A. (2013). Fabrication of nanofiber meltblown membranes and their filtration properties. *Journal of Membrane Science*, 336-344.

Haworth, B., & Jumpa, S. (1999). Extensional flow characterization and extrusion blow molding of high density polyethylene modified by calcium carbonate. *Plastics, Rubber and Composites*, 28(8), 363-378.

He, S.-S., We, M.-Y., Liu, M.-H., & Xue, W.–L. (2014). Characterization of virgin and recycled poly(ethylene terephthalate) (PET) fibers. *Journal of the Textile Institute*, 800-806.

Hegde, R. R., Dahiya, A., Kamath, M. G., Jangala, K., & Kotra, R. (2016). Introduction: Bicomponent Fibers. Institute of Science and Technology.

Helm, D. (2016, August). *Carpet Recycling Update: The pros and cons of subsidies and fees*. Retrieved June 12, 2020, from Floor Daily: https://www.floordaily.net/floorfocus/carpet-recycling-update-the-pros-and-cons-of-subsidies-and-fees-augsep-16

Hills Inc. (2013, Nov). Lab-scale-bicomponent. West Melbourne, FL.

Hind, J. (1999). *Recycling of Polymers.* Retrieved from Plastics Consultancy Network: http://www.pcn.org/Technical%20Notes%20-%20Recycle1.htm

Hiroo, I., & Shunichi, M. (1986). Chain extenders for polyesters. III. Addition-type nitrogen-containing chain extenders reactive with hydroxyl end groups of polyesters. *J Appl Polym Sci*, 2(4): 4581–94.

How Polymers Work. (2020). *Meaning of MW*. Retrieved June 13, 2020, from How Polymers Work: https://pslc.ws/macrog/weight.htm

How Polymers Work. (2020). *The meaning of mechanical*. Retrieved June 12, 2020, from How Polymers Work: https://pslc.ws/macrog/mech.htm#:~:text=A%20polymer%20has%20tensile%20strength,Fibers%20need%20good%20tensile%20strength.&text=A%20polymer%20sample%20has%20flexural,one%20tries%20to%20bend%20it.

Instron. (2018, April 18). *Melt Flow Rate*. Retrieved from Instron: https://www.instron.us/en-us/our-company/library/glossary/m/melt-flow

Intertek. (2018, June 11). *Melt Flow Rate ASTM D 1238, ISO 1133*. Retrieved from Intertek: http://www.intertek.com/polymers/testlopedia/melt-flow-rate-astm-d1238/

Intertek. (2018, June 11). *Rheology of Polymers*. Retrieved from Intertek: http://www.intertek.com/polymers/rheology/

Inuwa, I. M., Hassan, A., Wang, D. Y., Samsudin, S. A., Haafiz, M. K., Wong, S. L., & al, e. (2014). *Polym. Degrad. Stab.*, 110, 137.

J., S. (1998). *Polymer recycling, science, technology and applications.* New York: Wiley.

Jabarin, S. (1987). Crystallization kinetics of polyethylene II. Dynamic crystallization of PET. *J. Appl. Polym. Sci.* , 97–102.

Jabarin, S. (1987). Crystallization kinetics of polyethylene I. Isothermal crystallization from the melt. *J. Appl. Polym. Sci.*, 85-96.

Jeffries, R. (1971). *Bicomponent fibres.* Watford: Merrow Publishing Co. Ltd.

Jordi Labs. (2018). *Molecular Weight Analysis.* Boston: Jordi Labs.

Khan, Q., Mushtaq, M., Khan, S., Kiani, M., Zaman, F., & Khan, K. e. (2019). Enhancement of mechanical and electrical properties for in situ compatibilization of immiscible polypropylene/polystyrene blends. *Mater Res Express*, 6,105301.

Khatwani, P., & Yardi, S. (2003). Man Made Textiles. 46:19. India.

Khonakdar, H. A., Jafari, S. H., Mirzadeh, S., Kalaee, M. R., Zare, D., & Saeb, M. R. (2013). *Rheology-Morphology Correlation in PET/PP Blends: Influence of Type of Compatibilizer.* Retrieved May 20, 2020, from Online Library Wiley: https://onlinelibrary-wiley-com.prox.lib.ncsu.edu/doi/epdf/10.1002/vnl.20318

Kong, Y., & Hay, J. (2002). The measurement of the crystallinity of polymers by DSC. *Polymer*, 43, 3873-3878.

Körmendy, E. (2005). Phase Morphology of Polypropylene-Polyethylene Terephthalate Blend Fibres. *Fibres & Textiles in Eastern Europe*, 20-23.

Kunze, B. (1998). Nonwoven production with spun laid technology. *ITB Nonwovens-Industrial Textiles*, 3, 41-45.

Kusuktham, B. (2011). *Spinning of PET Fibres Mixed with Calcium Carbonate.* Retrieved May 20, 2020, from Science Alert: https://scialert.net/fulltextmobile/?doi=ajt.2011.106.113

L.T. (2018, April 24). *ENERGY DISPERSIVE X-RAY SPECTROSCOPY.* Retrieved from Lab Testing: https://www.labtesting.com/services/materials-testing/chemical-analysis/energy-dispersive-x-ray-spectroscopy/

LeBlanc, R. (2017, June 1). *Plastic Recycling Facts and Figures*. Retrieved from The Balance: https://www.thebalance.com/plastic-recycling-facts-and-figures-2877886

LeBlanc, R. (2017, March 1). *The basics of textile recycling*. Retrieved from The Balance: https://www.thebalance.com/the-basics-of-recycling-clothing-and-other-textiles-2877780

LeBlanc, R. (2017, February 15). *The Business Opportunity in Carpet Recycling*. Retrieved from The Balance: https://www.thebalance.com/the-business-opportunity-in-carpet-recycling-2877879

LeBlance, R. (2017, November 9). *An overview of carpet recycling*. Retrieved from The Balance: https://www.thebalance.com/an-overview-of-carpet-recycling-2877878

Lee, J. H., Lim, K. S., Hahm, W. G., & Kim, S. H. (2012). Properties of Recycled and Virgin Poly(ethylene terephthalate) Blend fibers. *Journal of Applied Polymer Science*, 1250-1256.

Lee, S., Won, J. S., Yoo, J. J., Hahm, W.-G., & Lee, S. G. (2012). Physical Properties of Recycled Polyester Yarns According to Recycling Methods. *Textile Coloration and Finishing*, 91-96.

Leonard C. Thomas. (2020). *Interpreting Unexpected Events and Transitions in DSC Results.* Retrieved June 12, 2020, from TA Instruments Literature: http://www.tainstruments.com/pdf/literature/TA039.pdf

Lepers, J. C., Favis, B. D., & Tabar, R. J. (1997). *J. Polym. Sci. B: Polym. Phys.*, 35, 2271.

Lewandowski, Z., Ziabicki, A., & Jarecki, L. (2007). The Nonwovens Formation in the Meltblown Process. *Fibres and Textiles*, 77-81.

Li, H., & Xie, X.-M. (2017). Morphology development and superior mechanical properties of PP/PA6/SEBS ternary blends compatibilized by using a highly efficient multi-phase compatibilizer. *Polymer*, 108, 1-10.

Lim, H. (2010). A review of spun bond process. *J Tex & Apparel, Technology & Management*, 6(3), 1-13.

Liu, T., Zhang, H., Zuo, M., Zhang, W., Zhu, W., & Zheng, Q. (2019). Selective location and migration of poly(methyl methacrylate)-grafted clay nanosheets with low grafting density in poly(methyl methacrylate)/poly(styrene-co-acrylonitrile) blends. *Compos Sci Technol*, 169, 110–119.

Malkan, S., & Wadsworth, L. (1993). Polymer-laid systems. In A. T. (Ed.), *Nonwovens: Theory, process, performance, and testing* (pp. 171-192). Atlanta: TAPPI Press.

Malvern. (2018, August 29). *GPC*. Retrieved from Malvern: https://www.malvernpanalytical.com/en/products/technology/gel-permeation-chromatography

Malvern Instruments. (2016). *A Basic Introduction to Rheology.* Malvern Instruments Limited.

Mariano, P., Federico, P., & Andrzej, G. (2002). Reactive compatibilization and properties of recycled poly(ethylene terephthalate)/polyethylene blends. *Polymer Bulletin*, 48, 67-74.

Mark, H., & Whitby, G. (1940). *The collected papers of W.H. Carothers.* New York: Interscience Publications Inc.

Materials Engineering. (2018, June 18). *ENGINEERING TRIPOS PART IIA: MODULE 3C1 MANUFACTURING ENGINEERING TRIPOS PART IIA: MODULE 3P1.* Retrieved from MANUFACTURING ENGINEERING: http://www-materials.eng.cam.ac.uk/3C1archive/handout5.pdf

McAmish, L. (2011). *US Patent No. US20110059287A1*.

McAmish, L., & Skelhorn, D. (2010). *US Patent No. US20120238175A1.* Retrieved May 20, 2020, from https://patents.google.com/patent/EP2150385B1

McGenity, P., Hooper, J., Paynter, C. D., & al, e. (1992). Nucleation and crystallization of polypropylene by mineral fillers: Relationship to impact strength. *Polymer*, 33(24), 5215-5224.

Merrington, A. C. (1943). The flow of viscoelastic materials in capillaries. *Nature*, 152, 663.

Michaud, J., Farrant, L., Jan, O., Kjær, B., & Bakas, I. (2010). *Environmental Benefits of Recycling.* UK: Final Report WRAP.

Midha, V. K., & Dakuri, A. (2017). Spun bonding Technology and Fabric Properties: a Review. *Journal of Textile Engineering & Fashion Technology*, 1 (4), 1-9.

Midha, V., & Kothari, V. (2004). Developments and recent trends in spunbonding. *The Indian Tex Journal*, 114: 17-24.

Mooney, P., John Shearer, P., Joey Mead, P., Carol Barry, P., Truong, Q., Welsh, E. A., . . . Hoffman, N. (2018). Bicomponent Fiber Extraction Process for Textile Applications. *Journal of Engineered Fibers and Fabrics*, 13(1); 33-39.

Morrison, F. A. (2001). Introduction. In F. A. Morrison, *Understanding Rheology* (pp. 1-11). Oxford University Press.

Mukhopadhyay, S. (2014). Bi-component and bi-constituent spinning of synthetic polymer fibres. In E. D. Zhang, *Advances in Filament Yarn Spinning of Textiles and Polymers* (pp. 113-127). Woodland Publishing Limited.

Muthu, S. S., Li, Y., Hu, J. Y., & Ze, L. (2012). Carbon footprint reduction in the textile process chain: Recycling of textile materials. *Fibers and Polymers*, 13 (8), 1065–1070.

Muthu, S. S., Li, Y., Hu, J. Y., & Ze, L. (2012). Carbon Footprint Reduction in the Textile Process Chain: Recycling of Textile Materials. *Fibers and Polymers*, 1065-1070.

Naito, K., Yang, J., Tanaka, Y., & Kagawa, Y. (2012). The effect of gauge length on tensile strength and weibull modulus of polyacrylonitrile (PAN)-and pitch-based carbon fibers. *J Mater Sci*, 47(2), 632-642.

Nanakoudis, A. (2019, November 28). *EDX Analysis with SEM: How Does it Work?* Retrieved from ThermoFisher: https://www.thermofisher.com/blog/microscopy/edx-analysis-with-sem-how-does-it-work/

Oerlikon. (2009). *A world survery on textiles and nonwovens industry.* Switzerland: Oerlikon.

Pang, Y., Jia, D., Hu, H., Hourston, D., & Song, M. (2000). Effects of a compatibilizing agent on the morphology, interface, and mechanical behaviour of polypropylene/poly(ethylene terephthalate) blends. *Polymer*, 41, 357-365.

Papadopoulou, C. P., & Kalfoglou, N. K. (2000). *Polymer*, 41, 2543.

Parsons, T. (2013, July 25-26). Multicomponent Fiber Extrusion Technology Applied to Precursors. *Carbon Fiber R&D Workshop*. Buffalo, NY.

Pattabiraman, P., Sbarski, D. I., & Spurling, P. T. (2005). *Thermal and Mechanical properties of recycled PET and its blends.* Retrieved June 12, 2020, from http://www.burchamintl.com/papers/petpapers/63.pdf

Pirzadeh, E., Zadhoush, A., & Haghighat, M. (2007). Hydrolytic and Thermal Degradation of PET Fibers and PET Granule: The Effects of Crystallization, Temperature, and Humidity. *Journal of Applied Polymer Science*, 1544-1549.

Polymer Database. (2015). *Stress-strain behaviour of polymers*. Retrieved June 12, 2020, from Polymer properties database: https://polymerdatabase.com/polymer%20physics/Stress-Strain%20Behavior.html

Polymer Database. (2020, April 23). *Polymer Properties Database*. Retrieved from Metallocene Coordination Catalyst: https://polymerdatabase.com/polymer%20chemistry/Metallocene.html

Polymer Database. (n.d.). *Polymer Phase Separation*. Retrieved May 20, 2020, from Polymer Database: https://polymerdatabase.com/polymer%20physics/Phase%20Equilibria3.html

Pracella, M., Pazzagli, F., & Galeski, A. (2002). Reactive compatibilization and properties of recycled poly(ethylene terephthalate)/polyethylene blends. *Polym Bull*, 48, 67–74.

Pukanszky, B., Belina, K., Rockenbauer, A., & Maurer, F. (1994). Effect of nucleation, filler anisotropic and orientation on properties of PP composites. *Composites*, 25(3), 205-214.

Qin, Y., Qu, M., Kaschta, J., & Schubert, D. W. (2018). Comparing recycled and virgin poly (ethylene terephthalate) melt-spun fibers. *Polymer Testing*, 364-371.

Raheem, B., & Uyigue, L. (2010). The conversion of post-consumer polyethylene terephthalate (PET) into a thermosetting polyester resin. *Scholars Research Library*, 2 (4), 240-254.

Ramamoorthy, S. K., Persson, A., & Skrifvars, M. (2014). Reusing Textile Waste as Reinforcements in Composites. *Journal of Applied Polymer Science*, 131 (17).

Rawal, A., & Mukhopadhyay, S. (2014). Melt spinning of synthetic polymeric filaments. In A. i. polymers, *D. Zhang* (pp. 75-99). Woodhead Publishing.

Razak, N. A., Inuwa, I., Hassan, A., & Samsudin, S. (2013). Effects of compatibilizers on mechanical properties of PET/PP blend. *Composite Interfaces*, 507–515.

Royal Society of Chemisty. (2020, April 20). *Compatibilization strategies in poly(lactic acid)-based blends*. Retrieved from Royal Society of Chemistry: https://pubs.rsc.org/en/content/articlelanding/2015/ra/c5ra01655j#!divAbstract

RTI Laboratories. (2019, September 15). *FTIR Analysis*. Retrieved from RTI Laboratories Techniques: https://rtilab.com/techniques/ftir-analysis/

Rudin, A., Loucks, D., & Goldwasser, J. (1980). Oriented monofilaments from blends of poly(ethylene terephthalate) and polypropylene. *Polym Eng Sci*, 20, 741–746.

Salipante, P. F., Little, C. A., & Hudson, S. D. (2017). Jetting of a shear banding fluid in rectangular ducts. *Phys Rev Fluids*.

Scheirs, J. (1998). *Polymer Recycling: Science, Technology, and Applications.* Wiley Series.

Scientific American. (2012, September 14). *Use It and Lose It: The Outsize Effect of U.S. Consumption on the Environment*. Retrieved May 27, 2020, from Scientific American: https://www.scientificamerican.com/article/american-consumption-habits/

Sevencan, F., & Vaizoğlu, S. (2007). PET ve geri dönüşümü Kor Hek . 6 (4); 307-312.

Sharobem, T. T. (2010, May). *Tertiary Recycling of Waste Plastics: An Assessment of Pyrolysis by Microwave Radiation.* Retrieved from Department of Earth and Environmental Engineering; Columbia University: http://www.seas.columbia.edu/earth/wtert/sofos/Sharobem_thesis.pdf

Shell Chemicals. (2020, May 14). *Polytrimethylene terephthalate (PTT)*. Retrieved from Swicofil: http://old.swicofil.com/ptt.html

Sia, X., Guoa, L., Wanga, Y., & Lau, K. (2008). Preparation and study of polypropylene/polyethylene terephthalate composite fibres. *Compos Sci Technol*, 68, 2943–2947.

Simons, C. (2020, April 29). *Triexta PTT Carpet Fiber*. Retrieved from The Spruce: https://www.thespruce.com/triexta-ptt-carpet-fiber-2908799

Special Chem. (2020, April 23). *How to Improve Adhesion of Polymers?* Retrieved from Special Chem: https://polymer-additives.specialchem.com/selection-guide/adhesion-promoters-for-polymers

Standard Textiles. (2020, May 18). *About Denier*. Retrieved from Standard Textiles: https://standardfiber.com/about-denier

Starý, Z., Pemsel, T., Baldrian, J., & Münstedt, H. (2012). Influence of a compatibilizer on the morphology development in polymer blends under elongation. *Polymer*, 1881-1889.

Tanrattanakul, V., Jaratrotkamjorn, R., & Juliwanlee, W. (2019). Effect of maleic anhydride on mechanical properties and morphology of poly(lactic acid)/natural rubber blend. *Mater Sci Forum*, 819, 284–289.

Tapia-Picazo, C., Luna-Bárcenas, J. G., García-Chávez, A., Gonzalez-Nuñez, R., Bonilla-Petriciolet, A., & Alvarez-Castillo, A. (2014). Polyester Fiber Production Using Virgin and Recycled PET. *Fibers and Polymers* , 547-552.

Tavares, A. A., Silva, D. F., Lima, P. S., Andrade, D. L., Silva, S. M., & Canedo, E. L. (2016). Chain extension of virgin and recycled polyethylene terephthalate. *Polymer Testing*, 26-32.

Telli, A., & Özdil, N. (2013). Properties of the yarns produced from r-pet fibers and their blends. *Tekstil ve Konfeksiyon* , (23); 3-10.

Textile World. (2010, July 19). *Specialty Markets — Bicomponent Fibers*. Retrieved from Textile World: https://www.textileworld.com/textile-world/nonwovens-technical-textiles/2010/07/specialty-markets-bicomponent-fibers/

Thomas, S., Grohens, Y., & Jyotishkumar, P. (2014). *Characterization of polymer blends: miscibility, morphology and interfaces.* Hoboken: Wiley.

Torres, N., Robin, J., & Boutevin, B. (2000). Study of thermal and mechanical properties of virgin and recycled poly(ethylene terephthalate) before and after injection molding. *European Polymer Journal*, 2075-2080.

Torres, N., Robin, J., & Boutevin, B. (2001). Chemical modification of virgin and recycled poly(ethylene terephthalate) by adding of chain extenders during processing. *J Appl Polym Sci*, 9(10): 1816–24.

Ucar, M., & Wang, Y. (2011). Utilization of recycled postconsumer carpet waste fibers as reinforcement in lightweight cementitious composites. *International Journal of Clothing Science and Technology*, 242-248.

University of Calgary. (2020). *Polymers and plastics.* Retrieved May 27, 2020, from CHEM 351: http://www.chem.ucalgary.ca/courses/351/laboratory/expt353_plastics.pdf

Utracki, L., & Shi, Z. (1992). Development of polymer blend morphology during compounding in a twinscrew extruder. Part I: droplet dispersion and coalescence—a review. *Polym Eng Sci*, 32, 1824–1833.

Vadicherla, T., Saravanan, D., & Muthu, S. S. (2015). Polyester Recycling—Technologies, Characterisation, and Applications. In S. S. Muthu, *Environmental Implications of Recycling and Recycled Products* (pp. 149-166). Hong Kong: Springer.

Vargas, E. (1993). Meltblown Process. In V. (Ed.), *Meltblown Technology Today* (pp. 7-12). San Francisco: Miller Freeman Publications.

Vavilova, S. Y., Prorokova, N. P., & Kalinnikov, Y. A. (2003). The problem of cyclic oligomers in dyeing and processing polyester and ways of solving it. *Fibre Chemistry*, 35(2), 128-130.

Verlag, B. (2001). *Calcium carbonate from the cretaceous period into the 21st century.* Basel: Springer Publishing Group.

Vivek, D. (2009, April 3). *Carbon Footprint of Textiles*. Retrieved from http://www.domain-b.com/environment/20090403_carbon_footprint.html

Vlachopoulos, J. (2019). *The Role of Rheology in Polymer Extrusion.* Hamilton, Canada: McMaster University.

Volokhova, A., Waugh, J., Arrington, K., & Matson, J. (2019). Effects of graft polymer compatibilizers in blends of cellulose triacetate and poly(lactic acid). *Polym Int*, Polym Int 68:1263–1270.

Wagner, M. H., Wu, W., Liu, Y., Qian, Q., Zhang, Y., & Mielke, W. (2008). Study on Phase Separation of PET/PEN Blends by Dynamic Rheology. *Journal of Applied Polymer Science*, 110, 177-182.

Wang, Y. (2006). *Recycling in Textiles.* (Y. Wang, Ed.) Woodhead Publishing.

Wang, Y., Zureick, A.-H., Cho, B.-s., & Scott, D. (1994). Properties of fibre reinforced concrete using recycled fibres from carpet industrial waste. *Journal of Materials Science*, 4191-4199.

Wei, B., Chen, D., Wang, H., You, J., Wang, L., & Li, Y. e. (2019). In-situ grafting of carboxylic acid terminated poly(methyl methacrylate) onto ethylene-glycidyl methacrylate copolymers: one-pot strategy to compatibilize immiscible poly(vinylidene fluoride)/low density polyethylene blends. *Polymer*, 160, 162-169.

Wei, W. (2015). Sheath/Core Polymeric Structure and Tensile Property of PP Bicomponent Fibers added with Inorganic Particulate Fillers. *Structure-Process-Properties of Nonwoven and Fibers Containing Inorganic Particulate Fillers-Calcium Carbonate*. Raleigh, US.

Weiner, S., & Addadi, L. (1997). Design strategies in mineralized biological materials. *J. Mater. Chem.* , 7(5), 689-702.

Westmoreland Mechanical Testing & Research. (2020). *What is tensile testing?* Retrieved from Westmoreland Mechanical Testing & Research: https://www.wmtr.com/en.tensile-testing.html#:~:text=The%20tensile%20strength%20of%20a%20metal%20is%20essentially%20its%20ability,are%20more%20likely%20to%20rupture.

Whinfield, J., & Dickson, J. (. (, 1946). *London Patent No. 587 079.*

Wingard, D. A. (2004). *US Patent No. US6752336 B1*.

Y., W. (2006). *Recycling in textiles.* Cambridge, UK: Woodhead Publishing.

Yang, H., He, J., & Liang, B. (2001). Transesterification kinetics of poly(ethylene terephthalate) and poly(ethylene 2,6-naphthalate) blends with the addition of ,2-bis(1,3-oxazoline). *J Polym Sci B Polym Phys*, 39(21): 2607–14.

Yi, X., Xu, L., Wang, Y., Zhong, G., Ji, X., & Li, Z. (2010). Morphology and properties of isotactic polypropylene/poly(ethylene terephthalate) in situ microfibrillar reinforced blends: influence of viscosity ratio. *Euro Polym J*, 46, 719–730.

Yinyuda. (2020, 14 05). *Introduction of PBT yarn and PTT yarn*. Retrieved from Yinyuda: http://www.yinyuda.com/News/Introduction-of-PBT-yarn-and-PTT-yarn.html

Yong Wan, P., Mira, P., Hak Yong, K., Hwan Chul, K., Jong Cheol, L., Fan-Long, J., & Soo-Jin, P. (2018). Thermal and curl properties of PET/PP blend fibres compatibilized with EAG ternary copolymer. *Bull. Mater. Sci.* , 41:104.

Zaschke, B., Hoppe, A., Schuster, M., Wenzel, M., & Wagner, K. (2012). *US Patent No. US8106121B2.*

Zhen, C., & ShouKe, Y. (2013). Structural variation of melt-crystallized PTT during the heating process revealed by FTIR and SAXS. *Chinese Science Bulletin - Polymer Chemistry*, 3, 328-335.

Zhou, C., Ma, J., Pan, L., & Liang, B. (2002). Transesterification kinetics in the reactive blends of liquid crystalline copolyesters and poly(ethylene terephthalate). *Eur Polym J*, 8(5):1049–53.

Zou, Y., Reddy, N., & Yang, Y. (2011). Reusing polyester/cotton blend fabrics for composites. *Composites, Part B: Eng*.